TOUCH-AND-GO CHEMISTRY: DEVELOPMENT OF MATERIALS FOR AND DEMONSTRATION OF A CONTACT-INITIATED POLYMERIZATION

BY

NINA MARIE SEKERAK

DISSERTATION

Submitted in partial fulfillment of the requirements
for the degree of Doctor of Philosophy in Chemistry
in the Graduate College of the
University of Illinois at Urbana-Champaign, 2015

Urbana, Illinois

Doctoral Committee:

Professor Jeffrey S. Moore, Chair
Professor Scott K. Silverman
Professor Douglas A. Mitchell
Professor Paul V. Braun

Abstract

My graduate research has focused on demonstrating the concept of a contact-initiated, or touch-and-go, reaction. One of the foundational concepts of organic chemistry is that an intermolecular reaction can only occur once two or more reactive molecules come into proximity in the correct orientation. Enzymatic reactions display improved reaction rates because catalytic groups are prearranged in proximity to the substrate. It follows that one can control a reaction rate by controlling the spatial proximity of two reactive groups. To demonstrate this concept, I developed a series of particle sizes that could be functionalized with reactive groups. These particles varied in size from 50 nm to 360 μm in diameter. Particles were then functionalized with *N*,*N*-dimethylaniline (DMA) and benzoyl peroxide (BPO) groups which co-initiate free radical polymerizations. The mechanism by which they co-initiate requires contact between the DMA and BPO molecules. When DMA and BPO were conjugated to complementary particles, a free radical polymerization was observed following contact between the particles. However, when the particles were physically separated, no reaction was observed. These experiments demonstrated touch-and-go chemistry, a reaction that could be controlled by controlling contact between two macroscopic objects.

Acknowledgments

The last six years have been a challenge, but I am deeply thankful to those who have encouraged me along the way. Thank you to Profs. Scott Silverman, Doug Mitchell, and Steve Granick for giving me a second chance in the graduate program. Your advice encouraged me to stay in graduate school and complete my degree, and I am grateful for the perspective you provided. Thank you also to Prof. Paul Braun for being willing to serve on my committee for the final days of my doctorate. Much appreciation is due Dr. Dean Olson and the staff in the NMR lab for fielding various questions and troubleshooting the instruments as well as offering a chance to relax and laugh.

Many thanks to my advisor, Prof. Jeff Moore. Thank you for being willing to meet and talk with me about research and career goals. Your perspective and encouragement helped me to keep going. You also helped me drop various projects that had no hope of success. Learning to value independence and creativity has come gradually, but you gave me the space and resources I needed to explore. I have appreciated the time in the "incubator" where I am free to fail and learn from those failures. Thank you also for teaching me that failure is a necessity in scientific research.

The Moore lab as a whole has been a wonderful group in which to work, and I am so thankful for my supportive coworkers here. There would have been no getting through grad school without your advice, laughter, and encouragement. There are too many to list you all by name, but I thank you for all your help over the years. Thank you to Dr. Josh Ritchey who introduced me to various facilities and to research in a wet chemistry lab. Dr. Scott Sisco was another tried-and-true source of knowledge.

Whenever I had a question about synthesis or purification, Scott was there with ideas and a few sarcastic rejoinders. Dr. Preston May consistently offered an encouraging smile and general advice about getting through school. Dr. Dustin Gross was a gentle teacher in the lab, as was Dr. Zheng Xue. Dr. Charles Diesendruck, thank you for your encouragement and excitement about my project. There were certainly moments that you had more faith in my project than I. Dr. Josh Kaitz, also known as "Papa Josh," thank you for restoring balance to the RAL labs as lab manager. Thanks to Dr. Olivia Lee for putting up with my many questions and general silliness. You have gently pushed me and encouraged me when I needed it. Thank you especially for your help in drafting an exit plan and in editing. When it comes to general encouragement and fun, I could not go through an acknowledgments section without mentioning Yi Ren, my faithful friend in the Moore lab. I am so glad for our times together, and you are becoming a great leader in the group. I also appreciate my labmates Ke Yang, Yang Song, Catherine Possanza, Anna Yang, Marissa Giovino, and Kevin Cheng for the discussions and questions. I am honored to have worked with all of you.

Thanks are also due the friends and family outside of my lab that have supported me through graduate school. Discussions and dinners with Amy Freeman, Janelle Sander, Hannah Ihms, Jennifer Lansing, Bethany Hausch, and Beth Ann Williams have been a welcome and needed break from the lab. My church family at Stratford Park Bible Chapel and my small group there have kept me grounded. Thank you to my family for supporting me *via* frequent phone calls and prayer.

Finally, I am thankful to my God and Savior for being faithful when I was faithless, for providing hope when I had none, and for giving me grace to continue. He has blessed me richly through the friendships, opportunities, and challenges of graduate school.

Table of Contents

Chapter 1: An Overview of Polystyrene Particle Synthesis and the Mechanism of Benzoyl Peroxide/Dimethylaniline Radical Redox Initiation

1.1 An Overview of Polystyrene Particle Synthesis

The current study of touch-and-go (TAG) chemistry is built on the foundation of two long-studied fields. The first is that of particle synthesis. The unique properties of particle emulsions and dispersions have attracted researchers to study them for decades. Particle synthesis is a sensitive science that depends on a variety of factors; varying one factor significantly alters the net result. For example, altering the reaction vessel design changes the flow dynamics, which manifests in the size, shape, or presence of distinguishable particles. Although nearly a century of research has accompanied this field, it is still difficult to predict the results when synthesizing a new set of functionalized particles. The first aspect of the research described in this thesis expands the current knowledge to synthesizing particles of various sizes that were subsequently functionalized with peroxides and anilines. In order to prepare particles with sizes ranging from 60 nm to 500 μm, four classes of polymerization were studied.

1.1.1 Emulsion Polymerization

A traditional oil-in-water emulsion polymerization is a biphasic reaction which produces small, monodisperse particles.[1] At the beginning of the reaction, the two main phases are the aqueous phase and the organic monomer phase. A surfactant such as sodium dodecyl sulfate acts not only to stabilize

monomer droplets but also to create micelles in the aqueous phase. To attain small, controlled particle sizes *via* emulsion polymerization, a water-soluble initiator such as potassium persulfate or ammonium persulfate is used. Since the charged initiator is soluble in the aqueous layer, polymerization begins in the aqueous or micellar phase. Monomer moves from the droplets to the micellar phase where it continues to be consumed in the polymerization. Thus, primary particles are formed which continue to grow by migration and incorporation of new monomer units or by coagulation of particles. As expected, surfactant concentration is instrumental in controlling the particle size and number of particles. This method yields a monodisperse set of nanoparticles under 500 nm in diameter, generally in the range of 50-300 nm.[2]

1.1.2 Surfactant-Free Emulsion Polymerization

An extension of the traditional emulsion polymerization is the surfactant-free emulsion polymerization. As its name suggests, no surfactant appears in the list of reagents for this procedure. While the lack of surfactant might suggest a vastly different mechanism, the accepted mechanism is fairly similar to that reported above. No surfactant is added, but a type of surfactant forms *in situ*.[3] The persulfate initiator homolytically cleaves and attacks a vinyl monomer to initiate polymerization. Propagation of the radical reaction leads to the formation of an ionic oligomer with a sulfate end group. These ionic oligomers act as surfactants and form micelles in the reaction mixture, forming the micellar phase necessary for the growth of primary particles. As in traditional emulsion polymerization, these particles continue to increase in size upon absorption and polymerization of monomer as well as coagulation of primary particles. The surfactant-free emulsion polymerization yields particles that are somewhat larger than their traditional analogues, though, ranging from 350 nm to 1.4 μm.[4-5] This procedure also affords monodisperse products.

1.1.3 Dispersion Polymerization

Dispersion, or precipitation, polymerization differs in its mechanism from emulsion or surfactant-free emulsion polymerization. Rather than employing an aqueous phase, dispersion

polymerizations are conducted in organic media, in which the monomer and oligomers are soluble. Early examples reported hydrocarbons as the solvents.[6] Within ten years of these reports, alcohols emerged as acceptable solvents for dispersion polymerization.[7] Whether hydrocarbons or alcohols are used as the solvent, the driving principle of the mechanism remains the same. The reaction begins as one phase as monomer remains soluble in the organic media; as the polymer reaches a threshold molecular weight, it begins to aggregate and form particle nuclei. Similar to an emulsion polymerization, particle nuclei form within the first few minutes of the reaction, leading to increasing turbidity of the mixture. These particle nuclei continue to grow and expand by the addition of monomer, oligomers, and polymer chains.

Like emulsion polymerization, dispersion polymerization requires a stabilizer that is either added at the beginning of the reaction or formed *in situ*. Since the reaction occurs in an organic solvent, selection criteria for the stabilizer do not match those for an emulsion polymerization, which often uses ionic sufactants. However, ions are less effective stabilizers in hydrocarbons and alcohols. Thus, the stabilizer used for dispersion polymerization is generally a steric stabilizer, a soluble polymer that adsorbs to the interface between the particle nuclei and the solvent. This adsorbed polymer prevents coagulation of particle nuclei once the particles attain a critical mass. Dispersion polymerization produces monodisperse batches of particles between 0.5-10 μm. Prior to dispersion methods, this larger size range was only attainable by seeded emulsion methods which require two or more steps, but the advent of dispersion polymerization allowed for the one-step synthesis of monodisperse microparticles.

1.1.4 Suspension Polymerization

The procedure of a suspension polymerization appears almost identical to that of an emulsion polymerization, but suspension polymerization proceeds by a different mechanism, thereby yielding a different outcome.[8] The similarities include the presence of an aqueous phase and an organic monomer phase as well as the addition of stabilizer. The initiator differentiates the two types of polymerization. While a hydrophilic molecule initiates polymerization in the micellar phase in an emulsion, a hydrophobic molecule such as benzoyl peroxide or azobisisobutyronitrile initiates polymerization in the

organic phase in a suspension. Thus, a suspension polymerization is considered a micro-bulk polymerization since polymerization begins and proceeds within the droplet, which subsequently becomes a polymer bead. Hence, droplet size determines bead size. Prior to polymerization, droplets are dynamic, coalescing and breaking until polymer content reaches a threshold. While droplet coalescence and splitting is not problematic in the early stages of the polymerization, it can result in irregularly shaped particles once polymerization has significantly progressed. The stabilizer serves the purpose of not only stabilizing droplets at a particular size but also preventing partially polymerized particles from adhering and bonding to each other upon collision. Since it is crucial to maintain particle integrity as polymerization proceeds, this type of system is sensitive to factors such as vessel design, vessel size, monomer-to-water ratio, stabilizer identity, stabilizer concentration, stir rate, and temperature. Suspension polymerization completes the toolkit of particle synthesis, creating polydisperse beads that are 10 μm to 5 mm in diameter.

1.2 Redox Initiators and the Benzoyl Peroxide-Dimethylaniline System

1.2.1 Definition of Redox Initiators

Investigation and demonstration of touch-and-go chemistry requires two reagents that efficiently react with each other and produce an observable outcome. This work draws from the field of redox initiation of radical polymerizations for a promising system to visualize TAG reactions. While the most common initiators for free radical polymerization undergo homolytic cleavage upon exposure to light or heat, a second class of radical initiators exists: the redox initiator.[9] In a redox initiator system, intermolecular electron transfer occurs to generate radicals as initiators for chain polymerizations. For example, suitable metal cations paired with peroxides and disulfides generate radicals by an electron transfer process. One redox initiator pair is that of a ferrous salt with hydrogen peroxide, otherwise known as Fenton's reagent. The Fe^{2+} cation transfers an electron to the peroxide. The unstable radical anion formed from the reduced peroxide leads to cleavage of the intermediate into a hydroxide anion and a hydroxyl radical. The hydroxyl radical then proceeds to initiate chain polymerization. In addition to direct

electron transfer, redox initiators comprise pairs of molecules that generate an intermediate covalent compound of oxidant and reductant. Benzoyl peroxide and *N,N*-dimethylaniline are found in this latter class of redox initiators that form a covalent intermediate of the oxidant and reductant.

1.2.2 Benzoyl Peroxide and N,N-*Dimethylaniline as Co-initiators*

In the redox mechanism of free radical initiation, a tertiary amine such as *N,N*-dimethylaniline (DMA) activates benzoyl peroxide (BPO). The unimolecular reaction of organic peroxides such as benzoyl peroxide to form radicals occurs upon exposure to light or heat. The peroxide undergoes homolytic cleavage to yield two oxygen-centered radicals which attack a vinyl monomer or decarboxylate to afford the more stable phenyl radical. This latter phenyl radical also initiates chain polymerization. In addition to its unimolecular decomposition, benzoyl peroxide may also react with a co-initiator, or activator, molecule to produce free radicals (Scheme 4.1). These activators are nucleophilic molecules that attack a peroxide oxygen in an S_N2 fashion at or below room temperature. In this step, a benzoate anion is the leaving group; and the proposed benzoyloxyanilinium cation is unstable and homolytically cleaves to yield a benzoyl radical and an anilinium radical cation. It is postulated that the benzoyl radical generally undergoes decarboxylation to generate a phenyl radical. The phenyl radical then attacks a vinyl monomer, thereby initiating chain polymerization. The fate of the anilinium radical cation is more debated than that of benzoyl peroxide. Some have proposed that the anilinium radical cation rearranges to form a more stable radical cation (second structure in Scheme 1.2); however, the role of the anilinium cation, whether rearranged or not, remains controversial.[10-11] Some studies suggest that the anilinium radical cation initiates chain polymerization while others support its inactivity. The consensus is that, regardless of its role with regard to initiation, dimethylaniline does act as a radical inhibitor in addition to its role as a co-initiator as an excessive concentration of dimethylaniline causes a decrease in the rate of a reaction.

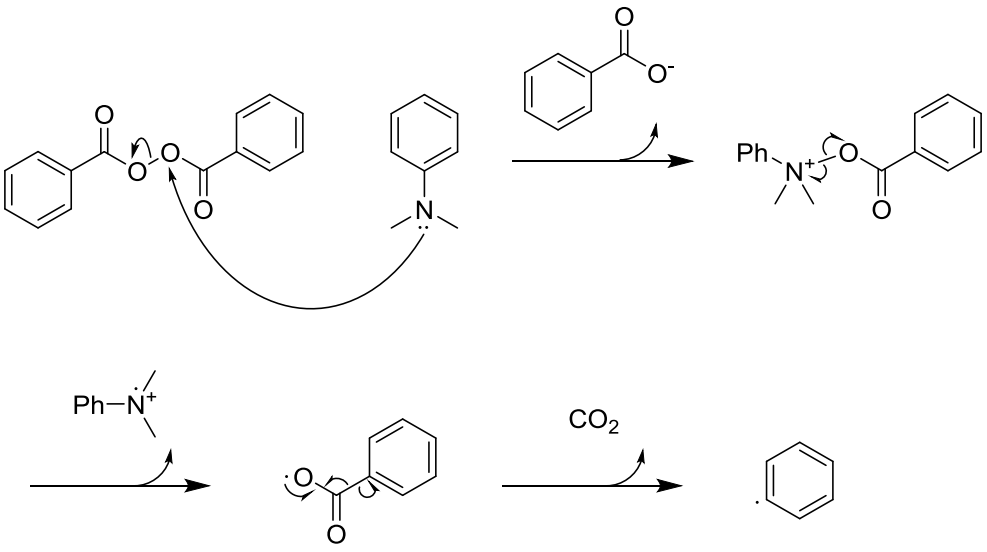

Scheme 1.1. Proposed mechanism of radical initiation by BPO/DMA redox system.

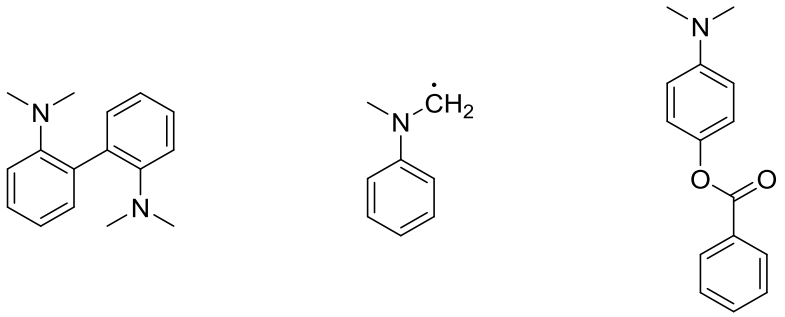

Scheme 1.2. Identified rearrangements of the anilinium radical cation upon loss of H^+.

1.2.3 Studies on the Benzoyl Peroxide-Dimethylaniline Mechanism

The mechanism of the BPO/DMA co-initiator system has been a point of discussion among polymer chemists for approximately 65 years. Horner and Schwenk first reported this radical-generating co-initiator system in 1949 and showed that it initiated free radical polymerizations of vinyl monomers.[12] In comparison to BPO alone, the BPO/DMA system presents high efficiency and reactivity at low temperatures. These advantages inspired several studies in the coming decades to probe the mechanism of initiation. Meltzer and Tobolsky undertook a study of the rate law for the polymerization of styrene initiated by BPO/DMA.[13] They found that the rate of initiation $R_i' = 3.07 \times 10^{-5}$[BPO][DMA] at 0 ºC.

Thus, since the rate law was first order in both BPO and DMA, Meltzer and Tobolsky hypothesized that a bimolecular reaction between BPO and DMA generates radicals. Supporting this idea of an intermolecular reaction was the study by Horner and Scherf in 1951.[14] They tested various substituted anilines and discovered that electron-rich dimethylanilines displayed an increased rate of initiation. Ten years later, O'Driscoll and Ricchezza confirmed this result with their study of substituted diethylanilines.[15] Imoto and Choe performed the complementary study and tested various disubstituted peroxides in the presence of dimethylaniline to study the rate of peroxide decomposition.[11] The resulting Hammett plot indicated that the reaction exhibited a small positive reaction constant ρ when plotted with normal Hammett values σ. The presence of electron-withdrawing groups on the peroxide accelerated the decomposition while electron-donating groups displayed a decreased rate. This result contrasted with that for the unimolecular decomposition obtained by Swain and coworkers, who found a negative ρ value when rate was plotted against σ values.[16] While substituted peroxides with electron-withdrawing groups showed less activity for the unimolecular reaction in the absence of dimethylaniline, they displayed greater activity in the presence of dimethylaniline. These results further supported the proposed substitution mechanism. Walling and Indictor performed another study probing the hypothesized mechanism in 1958.[17] They investigated the decomposition of benzoyl peroxide in the presence of dimethylaniline in various solvents. While the rate of decomposition was expected to increase in more polar solvents, no clear trend emerged from this study, failing to support any mechanistic pathway.

Further studies elucidated the unstable intermediate but disagreed on the role of the anilinium radical cation. In 1970, Sato and Otsu successfully synthesized *N*-acyloxytrialkylammonium tetrafluoroborate from dibenzoyl peroxide and a trialkyl amine (Scheme 1.3).[18] This salt was shown to initiate the radical polymerization of methyl methacrylate upon decomposition. This study supported the existence of the benzoyloxyammonium intermediate and demonstrated that such compounds produce radicals. However, it did not explain the function of the anilinium radical cation. In 1971, Sato, Takada, and Otsu conducted kinetic studies of another redox initiator system consisting of dimethylaniline and

cupric nitrate.[19] While the rate law did not clarify the role of dimethylaniline, the solvent studies suggested that the polymerization occurred by a radical mechanism. The initiating group was characterized by UV-vis data, which supported the incorporation of a rearranged dimethylanilinium radical; yet the results did not indicate whether the dimethylanilinium radical were an initiating or terminating group. Also, this study did not directly probe the BPO/DMA co-initiator system. A few years later in 1975, Sato, Kita, and Otsu performed EPR studies of the radical intermediates for the BPO/amine system via spin trapping.[10] The results indicated the rearrangement of the anilinium radical cation but did not confirm its reaction with styrene monomer. Thus, the initiation step of this well-studied redox polymerization remains in debate as little has appeared in the literature since the work of Sato and Otsu. Our current work seeks to utilize the current knowledge of the BPO/DMA mechanism and expand that knowledge by demonstrating that contact between the co-initiators is required to initiate polymerization.

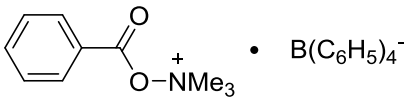

Scheme 1.3. Benzoyloxyammonium salt synthesized by Sato and Otsu. This species was shown to intiate radical polymerizations.

1.3 Summary

This work builds off of the established fields of particle synthesis and redox initiation to develop materials for and demonstrate a touch-and-go (TAG) reaction, one in which interfacial contact controls the chemistry of the system. Chapter 2 details our methods for synthesizing carboxypolystyrene particles of various sizes using emulsion, surfactant-free emulsion, dispersion, and precipitation polymerization. Chapter 3 outlines the choice of the benzoyl peroxide/dimethylaniline co-initiators to demonstrate TAG as well as the synthesis of appropriately functionalized materials for that test. Chapter 4 concludes the work by demonstrating a TAG reaction employing the particles described in Chapter 2 and the functionalization and methods offered in Chapter 3. This work serves to extend and apply these two areas of study by establishing synthetic procedures for functionalized polystyrene particles and using our

current knowledge of the mechanism of benzoyl peroxide/dimethylaniline co-initiation of radical reactions.

1.4 References

(1) Harkins, W. *J. Am. Chem. Soc*. **1947**, *69*, 1428-1444.

(2) Arshady, R. *Colloid Polym. Sci.* **1992**, *270*, 717-732.

(3) Goodall, A. R.; Wilkinson, A. C.; Hearn, J. *J. Polym. Sci.* **1977**, *15*, 2193-2218.

(4) Kotera, A.; Furusawa, K.; Takeda, Y. *Kolloid-Z.Z. Polym.***1970**, *239*, 677-681.

(5) Kotera, A.; Furusawa, K.; Kudo, K. *Kolloid-Z.Z. Polym.***1970**, *240*, 837-842.

(6) Barrett, K. E. J. *Br. Polym. J.* **1973**, *5*, 259-271.

(7) Almog, Y.; Reich, S.; Levy, M. *Br. Polym. J.* **1982**, *14*, 131-136.

(8) Vivaldo-Lima, E.; Wood, P. E.; Hamielec, A. E. *Ind. Eng. Chem. Res.* **1997**, *36*, 939-965.

(9) Sarac, A. S. *Prog. Polym. Sci.* **1999**, *24*, 1149-1204.

(10) Sato, T.; Kita, S.; Otsu, T. *Die Makromol. Chem.* **1975**, *176*, 561-571.

(11) Imoto, M.; Choe, S. *J. Polym. Sci.* **1955**, *15*, 485-501.

(12) Horner, L.; Schwenk, E. *Angew. Chem.* **1949**, *61*, 411-413.

(13) Meltzer, T.; Tobolsky, A. *J. Am. Chem. Soc.* **1954**, *76*, 5178-5180.

(14) Horner, L; Scherf, K. *Justus Liebigs Ann. Chem.* **1951**, *573*, 35-55.

(15) O'Driscoll, K.; Ricchezza, E. *Die Makromol. Chem.***1961**, *47*, 15-18.

(16) Swain, C.; Stockmayer, W.; Clarke, J. *J. Am. Chem. Soc.* **1950**, *72*, 5426-5434.

(17) Walling, C.; Indictor, N. *J. Am. Chem. Soc.* **1958**, *80*, 5814-5818.

(18) Sato, T.; Takada, M.; Otsu, T. *Die Makromol. Chem.* **1971**, *148*, 239-249.

(19) Sato, T.; Takada, M.; Otsu, T. *Die Makromol. Chem.* **1971**, *148*, 239-249.

.

Chapter 2: Synthesis of Carboxypolystyrene Particles Spanning Four Orders of Magnitude

2.1 Abstract

This chapter discusses the synthesis of a systematic series of functionalized polystyrene particles that can be easily derivatized and used for a variety of size-dependent applications such as biomedical imaging or solid-state catalysis. Various methods including emulsion, surfactant-free emulsion, dispersion, and suspension polymerization produced functionalized particles ranging from 50 nm to 360 μm. The functionality chosen for this work was the benzoic acid group since the carboxy group can be quantitatively converted to a variety of functional groups via coupling techniques. No prior reported methods produce acid-functionalized, cross-linked nanoparticles that can be used in organic solvents; and the synthesis of carboxypolystyrene resins is often lengthy or harsh. In contrast to reported procedures, our method provides an elegant approach to cross-linked carboxypolystyene nano- and microparticles. The route to installing the carboxy functionality was straightforward, involving post-polymerization cleavage of protected 4-vinylbenzoic acid. This simple approach succeeded to incorporate acidic groups in polymeric particles of all sizes. Carboxypolystyrene particles were then derivatized to afford peroxide, ester, and amide bonds. The functionalization was characterized by spectroscopic, imaging, and chemical techniques. We provide systematic and reproducible methods to synthesize carboxyPS particles of various sizes.

2.2 Introduction

Monodisperse polystyrene particles have been the subject of extensive research with roles varying from biomedical imaging agents[1] to gel modulators,[2] catalytic scaffolds[3] to building blocks for photonic crystals,[4] and drug delivery agents[5] to binders for paints and coatings.[6] Useful applications are not limited to the smaller sizes and low polydispersity. Polydisperse resins that are tens of microns in diameter or more serve as solid-state supports for reagents,[7] packing materials for ion-exchange columns,[8] and supports for solid-state synthesis.[9] To modify these particles for the numerous applications, a variety of functionalities have been introduced.[10-14] While much research has been devoted to the topic of functionalized organic particles, the incorporation of certain functionalities, such as benzoic acids or alkoxyamines, into polymeric particles has not been demonstrated or sufficiently optimized.

Incorporating carboxylic acid groups into cross-linked polystyrene particles is desirable for conjugating a number of groups to the particles via coupling chemistry and for displaying orthogonal reactivity with respect to the click reactions. However, this approach presents a specific challenge. One current gap in the literature is the synthesis of cross-linked carboxypolystyrene (carboxyPS) particles less than 1 μm in diameter. Reported methods are limited to polymer particles which fully dissolve in organic solvents and lose their morphology. The introduction of a cross-linker, although potentially yielding polydisperse samples, allows for particles to be manipulated in organic solvents and broadens potential applications. Unlike the synthesis of nanoparticles, the synthesis of cross-linked carboxyPS resins is reported but requires multiple steps post polymerization with harsh conditions. To address these synthetic challenges, we propose an elegant approach to synthesizing cross-linked carboxypolystyrene particles. In this work, the monomer 4-vinylbenzoic acid is protected as a *tert*-butyl ester, which is then copolymerized with styrene and a divinyl monomer. Following the polymerization, the ester is cleaved to yield cross-linked carboxyPS. We demonstrate that this simple yet general approach is applicable to the synthesis of both nanoparticles and resins with sizes spanning four orders of magnitude, thus providing a toolbox of particles suitable for modification for various applications in chemistry and materials science.

Different polymerization methods are available for the preparation of particles with a variety of sizes. Emulsion polymerization or mini-emulsion polymerization produces particles that are below 600 nm in diameter.[15] A traditional emulsion polymerization consists of two phases, an aqueous phase and an oily monomer phase. A radical initiator is dissolved in the aqueous phase, and polymerization begins in the micellar phase. The surfactant identity and concentration largely determines the particle size stabilized and produced by this method. Surfactant-free emulsion polymerizations (SFEP) produce nanoparticles below 2 μm in diameter, slightly larger than traditional emulsion polymerization.[16] The absence of a surfactant leads to the larger particle size in SFEP in relation to that of traditional emulsion polymerization since surfactant is not present to stabilize the larger suface-area-to-volume ratio of the smaller sizes. Although a surfactant is absent in SFEP, a cosolvent such as methyl alcohol is often dissolved in the aqueous layer and contributes to size determination. Accessing monodisperse particles between 1 and 10 μm in diameter requires dispersion, or precipitation, polymerization.[17] This reaction begins as a monophasic reaction in which the monomer is dissolved in an organic solvent, often an alcohol. As the polymerization progresses, the polymer precipitates. To obtain larger particles, from tens of microns to millimeters in diameter, suspension polymerization is employed. Suspension polymerization is similar to emulsion polymerization in the respect that both are biphasic, having an aqueous and an oily monomer phase.[18] However, the initiator is dissolved in the monomer phase. Thus, in a suspension polymerization, unlike in an emulsion polymerization, particle size is ultimately determined by the size of the monomer droplets. Since droplet size is polydisperse within the reaction mixture, the particles obtained are also polydisperse. If a certain size range is desired, particles can be separated by size via sieves. In this chapter, we report the synthesis of carboxyPS particles via emulsion, surfactant-free emulsion, dispersion, and suspension polymerization methods, thereby obtaining a series of particles of varying sizes.

2.3 Results and Discussion

2.3.1 Monomer Synthesis

As the most straightforward synthetic route, copolymerizing 4-vinylbenzoic acid with styrene and divinylbenzene presented itself as the ideal approach to carboxyPS particles. Two reports described the synthesis of carboxypolystyrene nanoparticles with 4-vinylbenzoic acid as comonomer; however, these procedures have not been reproduced in the literature to date.[19] In addition to being hydrophilic and thereby altering the properties of the biphasic polymerizations, 4-vinylbenzoic acid is crystalline with limited solubility in styrene. In order to bypass the use of 4-vinylbenzoic acid, we masked 4-vinylbenzoic acid as a *tert*-butyl ester to yield a hydrophobic oil fully miscible with styrene. Following copolymerization of the masked monomer with styrene and a cross-linker, the *tert*-butyl group is easily removed under acidic conditions to yield a carboxylic acid. This approach, although adding a couple steps to the overall synthesis, successfully enables an elegant route to polystryene particles functionalized with benzoic acid groups.

To synthesize *tert*-butyl 4-vinylbenzoate (*t*BuVB), we altered a procedure by Smith and coworkers (Scheme 2.1). Reaction between 4-vinylbenzoic acid and *N,N'*-carbonyldiimidazole (CDI) afforded a carbonyl imidazole intermediate. In the presence of 1,8-diazabicyclo[5.4.0]undec-7-ene (DBU) as the catalyst, subsequent displacement of the imidazole group by *tert*-butyl alcohol yielded the *tert*-butyl ester. The reaction proceeded cleanly, requiring only a wash for work-up. Since the monomer readily polymerized in the refrigerator or freezer over the course of weeks, butylated hydroxytoluene (BHT) was added to the monomer to inhibit polymerization during storage. Although protecting acids as *tert*-butyl esters can be challenging because of the bulky nature of the *tert*-butyl group, CDI coupling chemistry provided a simple route to the desired monomer.

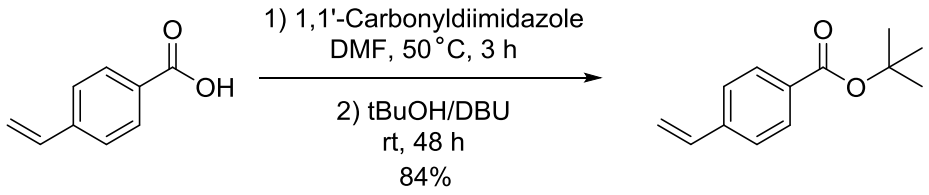

Scheme 2.1. Synthesis of *tert*-butyl 4-vinylbenzoate

2.3.2 Synthesis of Protected CarboxyPS Particles

The comonomer *t*BuVB was incorporated into cross-linked polystyrene by all four aforementioned polymerization methods, thereby yielding a range of particle sizes (Table 2.1). We modified the emulsion polymerization procedure of Zukoski and coworkers to obtain the smallest set of particles.[20] Initial trials were conducted in one stage in which all reagents were added to the reaction flask at the beginning of the procedure. However, this method led to particles with low percentages of cross-linker and did not demonstrate robustness in organic solvents. Adding *t*BuVB and using high concentrations of DVB resulted in a broad size distribution; thus, the particle synthesis was split into two stages. The first stage consists of copolymerization between styrene and a high percentage of DVB for 1 h to allow seed particles to form *in situ*. Comonomer *t*BuVB and an additional amount of DVB were subsequently added to the reaction mixture. Following 12 h of polymerization, the particles were washed with ethanol and tetrahydrofuran (THF) to remove surfactant and any remaining monomer. The weight percent of DVB was relatively high for nanoparticles at 5 wt %. Typically, cross-linking densities for nanoparticles are less than or equal to 2 wt %. We found that at lower cross-linking densities, the particles did not withstand washing and *tert*-butyl ester cleavage conditions. In contrast, particles with high cross-linking density are stable in various organic solvents without drastic changes in morphology. The two-stage emulsion polymerization yielded particles that were 50 ± 10 nm in diameter before ester removal.

To obtain particles an order of magnitude larger in diameter, we modified the surfactant-free emulsion polymerization procedure by Homola and coworkers.[21] When the polymerization was conducted

in one stage, the particles were slightly more polydisperse than when the addition of reagents was split between two stages. Thus, like the traditional emulsion polymerization, styrene was added at the beginning of the reaction in order to produce seed particles *in situ* in the first hour of the polymerization, followed by addition of a mixture of *t*BuVB and DVB. Following 12 h of polymerization, the particles were washed with THF and ethanol to remove unreacted monomers. Monodisperse particles of diameter 650 ± 50 nm were successfully obtained by this procedure. Effects of low cross-linking densities were similar to those observed for the 50-nm particles. At 1 wt % cross-linker, the particles were unable to withstand washing in organic solvents. However, the use of 2 wt % cross-linker proved sufficient to stabilize the particles in organic solvents. In contrast to previous reported methods, our procedures by emulsion and SFEP allow for the synthesis of robust, cross-linked nanoparticles.

Dispersion polymerization was attempted for the preparation of particles with roughly twice the diameter of the SFEP particles. Winnik and coworkers reported the successful synthesis of polystyrene copolymer spheres when the comonomer was added after the nucleation stage.[22-23] This method is similar to our emulsion polymerization procedures. In dispersion polymerization, we added cross-linker and comonomer 1 h following the beginning of the polymerization to allow for the formation of polystyrene seed particles *in situ*. Instead of spherical particles, dimpling was observed for the particles synthesized by dispersion polymerization, resulting in monodisperse mushroom cap particles that were 1.4 ± 0.1 μm in diameter ("brim-to-brim") and 1.0 ± 0.1 μm in height ("crown-to-brim"). This dimpling phenomenon has been reported in seeded emulsion polymerizations when solvent or monomer is expelled from a swollen particle faster than solvent is entering a cross-linked particle.[24-27] A similar phenomenon may be occurring to produce this unusual shape during dispersion polymerizations. The time of comonomer addition was varied to probe the effect on particle morphology, but spherical particles were not obtained (Figure 2.1). When *t*BuVB and DVB were added at the beginning of the polymerization, the particles formed were dicolloids with some smaller particles formed. When the comonomers were added 2 h into the reaction, the particles appeared to form mushroom cap morphology with a spherical core exposed as

described by Watson.[27] When the addition took place at 3 h, the particles were irregularly shaped with broader size variation. Each particle displays between 3 and 12 dimples on the surface. Attempting the polymerization with ethylene glycol dimethacrylate (EGDMA) as cross-linker resulted in a polydisperse sample. It was determined from these experiments that spherical particles would be difficult to obtain with this method. We also concluded that dispersion polymerization yielded a narrow size distribution of particles with anisotropic shape.

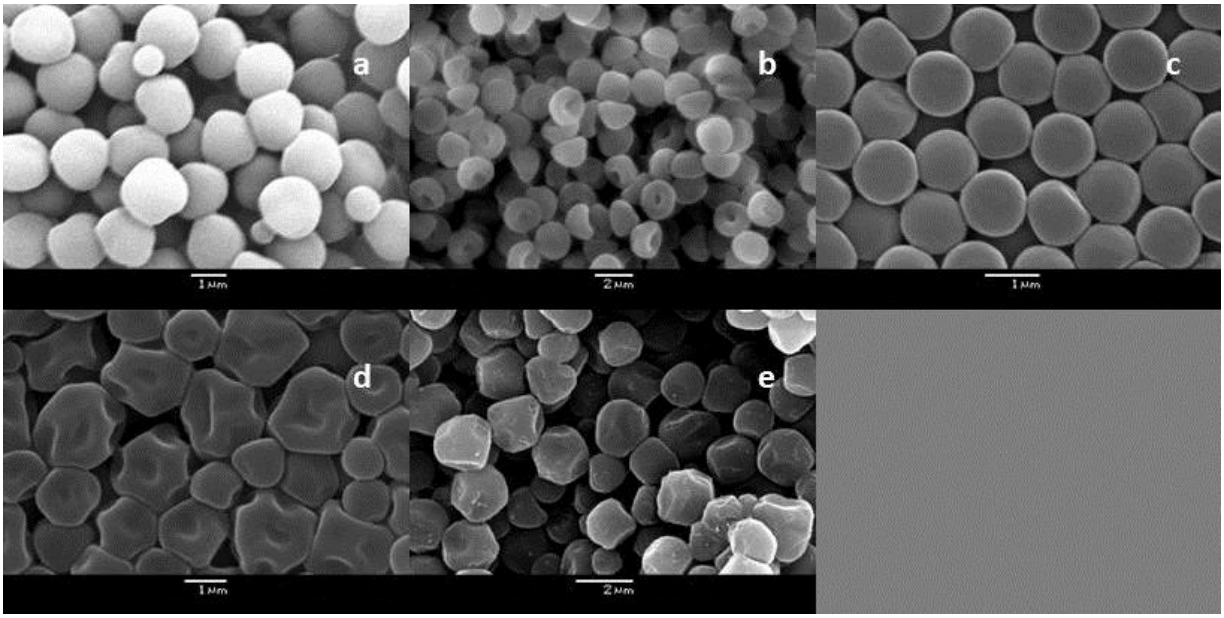

Figure 2.1. Protected carboxyPS microparticles synthesized by dispersion polymerization: *t*BuVB and DVB added to reaction mixture (a) at beginning of polymerization, (b) after one hour of polymerization, (c) after two hours, (d) after three hours, and (e) after four hours.

As noted in the introduction, suspension polymerization yields polydisperse samples because of the nature of the biphasic reaction, and it is sensitive to a variety of parameters such as the concentration and type of surfactant or stabilizer used. While initiator concentration significantly affects emulsion polymerizations, it does not impact suspension polymerizations as much. Many of the physical parameters are more important to the results of a suspension polymerization than to an emulsion polymerization. Stir rate affects the size distribution, and vessel design also plays a factor in the product due to flow dynamics. Factors as simple as the molecular weight of the stabilizer also affect the size and

morphology of the product. Thus, reproducing literature procedures becomes difficult when experimental procedures omit synthetic details or lack descriptions of specialized glassware and equipment. Furthermore, many of the older reports did not include micrographs to visualize the spherical shape of their particle product, which were separated by size range via sieves. Those reading the literature cannot determine from these papers whether the reported methods in fact yielded spheres or a variety of shapes. All of these aspects complicate the process of reproducing reported procedures.

To synthesize microparticles in a reproducible manner, we attempted and altered a number of suspension polymerization procedures. The procedure reported in our group by Douglas Davis was attempted first.[28] Davis reports the suspension polymerization of methyl methacrylate as initiated by the redox system of dimethylaniline (DMA) and benzoyl peroxide (BPO). Despite initiating the polymerization of methyl methacrylate, styrene did not polymerize under the same conditions. The DMA/BPO co-initiator system is known to be more sensitive to oxygen than thermal initiators such as azobisisobutyronitrile (AIBN). However, when AIBN replaced DMA/BPO as the radical initiator and the reaction mixture was heated to 80 °C, styrene polymerized but did not form individual particles. The next trial sought to reproduce Durie's results using a mixture of poly(vinyl alcohol) (PVA) and boric acid as stabilizers.[29] This attempt yielded particles which were dimpled and irregularly shaped. Acacia gum as a stabilizer as reported by Toy and coworkers[30] yielded non-spherical, irregular particles, indicating that the droplets were not sufficiently stabilized. As an alternative, polyvinylpyrrolidone was substituted as a suitable stabilizer as used by Greig and Sherrington;[31] but the particles formed from this procedure had agglomerated during the polymerization. ZeMac E400, a copolymer of ethylene and maleic anhydride; lignosulfonic acid; and methyl cellulose were substituted in turn for PVA in Melby's procedure but did not yield the desired spherical particles.The procedure by Melby and Strobach[32] did not list the molecular weight or percent hydrolyzation of PVA used as stabilizer. An attempt to reproduce their result with 85-kDa PVA, 97% hydrolyzed, and BPO as initiator yielded bulk polymer and no particles. Optimization of Melby's procedure was further attempted by altering stabilizer concentration and stir rate, but the

desired result was not achieved. At length, PVA with a molecular weight of 205 kDa and hydrolyzation of 88% was substituted for the lower molecular weight PVA previously used. This polymer worked effectively to stabilize the styrene droplets during polymerization, and the reaction produced spherical particles. This result agreed with the findings of Puig and coworkers who found that polyvinyl alcohol with high molecular weight and 88% hydrolyzation has effective stabilization properties for suspension polymerizations.[34] We subsequently optimized the reaction conditions by varying the stir rate and concentration of stabilizer to produce particles of different size ranges. With a 1.0 wt % solution of PVA and a stir rate of 400 rpm, suspension polymerization yielded spherical particles mostly 10-100 μm in diameter, exhibiting an average of 90 ± 30 μm. With a 0.23 wt % solution of PVA and a stir rate of 240 rpm, suspension polymerization afforded larger particles mostly 80-500 μm in diameter, exhibiting an average diameter of 360 ± 80 μm. By varying the methods used from emulsion polymerization to suspension polymerization, we obtained a wide range of particle sizes (Table 2.1).

2.3.3 Cleavage of tert-*Butyl Ester Protecting Group*

After the synthesis of the protected carboxyPS particles *via* radical polymerization, the *tert*-butyl ester was cleaved to afford particles of all sizes with free carboxylic acid groups (Scheme 2.2). The particles were immersed in a 1:1 mixture of dichloromethane and trifluoroacetic acid overnight. Subjecting particles to reaction conditions for 2 h or less resulted in incomplete removal of the *tert*-butyl ester. Although some discoloration and dimpling was observed for certain samples following cleavage of the ester, especially those with low degrees of cross-linking, the particles generally retain their shapes and sizes within error (Table 2.2).

The chemical functionality of the particles was characterized by Fourier-transform infrared (FTIR) spectroscopy, both by attenuated total reflectance (ATR) and diffuse reflectance (DRIFTS) techniques, as well as by gel-phase ^{13}C NMR spectroscopy. Results obtained from both techniques

Synthesis of protected carboxyPS particles					
Particle diameter	50 ± 10 nm	600 ± 50 nm	1.4 ± 0.1 µm	90 ± 30 µm	360 ± 80 µm
Polymerization method	Emulsion	SFEP	Dispersion	Suspension	Suspension
Dispersant	250 g H_2O	144 g H_2O	34.0 g EtOH	110 g H_2O	110 g H_2O
Surfactant, cosolvent, or stabilizer	0.35 g SDS	18.0 g MeOH	0.27 g PVP, 0.29 g Triton X-305	1.1 PVA g	0.25 g PVA
Initiator	0.78 g KPS	0.23 g KPS	0.205 g AIBN	0.50 g BPO	0.50 g BPO
Styrene (g)	19.0	16.1	6.0	16.1	16.1
***t*BuVB at t=0 (g)**	-	-	-	2.0	2.0
DVB at t=0 (g)	0.96	-	-	0.18	0.18
***t*BuVB (g) at t=1 h**	2.3	2.0	0.70	-	-
DVB (g) at t=1 h	0.21	0.18	0.06	-	-
Dispersant at t=1 h	-	-	15.0 g EtOH	-	-
Stir rate (rpm)	180	180	180	400	240

Table 2.1. Conditions for synthesis of protected carboxyPS particles of various sizes. Poly(vinyl alcohol) (PVA) was purchased under the name Mowiol® 40-88. Polyvinylpyrrolidone (PVP) had a MW = 360 kDa. The various initiators used were potassium persulfate (KPS), azobisisobutyronitrile (AIBN), and benzoyl peroxide (BPO). Water was purified through a Millipore filter prior to use. The ethanol used was 190 proof.

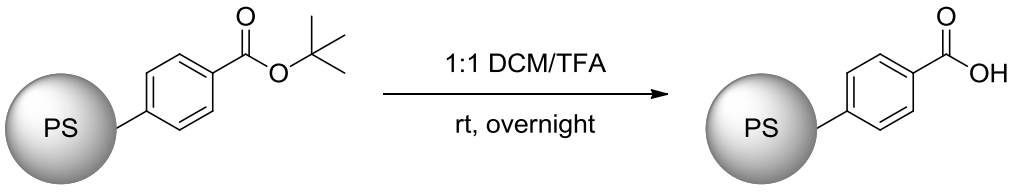

Scheme 2.2. Acid-catalyzed cleavage of the *tert*-butyl ester group.

Particle size before and after removal of *tert*-butyl protecting group

Polymerization method	Before cleavage	After cleavage
Emulsion	50 ± 10 nm	50 ± 10 nm
SFEP	600 ± 50 nm	620 ± 50 nm
Dispersion (diameter)	1.4 ± 0.1 μm	1.27 ± 0.06 μm
Dispersion (height)	1.0 ± 0.1 μm	0.94 ± 0.09 μm
Suspension (1.0 wt% PVA)	90 ± 30 μm	70 ± 30 μm
Suspension (0.22 wt% PVA)	360 ± 80 μm	360 ± 60 μm

Table 2.2. Particle size before and after ester cleavage. For each set of particles, 50 particles were measured and averaged. For the mushroom caps, both the diameter (brim-to-brim) and the height (crown to brim) were averaged.

displayed the same change in functionality between the ester and carboxy particles. In the IR spectra, the particles protected with *tert*-butyl ester groups showed one sharp carbonyl stretch at 1710 cm^{-1} and a methyl umbrella bend at 1290 cm^{-1}, while the carboxyPS particles showed two carbonyl stretches at 1740 and 1680 cm^{-1} corresponding to the free carboxylic acid and the dimerized carboxylic acid (Figure 2.3). A residual peak at 1710 cm^{-1} indicated incomplete cleavage for short reaction times. While DRIFT spectra were obtained for the 50-nm, 600-nm, and 1.4-μm particles, this technique was inconclusive for the resin microparticles. ATR-FTIR spectroscopy was effective for particles in the micrometer scale, and the spectra displayed the same chemical transformation as for the smaller particles. Additionally, the microparticles were characterized by gel-phase ^{13}C NMR spectroscopy before and after removal of the *tert*-butyl group (Figure 2.4). Before cleavage, peaks at δ 80.62 and 28.48 ppm indicate the presence of the *tert*-butyl group; these peaks do not appear in the spectra of the carboxy particles. Following ester cleavage, the carbonyl resonance shifts from δ 165.85 to 167.66 ppm. The changes observed in the IR and NMR spectra indicated that full removal of the protecting group was obtained following the overnight reaction in DCM and TFA.

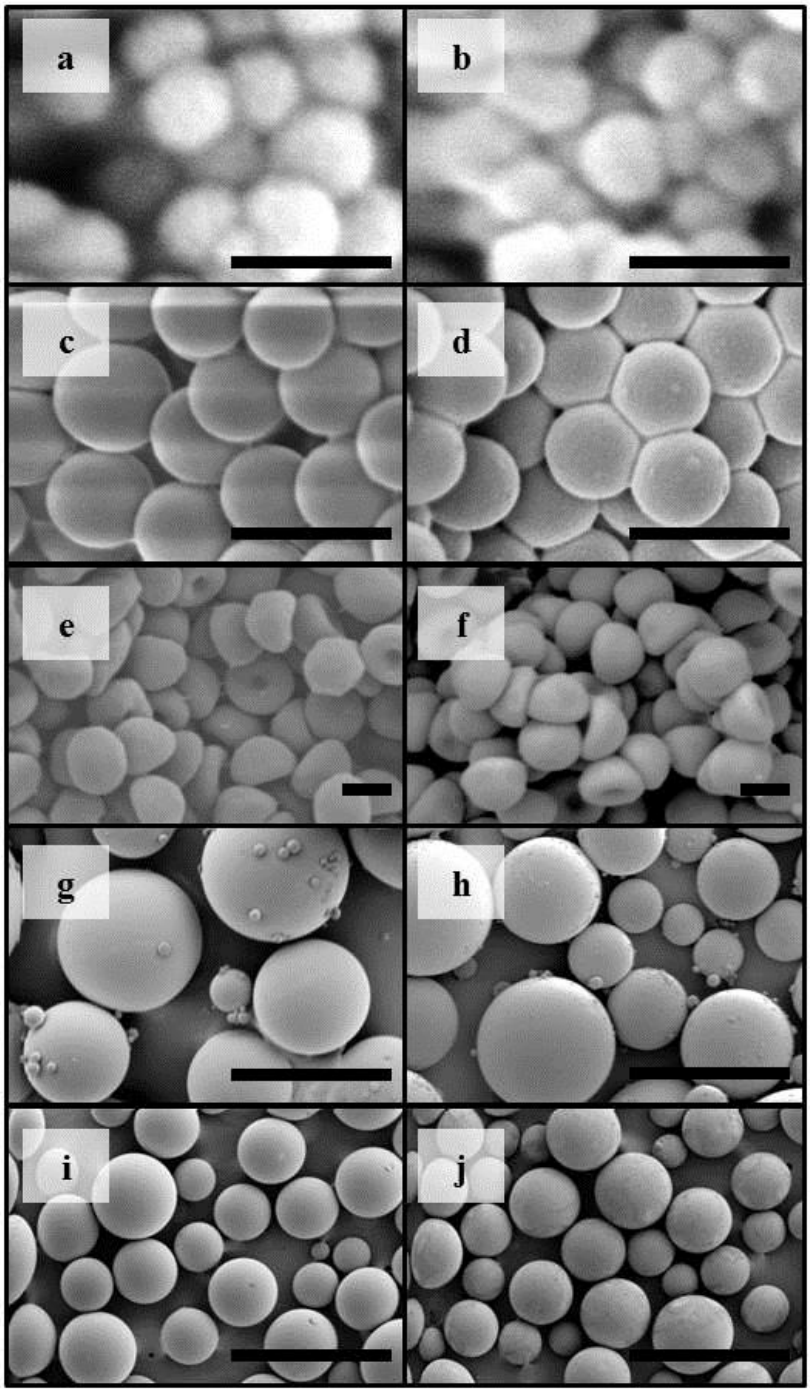

Figure 2.2. Particles before and after cleavage of the *tert*-butyl ester. Particles from the emulsion polymerization (a) before and (b) after removal of protecting group. Particles from SFEP (c) before and (d) after removal of protecting group. Particles from the dispersion polymerization (e) before and (f) after removal of protecting group. Particles from the suspension polymerization with 1.0 wt% PVA (g) before and (h) after removal of protecting group. Particles from the suspension polymerization with 0.22 wt % PVA (i) before and (j) after removal of protecting group. Scale bars represent 100 nm in (a-b), 1.00 μm in (c-f), 100 μm in (g-h), and 1.00 mm in (i-j).

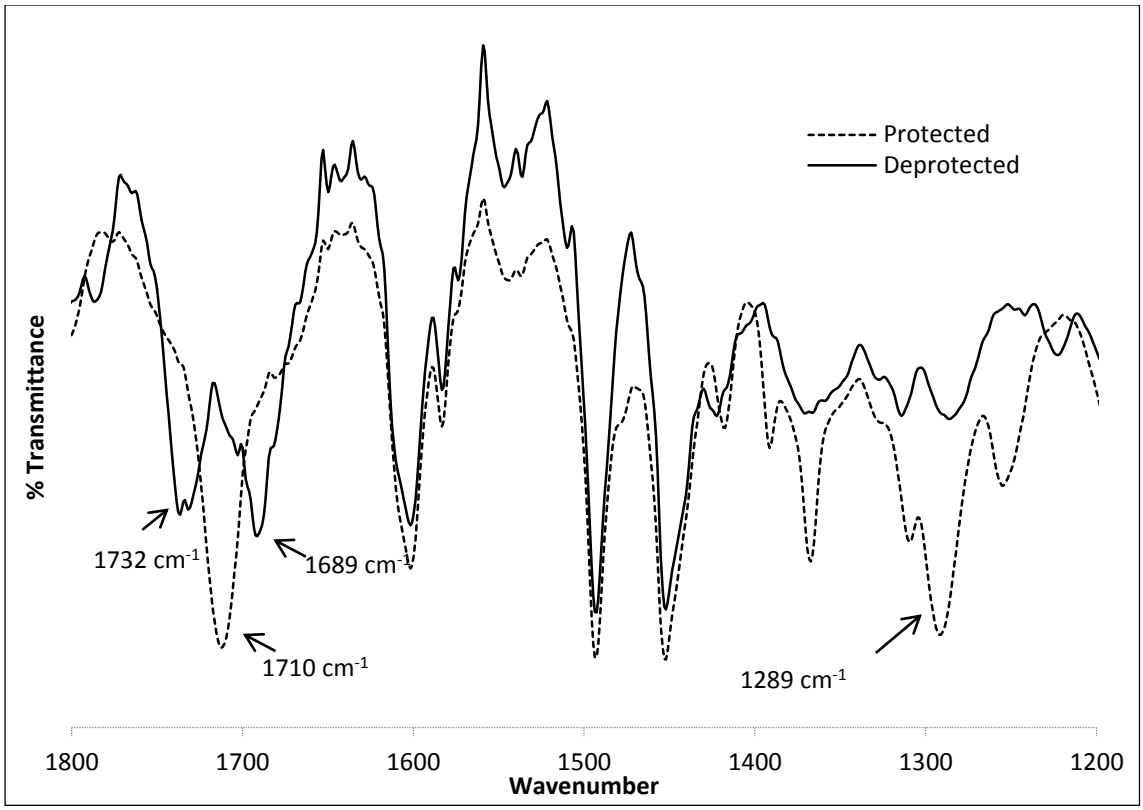

Figure 2.3. DRIFTS spectra of carboxyPS mushroom cap particles before (dotted line) and after (solid line) deprotection. The carbonyl stretch of the *tert*-butyl ester is found at 1710 cm^{-1} while the methyl umbrella bend is pronounced at 1289 cm^{-1}. Following hydrolysis of the ester, these characteristic peaks are no longer present in the spectrum. Instead, two carbonyl stretches at 1732 and 1689 cm^{-1} are present. The stretch at the higher wavenumber corresponds to a free carboxylic acid. The stretch at the lower wavenumber corresponds to a carboxylic acid that is dimerized with another acid.

2.3.4 Conjugation of Small Molecules to CarboxyPS Particles

Successful hydrolysis of the ester group enables further functionalization of the carboxylic acid by coupling techniques. Coupling alcohols, amines, and peroxyacids to the acid yields esters, amides, and dibenzoyl peroxides, respectively. To demonstrate the esterification of the particle-bound carboxylic acid, 1-pyrenebutanol (PB) was conjugated to the carboxyPS particles *via N,N*-diisopropylcarbodiimide (DIC) coupling (Scheme 2.3). The functionalized particles were imaged with confocal microscopy (Figure 2.5). Particles with protected carboxy groups were subjected to the same tagging conditions as particles with free carboxy groups, and they did not display fluorescence at the same gain setting. Likewise, carboxyPS particles were swollen in a DCM solution of DMAP and PB in the absence of DIC. These particles also

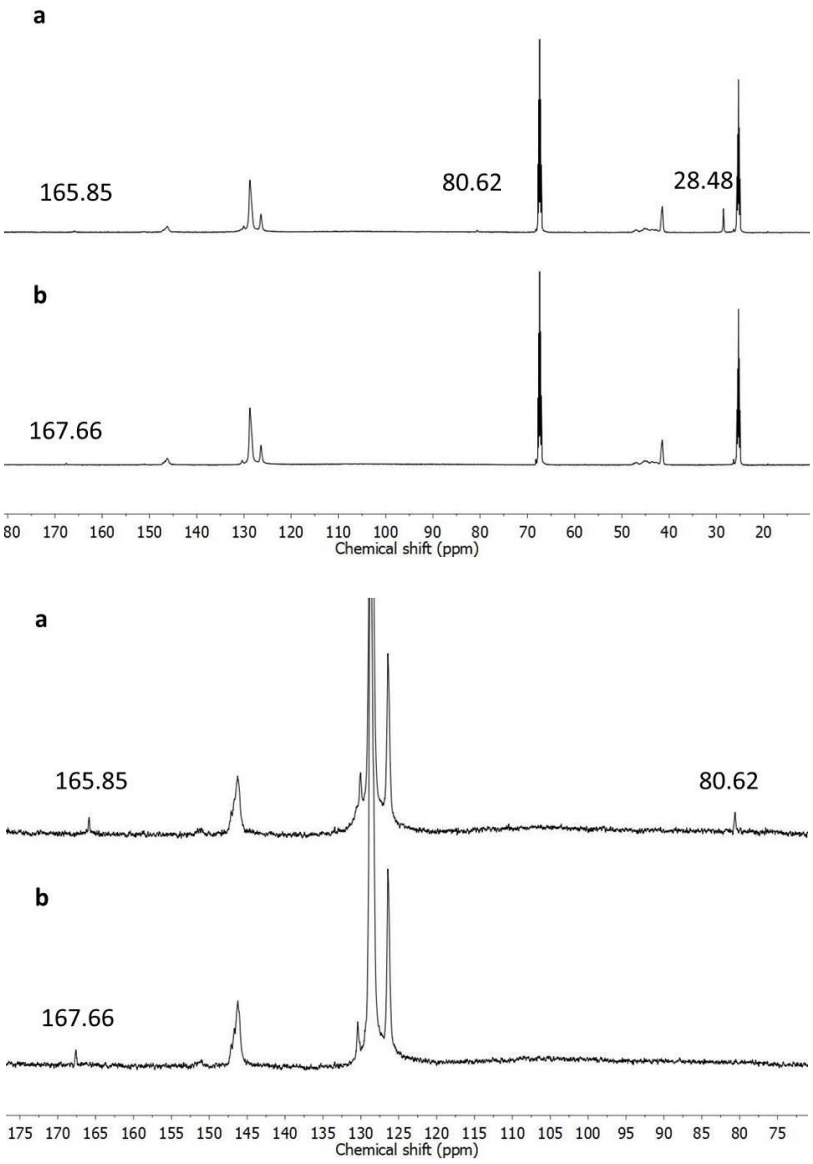

Figure 2.4. Gel-phase ^{13}C NMR spectra of carboxyPS microparticles in THF-d_8 (a) before and (b) after ester hydrolysis.

did not show fluorescence at the same gain setting. These control sets indicated that PB was conjugated to the particles and not merely adsorbed. Further characterization of the functionalized particles by IR and NMR spectroscopy demonstrated the formation of an ester bond. In the IR spectrum, the carbonyl stretches of the carboxylic acid were replaced by one sharp peak at 1715 cm^{-1}. In the NMR spectrum, the carbonyl peak shifted to δ 166.5 ppm while additional aromatic peaks appeared between δ 122-133 ppm.

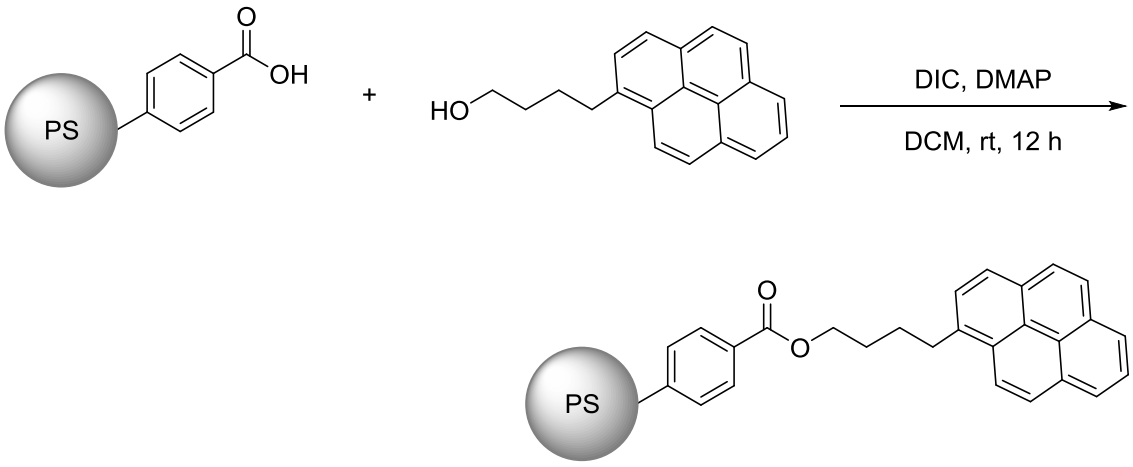

Scheme 2.3. Conjugation of 1-pyrenebutanol to carboxyPS particles *via* carbodiimide coupling.

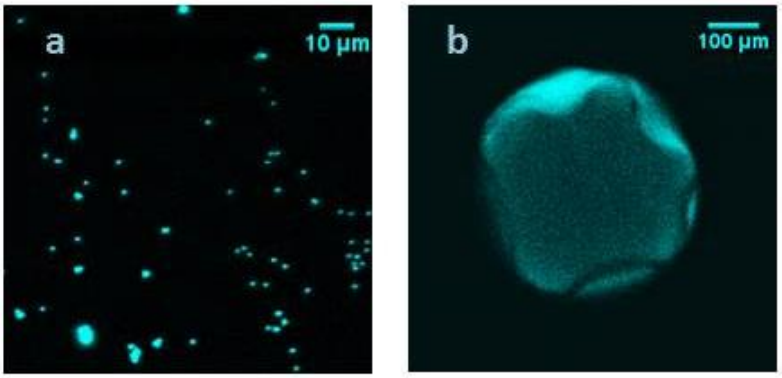

Figure 2.5. Confocal images of fluorescently labeled particles. (a) Pyrene-labeled 600-nm particles. (b) Pyrene-labeled 400-µm particle.

Additionally, peaks were present in the aliphatic region at δ 29.8, 29.2, 22.4, and 21.0 ppm. This characterization demonstrated that the PB was covalently bound to the particles.

A different coupling chemistry was used to synthesize an amide derivative (Scheme 2.4). Coupling *via* 1,1'-carbonyldiimidazole is an established method[33] that has gained interest in recent decades due to peptide synthesis. The coupling technique applies to a variety of products since the reactive acylimidazole intermediate serves as an alternative to an acid chloride. To demonstrate the formation of an amide, the 620-nm and 360-µm carboxyPS particles were activated with 1,1'-carbonyldiimidazole. Subsequent displacement of the imdiazole by a primary amine yielded the desired amide. The particles were characterized by gel-phase ^{13}C NMR and IR spectroscopy. In the

gel-phase NMR spectrum, new peaks corresponding to the alkyl chain appeared at δ 40.1, 33.1, 21.1, and 14.3 ppm. Additionally, the carbonyl peak shifted from δ 167.7 to 166.9 ppm. The difference between the FTIR spectra was more pronounced (Figure 2.6). Both methods displayed a change in the carbonyl region indicative of the formation of an amide.

Scheme 2.4. Conjugation of *n*-butylamine to carboxyPS particles *via* CDI coupling.

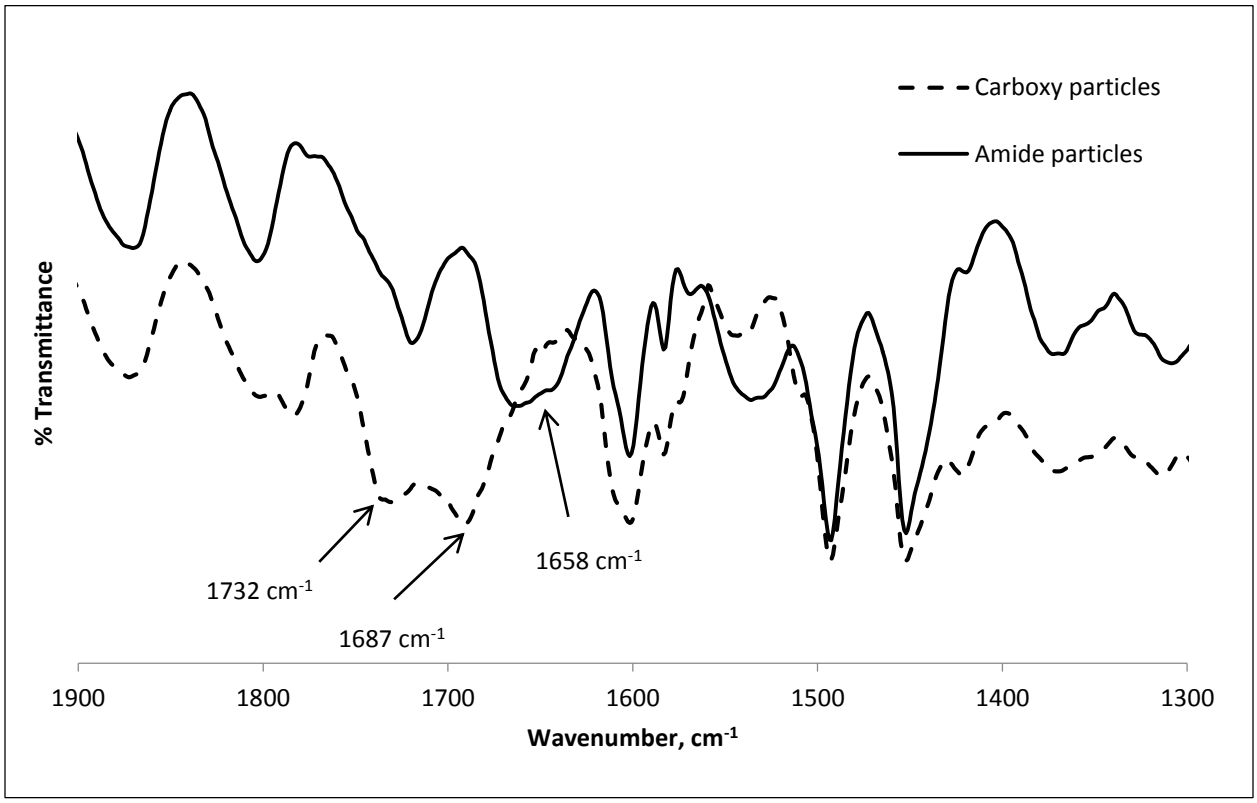

Figure 2.6. ATR-FTIR spectra of carboxyPS microparticles (dashed line) and particles with amide functionality (solid line). The peaks corresponding to the carboxylic acid at 1732 and 1687 cm^{-1} disappeared while a broad peak at 1658 cm^{-1} corresponding to the amide was present following functionalization.

Effective functionalization of the particles included not only the formation of ester and amides but also the formation of dibenzoyl peroxides (BPO). To our knowledge, we are the first to demonstrate the attachment of dibenzoyl peroxide to a polymer. Few methods exist to synthesize unsymmetrical peroxides.[35-37] We functionalized carboxyPS particles with BPO by reaction with DIC and *meta*-chloroperbenzoic acid (*m*CPBA). Particles were characterized by gel-phase ^{13}C NMR and IR spectroscopy and by iodometric titration. In the IR spectrum, the carbonyl stretches of the acid disappeared while two carbonyl stretches corresponding to the dibenzoyl peroxide appeared at 1791 and 1764 cm^{-1}. The ^{13}C NMR spectrum also indicated the disappearance of the carboxylic acid. Two peaks corresponding to the carbonyl groups of the peroxide appeared at δ 163.2 and 162.5 ppm while three new peaks in the aromatic region appeared at δ 135.8, 135.1, and 131.5 ppm. Results from iodometric titration indicated that the particles had 0.64 ± 0.02% active oxygen content, which suggests 78% functionalization of the acid functionality. Since the acid peak was not visible in the IR or NMR spectra, it can be assumed that the particles were completely functionalized. This functionalization allowed for quantification of the carboxylic acids on the particles by titration.

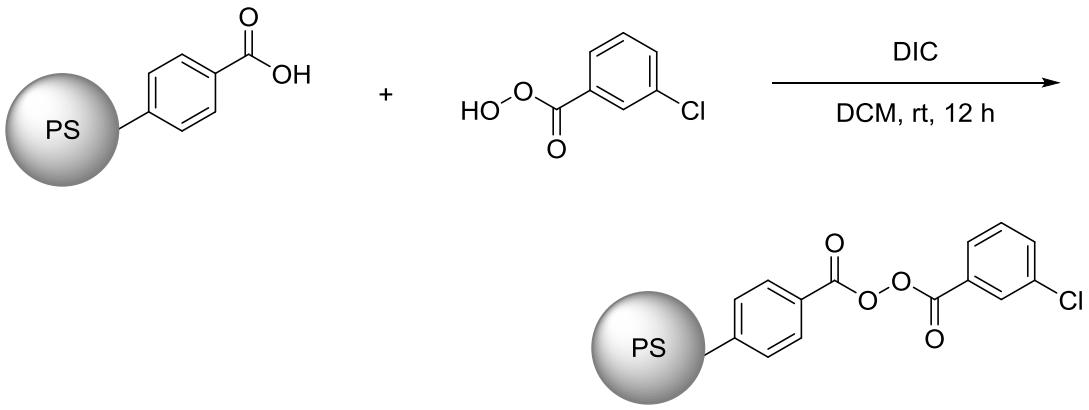

Scheme 2.5. Carbodiimide coupling to form particle-bound dibenzoyl peroxide.

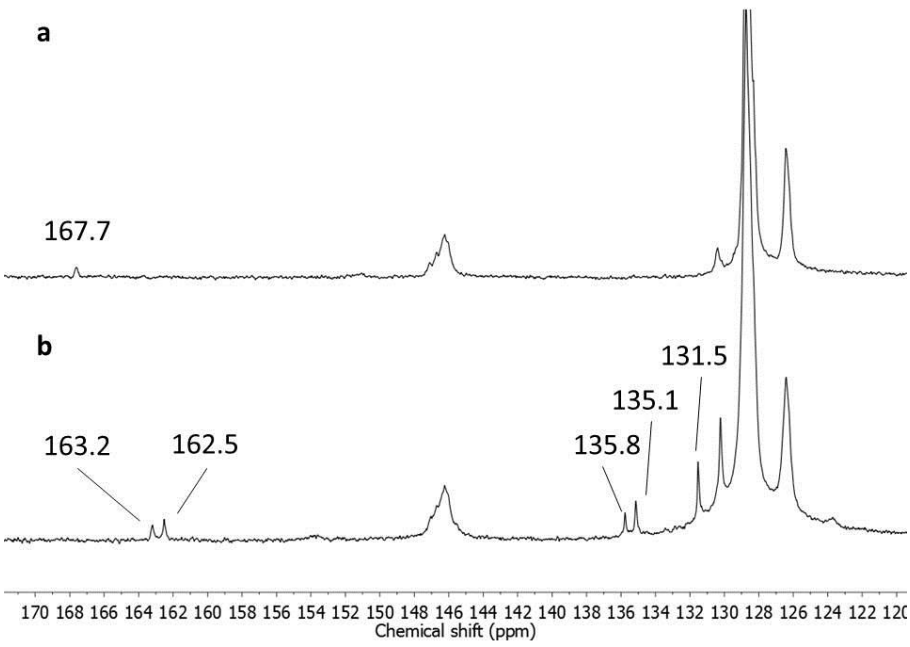

Figure 2.7. ^{13}C NMR spectra of (a) carboxyPS microparticles and (b) microparticles functionalized with peroxide in THF-d_8.

Particle size of protected carboxyPS	% Active oxygen (measured)	% Active oxygen (calculated)
50 ± 10 nm	0.64	0.80
600 ± 50 nm	0.62	0.82
90 ± 30 µm	0.67	0.81
360 ± 80 µm	0.63	0.81

Table 2.3. Results of iodometric titrations of peroxide-functionalized particles. Results of the iodometric titrations indicated that the particles had approximately 80% of the expected functionalization.

2.3.5 Variation of Cross-Linking Agent

To demonstrate the versatility of the suspension polymerization method, the cross-linker identity and density were varied. Three different cross-linkers were used: DVB, EGDMA, and poly(ethylene glycol) dimethacrylate (PEGDMA). Cross-linker loadings of approximately 0.03, 0.06, and 0.2 mmol/g particle were used. Following cleaning by centrifugation and repeated rinses, the particles were swollen in THF, DCM, and toluene. The volume percentage that each set of particles swelled is

listed in Table 2.4. Ten particles of each set were swollen in a good solvent. The diameter of the particle was measured by optical microscopy before and after swelling. The volume ratio is equal to the cube of the swollen particle diameter divided by the cube of the hard particle diameter. Particles showed the largest swelling ratio in THF and the smallest in toluene. Resins with higher degrees of cross-linking displayed lower swelling ratios than those with higher degrees of cross-linking. DVB constricted the degree of swelling that could be achieved in comparison to the other two cross-linkers. The particles cross-linked with EGDMA had the best swelling ratio. This small study demonstrated that the amount and identity of the cross-linker affects the swelling ratio. However, the trend is not always intuitive. Longer cross-linkers were expected to lead to larger swelling ratios, but this result was not the case for the resins studied. The cross-linker not only affected the swelling ratio but also the quality of the gel-phase ^{13}C NMR data. As the percentage of cross-linker was increased, the peaks in the spectrum broadened (Figure 2.8). Solid-state spectra of carboxyPS particles before and after hydrolysis displayed broad peaks which were not useful for interpretation. A densely cross-linked particle, though swollen in deuterated solvent, would still exhibit some solid-like behavior. Thus, the cross-linker may limit the data that can be obtained for a particular set of particles.

Cross-linker (mmol/g)	**THF swelling ratio**	**DCM swelling ratio**	**Toluene swelling ratio**
DVB (0.032)	7.1 ± 0.9	4.1 ± 0.4	3.7 ± 0.3
DVB (0.063)	5.1 ± 0.5	4.2 ± 0.4	3.7 ± 0.1
DVB (0.24)	3.7 ± 0.2	3.2 ± 0.2	3.0 ± 0.1
EGDMA (0.033)	14.1 ± 0.9	5.8 ± 0.8	4.9 ± 0.3
EGDMA (0.063)	8.4 ± 0.9	4.3 ± 0.5	3.9 ± 0.2
EGDMA (0.24)	4.0 ± 0.3	3.2 ± 0.3	3.2 ± 0.1
PEGDMA (0.031)	8.2 ± 0.9	4.3 ± 0.2	4.2 ± 0.3
PEGDMA (0.062)	6.1 ± 0.9	3.7 ± 0.3	3.6 ± 0.2
PEGDMA (0.22)	3.9 ± 0.3	2.9 ± 0.3	2.9 ± 0.2

Table 2.4. Volume swelling ratios of carboxyPS microparticles with different cross-linkers and cross-linker densities. For each value, the swelling of ten particles were measured and averaged.

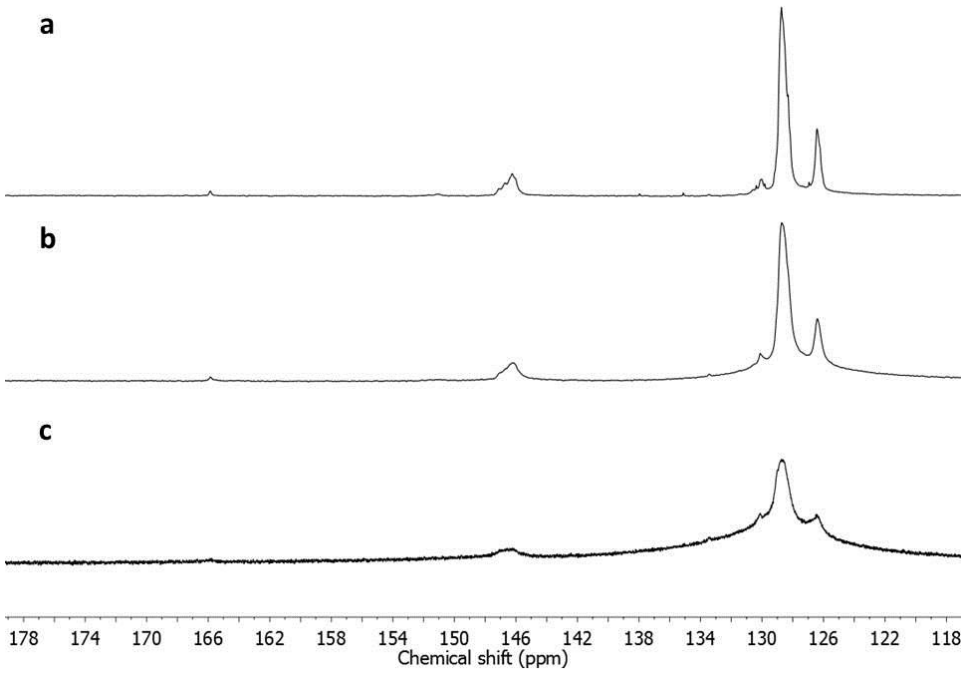

Figure 2.8. Gel-phase ^{13}C NMR spectra (THF-d_8) of protected carboxyPS microparticles: (a) 0.40 wt % DVB, (b) 0.80 wt % DVB, and (c) 3.1 wt % DVB. Line broadening was observed for higher percentages of cross-linking.

2.4 Conclusion

We have demonstrated an elegant, versatile route of synthesizing carboxy-functionalized polystyrene particles of various sizes. The copolymerization of a protected acid monomer with styrene and a cross-linker in an emulsion, surfactant-free emulsion, dispersion, or suspension polymerization produced particles of the desired size or size range. Removal of the *tert*-butyl protecting group exposed free benzoic acid groups which could be conjugated with alcohols, amines, and peracids to afford ester-, amide-, and peroxide-functionalized particles. The cross-linker was varied for the microparticles to probe particle swelling capacity. Particles with low percentages of EGDMA cross-linker displayed the highest volume-swelling ratio. These methods provide a toolkit of particle sizes that can be functionalized for a variety of applications.

2.5 Synthetic and Experimental Procedures

Materials and Reagents:

Unless otherwise stated, all starting materials were obtained from commercial suppliers and used without purification. Ethanol, 190 and 200 proof, (EtOH) and tetrahydrofuran (THF) were purchased from Fisher Scientific. The monomer precursor 4-vinylbenzoic acid (4-VBA) stabilized with butylated hydroxytoluene **(**BHT) was purchased from TCI America. Inhibitor was removed from styrene by passage through a basic alumina column. 1,1'-Carbonyldiimidazole (CDI) was purchased from AK Scientific, Inc. Magnesium sulfate was purchased from Fluka. Sodium dodecyl sulfate (SDS) was purchased from Biorad. All other reagents were purchased from Sigma Aldrich. Dimethylformamide (DMF) was purified by passage through packed columns of activated sieves as described by Pangborn and coworkers.[38] Water was obtained from a Millipore (Billerica, MA) MilliQ water purification system. An IKA 20 digital mechanical stirrer and a Glas-Col GT Series mechanical stirrer were used for emulsion and suspension polymerizations. ^{1}H NMR spectra were recorded on a Varian Unity 500 MHz spectrometer. Chemical shifts (δ) are reported in ppm from tetramethylsilane with the solvent resonance as the internal standard (deuterochloroform: 7.26 ppm). Data are reported as follows: chemical shifts, multiplicity (s = singlet, d = doublet, t = triplet, m = multiplet), and coupling constant (Hz). ^{13}C NMR (125 MHz) spectra were recorded on a Varian Unity 500 MHz Spectrometer with complete proton decoupling. Chemical shifts are reported in ppm from tetramethylsilane with the solvent resonance as the internal standard [deuterochloroform: 77.0 ppm, deuterated tetrahydrofuran (THF): 67.4 ppm]. Confocal images were obtained on a Leica SP2 UV & visible laser confocal microscope, optical images were obtained on a Leica microscope, FT-IR spectra were recorded on a Nicolet Nexus 670 spectrometer with DRIFTS and iTR attachments, and ESI-HRMS spectra were recorded on a Waters Q-TOF Ultima mass spectrometer. Scanning electron microscopy (SEM) images were acquired on a JEOL 6060LV at 10 kV and a Hitachi S4700 at 2 kV. The SEM samples were prepared by drying suspensions on aluminum stubs followed by sputter coating with a Au/Pd alloy.

Synthesis of *tert*-Butyl 4-Vinylbenzoate (*t*BuVB)

In DMF (18 mL), 4-VBA (6.0 g, 40.5 mmol) and CDI (10.0 g, 61.7 mmol) were dissolved and heated to 50 °C for 3 h. The reaction mixture was removed from heat, and tBuOH (5.0 mL, 52 mmol) and DBU (2.4 mL, 16 mmol) were added by syringe. After 48 h, the reaction mixture was diluted with diethyl ether (300 mL) and washed with 0.5 M HCl (3 x 100 mL) and saturated sodium carbonate (2 x 50 mL). The organic layer was dried over magnesium sulfate. To the organic layer, BHT (8.0 mg, 36 μmol) was added. The product was concentrated *in vacuo* to afford 5.7 g (73 % yield) of a pale yellow oil and stored at -30 °C. Inhibitor was removed from *t*BuVB before polymerization by passage through basic alumina.

^{1}H NMR ($CDCl_3$) δ 7.94 (d, 2H, *J* = 8.3 Hz), 7.44 (d, 2H, *J* = 8.3 Hz), 6.75 (dd, 1H, *J* = 17.6, 10.9 Hz), 5.85 (d, 1H, *J* = 17.7 Hz), 5.36 (d, 1H, *J* = 10.9 Hz), 1.59 (s, 9H).

^{13}C-NMR ($CDCl_3$) δ 165.53, 141.38, 136.09, 131.13, 129.67, 125.90, 116.09, 80.92, 28.18.

HRMS-ESI (*m/z*): calcd for $C_{13}H_{16}O_2Na$ $[M+Na]^+$, 227.1048; found, 227.1052.

Synthesis of 50-nm Nanoparticles *via* Emulsion Polymerization

In a 500-mL Morton flask, water (250 g), SDS (0.35 g, 1.2 mmol), potassium persulfate (KPS, 0.775 g, 2.87 mmol), styrene (19.0 g, 182 mmol), and divinylbenzene (DVB, 0.96 g, 5.9 mmol) were stirred at 60% by a Glas-Col GT Series mechanical stirrer (~180 rpm). The flask was purged with nitrogen for 15 min before being heated to 70 °C. A mixture of *t*BuVB (2.3 g, 11 mmol) and DVB (0.21 g, 1.3 mmol) was added to the reaction mixture 1 h following heating. The reaction mixture was cooled to room temperature 12 h after the addition. The particles were isolated by centrifugation for 15 min at 6000 rpm. The particles were redispersed in 15 mL THF, precipitated by addition of 35 mL EtOH, and centrifuged for 15 min at 6000 rpm. This process was repeated an additional 4 times. Particles were dried *in vacuo* to yield 18.2 g (82% yield).

Synthesis of 600-nm Nanoparticles *via* Surfactant-Free Emulsion Polymerization

In a 500-mL Morton flask, water (144 g), MeOH (18.0 g), KPS (0.225 g, 0.832 mmol), and styrene (16.1 g, 155 mmol) were stirred at 60% by a Glas-Col GT Series mechanical stirrer (~180 rpm). The flask was purged with nitrogen for 15 min before being heated to 70 °C. A mixture of *t*BuVB (2.0 g, 9.8 mmol) and DVB (0.20 g, 1.1 mmol) was added to the reaction mixture 1 h following heating. The reaction mixture was cooled to room temperature 12 h after the addition. The particles were isolated by centrifugation for 10 min at 6000 rpm. The particles were redispersed in 15 mL THF, precipitated by addition of 35 mL EtOH, and centrifuged for 10 min at 6000 rpm. This process was repeated an additional 4 times. Particles were dried *in vacuo* to yield 10.8 g (59% yield).

Synthesis of 1.4-µm Mushroom Caps *via* Dispersion Polymerization

In a 300-mL Morton flask, water (144 g), 190-proof EtOH (68.2 g), PVP (MW ~360 kDa, 0.54 g), Triton X-305 solution (0.58 g), AIBN (0.41 g), and styrene (12.0 g, 115 mmol) were stirred at 60% by a Glas-Col GT Series mechanical stirrer (~180 rpm). The flask was purged with nitrogen for 15 min before being heated to 70 °C. A mixture of *t*BuVB (1.4 g, 6.9 mmol) and DVB (0.24 g, 1.3 mmol) in EtOH (31.6 g) was added to the reaction mixture 1 h following heating. The reaction mixture was cooled to room temperature 12 h after the addition. The particles were isolated by centrifugation for 10 min at 6000 rpm. The particles were redispersed in 10 mL THF, precipitated by addition of 30 mL EtOH + 10 mL hexane, and centrifuged for 10 min at 6000 rpm. The particles were redispersed in 10 mL THF, precipitated by addition of 40 mL EtOH, and centrifuged for 10 min at 6000 rpm. This process was repeated an additional 3 times. Particles were dried *in vacuo* to yield 6.91 g (51% yield).

Synthesis of Microparticles 10 to 100 µm in Diameter *via* Suspension Polymerization

In a 300-mL Morton flask, water (110 g), Mowiol 40-88 (M_W ~205,000 g/mol, 88% hydrolyzation, 1.10 g), styrene (16.1 g, 155 mmol), DVB (0.18 g, 1.1 mmol), *t*BuVB (2.0 g, 9.8 mmol), and benzoyl peroxide (BPO, Luperox, 0.50 g, 1.5 mmol) were stirred at 400 rpm by an IKA 20 digital

mechanical stirrer, purged with nitrogen for 15 min, and heated to 70 °C. The reaction mixture was cooled to room temperature 12 h after heating. The particles were isolated by centrifugation for 3 min at 3000 rpm. Particles were then swollen in 30 mL THF, shrunken by addition of 70 mL EtOH, and centrifuged for 3 min at 3000 rpm. This process was repeated four times. Particles were dried *in vacuo* to yield 13.6 g particles (75% yield).

Synthesis of Microparticles 50 to 500 µm in Diameter *via* Suspension Polymerization

In a 300-mL Morton flask, water (110 g), Mowiol 40-88 (M_W ~205,000 g/mol, 88% hydrolyzation, 0.25 g), styrene (16.1 g, 155 mmol), DVB (0.20 g, 1.1 mmol), *t*BuVB (2.0 g, 9.8 mmol), and BPO (Luperox, 0.50 g, 1.5 mmol) were stirred at 240 rpm by an IKA 20 digital mechanical stirrer, purged with nitrogen for 15 min, and heated to 70 °C. The reaction mixture was cooled to room temperature 12 h after heating. The particles were isolated by centrifugation for 3 min at 3000 rpm. Particles were then swollen in 30 mL THF, shrunken by addition of 70 mL EtOH, and centrifuged for 3 min at 3000 rpm. This process was repeated four times. Particles were dried *in vacuo* to yield 17.1 g (94% yield).

Acid-Catalyzed Cleavage of *tert*-Butyl Esters

At room temperature, protected carboxyPS particles (5.65 g) were suspended in 1:1 DCM/trifluoroacetic acid (100 mL). The mixture was stirred for 12 h. The particles were precipitated by addition of 100 mL EtOH and centrifugation. The carboxyPS particles were washed 5 times in THF/EtOH by redispersion and centrifugation (the same conditions as the respective protected particles) and dried *in vacuo* to yield 4.3 g particles (80% yield).

Functionalization of CarboxyPS Particles with 1-Pyrenebutanol

CarboxyPS particles (0.30 g) were dispersed in 3.5 mL DCM. To this dispersion, 1-pyrenebutanol (0.20 g, 0.73 mmol) and DMAP (0.10 g, 0.80 mmol) were added followed by DIC (0.03 mL, 0.2 mmol). After 24 h, 10 mL EtOH was added to the reaction mixture. The particles were isolated by centrifugation,

washed 5 times in THF/EtOH by redispersion and centrifugation (the same conditions as the respective protected particles), and dried *in vacuo* to yield 0.20 g (59% yield).

Functionalization of CarboxyPS Particles with *n*-Butylamine

CarboxyPS particles (0.31 g) were swollen in a solution of 1,1'-carbonyldiimidazole (0.13 g, 0.80 mmol) in THF (8 mL). After 1 h, *n*-butylamine (0.08 mL, 0.8 mmol) in THF (2 mL) was added to the reaction mixture. After another hour, 10 mL EtOH was added to the reaction mixture. The particles were isolated by centrifugation, washed five times in THF/EtOH by redispersion and centrifugation (the same conditions as the respective protected particles), and dried *in vacuo* to yield 0.15 g (49% yield).

Functionalization of CarboxyPS Particles with 3-Chloroperbenzoic Acid

CarboxyPS particles (1.1 g) were swollen in a solution of *m*CPBA (0.98 g, 5.7 mmol) in DCM (25 mL). To this mixture, DIC (0.55 mL, 3.6 mmol) was added. After 12 h, 25 mL EtOH wase added to the reaction mixture. The particles were isolated by centrifugation, washed 5 times in THF/EtOH by redispersion and centrifugation (the same conditions as the respective protected particles), and dried *in vacuo* to yield 1.1 g (96% yield).

2.6 References

(1) Shi, D.; Cho, H. S.; Chen, Y.; Xu, H.; Gu, H.; Lian, J; Wang, W.; Liu, G.; Huth, C.; Wang, L.; Ewing, R. C.; Budko, S.; Pauletti, G. M.; Dong, Z. *Adv. Mater.* **2009**, *21*, 2170-2173.

(2) Bhattacharya, S.; Srivastava, A.; Pal, A. *Angew. Chem.* **2006**, *118*, 3000-3003.

(3) Stevens, P. D.; Fan, J.; Gardimalla, H. M. R.; Yen, M.; Gao, Y. *Org. Lett.* **2005**, *7*, 2085-2088.

(4) Xu, X.; Asher, S. A. *J. Am. Chem. Soc.* **2004**, *126*, 7940-7946.

(5) Soppimath, K. S.; Aminabhavi, T. M.; Kulkarni, A. R.; Rudzinski, W. E. *J. Control. Release* **2001**, *70*, 1-20.

(6) Scholz, H. A. *Ind. Eng. Chem.* **1953**, *45*, 710-711.

(7) Ley, S. V.; Baxendale, I. R.; Beam, R. N.; Jackson, P. S.; Leach, A. G.; Longbottom, D. A.; Nesi, M.; Scott, J. S.; Storer, R. I.; Taylor, S. J. *J. Chem. Soc., Perkin Trans. 1* **2000**, 3815-4195.

(8) Fritz, J. S. *J. Chromatogr. A* **2005**, *1085*, 8-17.

(9) Hermkens, P. H. H.; Ottenheijm, H. C. J.; Rees, D. C. *Tetrahedron*, **1996**, *52*, 4527-4554.

(10) Breed, D. R.; Thibault, R.; Xie, F.; Wang, Q.; Hawker, C. J.; Pine, D. J. *Langmuir* **2009**, *25*, 4370-4376.

(11) Lunov, O.; Syrovets, T.; Loos, C.; Nienhaus, G. U.; Mailander, V.; Landfester, K.; Rouis, M.; Simmet, T. *ACS Nano* **2011**, *5*, 9648-9657.

(12) Bucsi, A.; Forcada, J.; Gibanel, S.; Heroguez, V.; Fontanille, M.; Gnanou, Y. *Macromolecules* **1998**, *31*, 2087-2097.

(13) Frechet, J. M. J.; de Smet, M. D.; Farrall, M. J. *Polym.* **1979**, *20*, 675-680.

(14) Stranix, B. R.; Gao, J. P.; Barghi, R.; Salha, J.; Darling, G. D. *J. Org. Chem.* **1997**, *62*, 8987-8993.

(15) Gardon, J. L. *J. Polym. Sci. Part A* **1968**, *6*, 623-641.

(16) Goodall, A. R.; Wilkinson, A. C.; Hearn, J. *J. Polym. Sci.* **1977**, *15*, 2193-2218.

(17) Lok, K. P.; Ober, C. K. *Can. J. Chem.* **1985**, *63*, 209-216.

(18) Vivaldo-Lima, E.; Wood, P. E.; Hamielec, A. E. *Ind. Eng. Chem. Res.* **1997**, *36*, 939-965.

(19) Prasath, R. A.; Margarit-Puri, K.; Klapper, M. *J. Appl. Polym. Sci.* **2007**, *103*, 2910-2919.

(20) Mock, E. B.; De Bruyn, H.; Hawkett, B. S.; Gilbert, R. G.; Zukoski, C. F. *Langmuir* **2006**, *22*, 4037-4043.

(21) Homola, A.M.; Inoue, M.; Robertson, A. A. *J. Appl. Polym. Sci.* **1975**, *19*, 3077-3086.

(22) Song, J.-S.; Chagal, L.; Winnik, M. A. *Macromolecules* **2006**, *39*, 5729-5737.

(23) Song, J.-S.; Winnik, M. A. *Macromolecules* **2005**, *38*, 8300-8307.

(24) Okubo, M.; Minami, H. *Macromol. Symp.* **2000**, *150*, 201-210.

(25) Xu, L.; Li, H.; Jiang, X.; Wang, J.; Li, L.; Song, Y.; Jiang, L. *Macromol. Rapid Commun.* **2010**, *31*, 1422-1426.

(26) Srisopa, A.; Ali, A. M. I.; Mayes, A. G. *J. Polym. Sci. Part A* **2011**, *49*, 2070-2080.

(27) Fung, E. Y. K.; Muangnapoh, K.; Watson, C. M. L. *J. Mater. Chem.* **2012**, *22*, 10507-10513.

(28) Davis, D. A.; Hamilton, A.; Yang, J.; Cremar, L. D.; Van Gough, D.; Potisek, S. L.; Ong, M. T.; Braun, P. V.; Martínez, T. J.; White, S. R.; Moore, J. S.; Sottos, N. R. *Nature* **2009**, *459*, 68-72.

(29) Durie, S.; Jerabek, K.; Mason, C.; Sherrington, D.C. *Macromolecules* **2002**, *35*, 9665-9672.

(30) Toy, P. H.; Reger, T. S.; Garibay, P.; Garno, J. C.; Mailikayill, J. A.; Liu, G.; Janda, K. D. *ACS Comb. Chem.* **2001**, *3*, 117-124.

(31) Greig, J. A.; Sherrington, D. C. *Eur. Polym. J.* **1979**, *15*, 867-871.

(32) Melby, L. R.; Strobach, D. R. *J. Am. Chem. Soc.* **1967**, *89*, 450-453.

(33) Mendizabal, E.; Castellanos-Ortega, J. R.; Puig, J. E. *Colloid Surface* **1992**, *63*, 209-217.

(34) Staab, H. A. *Angew. Chem. Int. Ed.***1962**, *1*, 351-367.

(35) Swain, C. G.; Stockmayer, W. H.; Clarke, J. T. *J. Am. Chem. Soc.* **1950**, *72*, 5428-5434.

(36) Cadogan, J. I. G. *J. Chem. Soc.* **1959**, 2844-2846.

(37) Linhardt, R. J.; Murr, B. L.; Montgomery, E.; Osby, J.; Sherbine, J. *J. Org. Chem.* **1982**, *47*, 2242.

(38) Pangborn, A. B.; Giardello, M. A; Grubbs, R. H.; Rosen, R. K.; Timmers, F.J. *Organometallics* **1996**, *15*, 1518-1520.

Chapter 3: Development of a Particle-Bound Benzoyl Peroxide/Dimethylaniline Co-initiator System

3.1 Abstract

The concept of a contact-initiated or contact-catalyzed reaction offers potential in the areas of organic synthesis, battery energy, and self-healing materials. In order to provide a proof-of-concept reaction, an initiator or catalytic system must offer large turnover and insignificant background signals. This chapter describes the choice of the benzoyl peroxide and dimethylaniline co-initiators as a proof-of-concept system since it meets these qualifications. It also presents the synthesis and testing of benzoyl peroxide- and dimethylaniline-functionalized particles for a proximity-induced radical initiation. We established appropriate synthetic routes for attaching benzoyl peroxide and dimethylaniline to carboxypolystyrene resins. Furthermore, both particle-bound dimethylaniline and peroxide co-initiated radical polymerizations in the presence of the small molecule benzoyl peroxide and dimethylaniline, respectively.

3.2 Introduction

Bifunctional catalysis has been highlighted in the areas of enzymatic catalysis, bimetallic catalysis, and organocatalysis.[1-3] Spatial proximity of two catalytic or initiating precursors—vital to many of these reactions—has not been exploited to create controllable catalysts. Controlling the the proximity of the two precursors by environmental stimuli is one means hypothesized to alter the catalytic activity of

a system. For example, by grafting two different precursors onto separate colloidal particles, the proximity of the precursors would be controlled via the aggregation or dispersion state of the particles. This type of system is particularly interesting since local concentrations are spatially variable according to the positions of nanoscopic objects—the particle carriers. Additionally, the possible reaction between precursors would be "touch and go" (TAG), only proceeding when the surfaces are in contact with each other. Applications of TAG reactions include energy production,[4-5] battery design,[6-8] microfluidic reactions,[9-11] and simple organic syntheses. A few platforms suitable for studying TAG reactions consist of a mixture of colloids, two complementary planar surfaces, or a spherical particle with a planar surface. Figure 3.1 illustrates the concept of a TAG reaction in the form of a catalytic, binary-nanoparticle system.

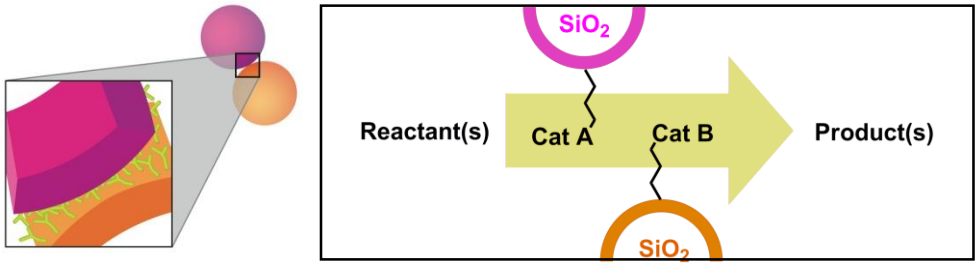

Figure 3.1. Schematic drawing of proposed TAG reaction between colloidal silica particles.

One example of this concept has appeared previously in the field of enzyme mimics. In 2005, Morse and coworkers attempted to demonstrate the polycondensation of tetraethoxysilane catalyzed by a binary-nanoparticle system (Figure 3.2).[12] The hydroxyl group grafted onto one surface acted as a nucleation site while the imidazole on another surface acted as a base. This mechanism would not require contact or proximity of the catalytic groups in order to obtain the desired results. No control experiments were conducted to verify that the polycondensation failed in the presence of physically separated nanoparticles; thus, the work failed to show a TAG reaction. A second publication by Morse and coworkers demonstrated that this condensation occurred preferentially at an interface between the two catalytic groups.[13] This work succeeded to show that proximity was an important parameter in the reaction but failed to show that it was necessary.

To demonstrate a TAG reaction, we chose to investigate the radical polymerization initiated by dimethylaniline (DMA) and benzoyl peroxide (BPO) as a model reaction.[14] Prior to selecting the DMA/BPO co-initiator system, we had considered another promising candidate: the thiourea/amine-catalyzed living ring-opening polymerization of lactide.[15] Several aspects of this system are advantageous for demonstrating a TAG reaction, including simple attachment of the catalytic groups to silica particles and straightforward reaction monitoring by analytical methods. We hypothesized that, as the polymerization progressed, the colloidal particles would aggregate in the presence of non-adsorbing polymer, increasing the number of contact events and leading to an autoaccelerating reaction. However, simple calculations demonstrated that the TAG reaction would be too slow to observe. If one assumes that the particles are perfect spheres that are closest packed and that each particle touches three complementary particles, then the catalytic contact area C_A of one particle is defined by the equation

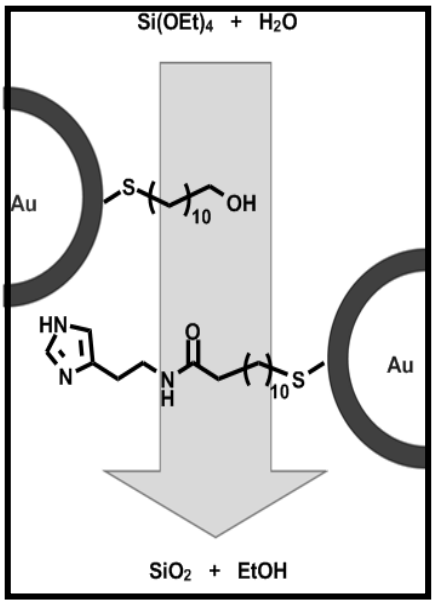

Figure 3.2. Schematic drawing of the polycondensation reaction performed by the Morse lab.

$$C_A = 6\pi Rh$$

in which R is the radius of the particle and h is the depth from the contact point at which functional groups may still come into contact. It was assumed that h = 10 Å, meaning that any groups on complementary particles that were within 20 Å of each other had the potential to react. This allowed for basic thermal agitation and rotation of the spheres. If there were 2.5 grafted groups per nm^2, then the moles of catalyst per particle $n_{particle}$ is equal to

$$n_{particle} = C_A \cdot \left(2.5\ \frac{catalytic\ groups}{nm^2}\right) \cdot \left(\frac{1}{N_A}\right) = \frac{15\pi R\ nm^{-1}}{N_A}$$

in which N_A represents Avogadro's constant. Assuming that 34.5 μmol of catalyst is needed per milliliter of solvent, then the mass of particles needed for each co-catalyst $m_{particles}$ is

$$m_{particle} = 3.45 \text{ x } 10^{-5}\ mol\ \cdot \frac{1}{n_{particle}} \cdot V_{particle}\ \cdot d_{particle}$$

in which $V_{particle}$ is the volume of one particle and $d_{particle}$ is the density of the particles. Expanding the fomula gives

$$m_{particle} = 3.45 \text{ x } 10^{-5}\ mol\ \cdot \left(\frac{N_A}{15\pi R\ nm^{-1}}\right) \cdot \left(\frac{4}{3}\pi R^3\right) \cdot d_{particle}$$

$$= 3.45 \text{ x } 10^{-5}\ mol\ \cdot \left(\frac{4}{45}\ N_A R^2\ nm\right) \cdot d_{particle}$$

Given that the density of silica is 2.2 g/cm^{-3}, the equation can be simplified to

$$m_{particle} = (4.06 \text{ x } 10^{-3}\ g \cdot nm^{-2})R^2$$

Using this equation, we calculated the amount of each particle that we would need to mimic the catalytic concentration reported by Hedrick and coworkers. Approximately 1 g of 20-nm particles (both co-catalystys) or 20 g of 100-nm particles would have to be mixed in 1 mL solvent to mimic solution concentrations. Therefore, we chose to study the BPO/DMA co-initiating system, which requires somewhat lower loadings of the particles and exhibits higher turnover frequency than the thiourea-amine co-catalyst. To mimic conditions in the literature, only 1 μmol of each co-initiator is needed in 1 mL solvent as opposed to 34.5 μmol. Assuming that silica particles would be used, the mass of each type of particle needed for the BPO/DMA system is calculated by the equation

$$m_{particle} = (1.18 \text{ x } 10^{-4}\ g \cdot nm^{-2})R^2$$

Approximately 12 mg of 20-nm particles (both co-initiators) or 0.58 g of 100-nm particles would have to be mixed in 1 mL solvent to mimic solution concentrations according to this equation. These loadings seemed more feasible than those for the thiourea-amine catalytic system.

The mechanism of the BPO/DMA co-initiation of a radical polymerization further recommended its choice for TAG chemistry. The current mechanistic proposal suggests that the radical initiation of BPO/DMA proceeds by a rate-limiting S_N2 mechanism in which the nitrogen of the aniline attacks the peroxide bond to form a quaternary benzoyloxyammonium species.[16-18] Thus, the reaction requires not only the presence of both BPO and DMA at room temperature but also contact between the two molecules. The transient cation formed undergoes homolytic cleavage, producing the benzoyl radical which can attack a vinyl monomer. The radical undergoes a series of propagation steps to form a polymer chain, thus amplifying the signal of the reaction between BPO and DMA. Although the contact events and hence initiation events may be few, the ensuing radical polymerization will indicate the occurrence of that reaction. We also anticipate that the TAG studies would elucidate additional details of the BPO-DMA initiating mechanism, such as the role of the anilinium radical cation and the behavior of unsymmetrical peroxides.

3.3 Results and Discussion

3.3.1 Synthesis of Unsymmetrical Peroxides

In order to successfully implement the BPO/DMA co-initiating system, we developed an efficient functionalization chemistry which was compatible with the peroxide and amine functional groups. Since maintaining the integrity of the peroxide bond was crucial, a polymer bead or nanoparticle is preferable to surface-functionalized silica, which catalyzes the degradation of some unsymmetrical peroxides.[19] We investigated several routes to functionalize the polymer particles: an activated ester approach,[20] "click" chemistry,[21] and carbodiimide coupling. The reaction between an *N*-hydroxysuccinimide (NHS) ester and a peracid was attempted in the presence of pyridine or cesium carbonate but was unsuccessful. Thus, we considered the use of a more active ester since nucleophilic bases such as dimethylaminopyridine react with benzoyl peroxides.[22] While an activated ester such as a thioester was expected to generate a nucleophilic thiol byproduct which would disrupt the peroxide bond formed, the 2,4-dinitrophenyl (DNP) ester alternative appeared to have no undesired reactivity . Results from ^{1}H NMR studies showed that

pyridine was too weak a base for the reaction to proceed while cesium carbonate was effective for synthesizing diaroyl peroxides (Scheme 3.1). In the presence of cesium carbonate, the DNP ester reacted with a peracid slowly to form a dibenzoyl peroxide in about 60% yield in 18 h; however, a faster rate was desired.

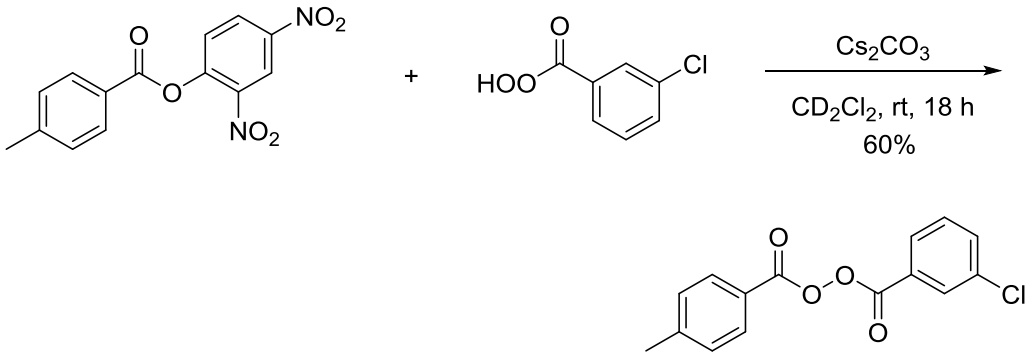

Scheme 3.1. Synthesis of unsymmetrical peroxide *via* activated DNP ester. Test reactions were monitored by ^{1}H NMR spectroscopy.

In addition to an activated ester starting material, we considered "click" chemistry as a viable functionalization route for attaching peroxide groups to polymer particles. Traditional azide-alkyne chemistry was not attempted as residual copper would be undesirable in radical polymerization tests. The copper-free azide-alkyne click reaction requires a lengthy synthesis of the precursor and was not tested. Thiol-ene chemistry was not a candidate reaction because both the nucleophilic thiol and the radicals generated during the thiol-ene reaction react with the peroxide bond. Results from NMR spectroscopic experiments also showed that the nucleophic alkoxyamine necessary for aldoxime, or oxime, chemistry interfered with the peroxide bonds (Scheme 3.2). Although alkoxyamine-functionalized polystyrene nanoparticles were synthesized, attempted derivatization with a peroxide containing a formyl group was unsuccessful. Thus, we explored other routes to attach peroxides to polymer particles.

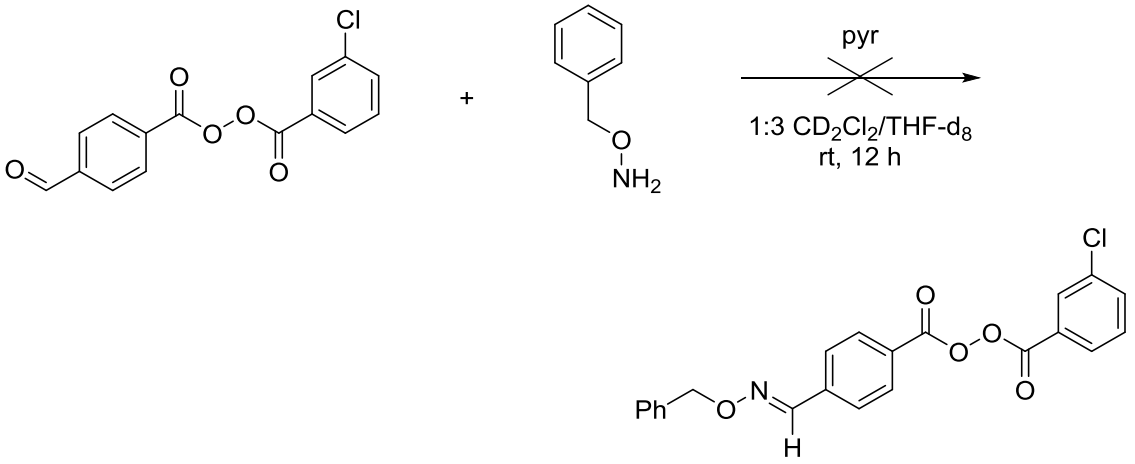

Scheme 3.2. Synthesis of unsymmetrical peroxide *via* oxime click chemistry. The desired product was not observed.

We demonstrated successful synthesis of diaroyl peroxides via carbodiimide coupling, a known approach to synthesizing unsymmetrical peroxides.[23] Studies by ^{1}H NMR spectroscopy indicated that the coupling reaction occurred almost quantitatively overnight and that the integrity of the peroxide bond was maintained through the progress of the reaction. Even though carbodiimide coupling presented a potential problem of cross-linking an acid-functionalized particle by forming anhydride bonds, we chose this route to functionalize polymeric particles with diaroyl peroxides.

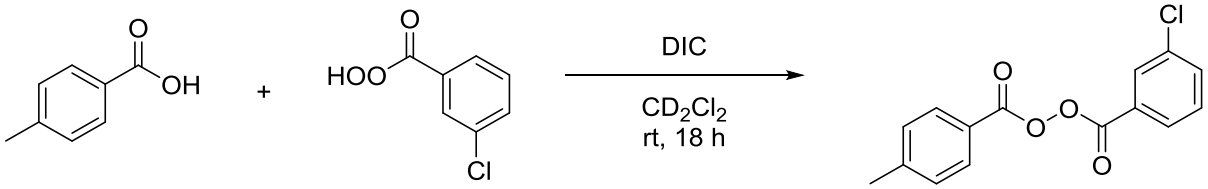

Scheme 3.3. Synthesis of unsymmetrical peroxide *via* carbodiimide coupling. ^{1}H NMR spectra indicated near quantitative yield of the desired product.

3.3.2 Tests of Unsymmetrical Benzoyl Peroxides and N,N-*Dimethylaniline Derivatives*

Before functionalizing particles of any kind with DMA or peroxides, it was necessary to determine the activity of the small molecule analogues. Three different peroxides were synthesized as well as two DMA derivatives (Scheme 3.4). Comparing the DMA derivatives, DMA ester **5** is electronically similar to compounds used in the literature while DMA amide **4** is more electron-rich than

the reported activators.[24-25] In the presence of benzoyl peroxide and styrene, DMA **4** showed an inhibitory effect on polymerization while DMA **5** was found to be an active co-initiator. The different peroxides were then tested in the presence of DMA **5** and styrene.[26] The initial progress of the reaction was monitored by ^{1}H NMR. Assuming that the rate equation for initiation is $R_i = K[BPO]^{0.5}[DMA]^{0.5}$ at room temperature, the rate constants for BPO **1**, **2**, and **3** were 1.8 x 10^{-3}, 1.8 x 10^{-3}, and 9.3 x 10^{-4}, respectively. Since the rate constants for initiation were all similar and *m*-chloroperbenzoic acid is commercially available, peroxide **2** was selected for particle functionalization to simplify the synthesis.

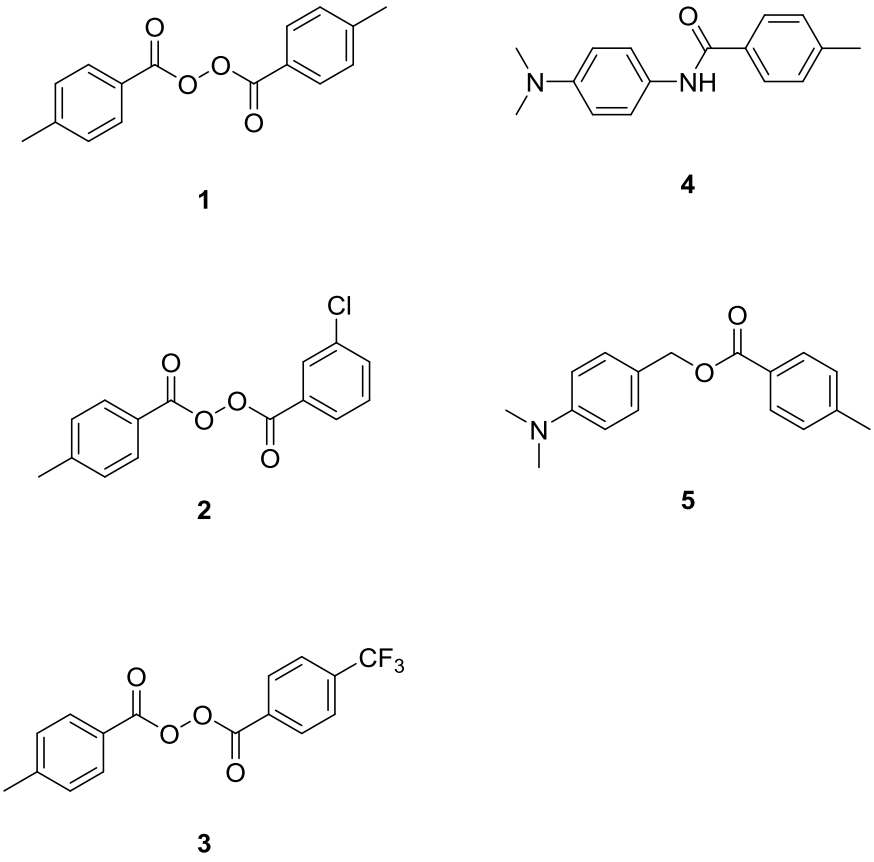

Scheme 3.4. Small molecules synthesized for kinetics tests.

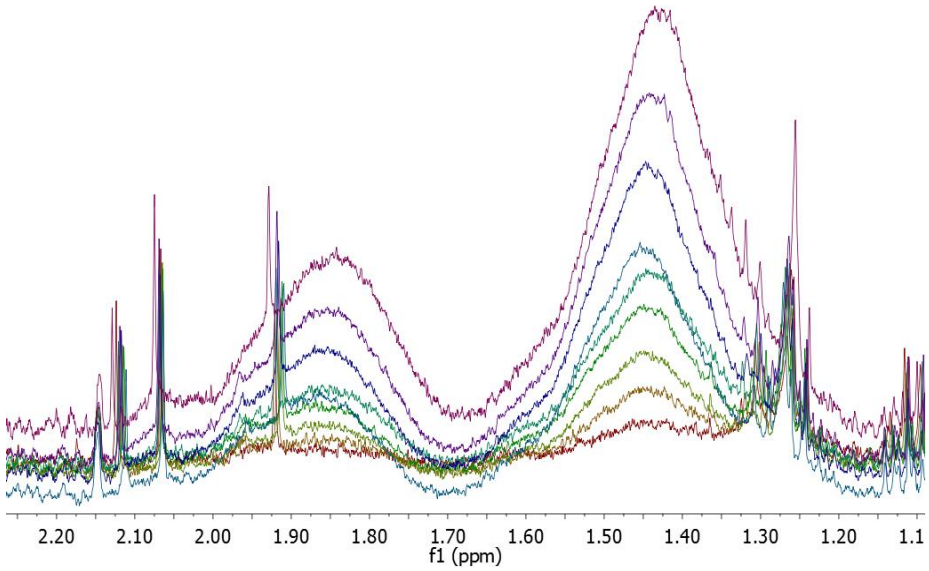

Figure 3.3. Methine and methylene peaks of polystyrene in ^{1}H NMR kinetic study of peroxide **2** and DMA **5**. Spectra werecollected at 2, 5, 10, 15, 20, 25, 30, 40, 50, and 60 min. The area of the peaks increased over the observed period. An internal standard, 18-crown-6, was used as an integration reference.

3.3.3 Functionalization of CarboxyPS Resins with Co-initiators

Following the promising results from studying the small molecule analogues, we attached the BPO and DMA derivatives to commercially available, benzoic acid-functionalized polystyrene resins *via* carbodiimide coupling and tested for their activity as particle-bound initiators (Scheme 3.5). A batch of control resin was subjected to the same reaction conditions but in the absence of coupling agent. DRIFTS confirmed successful functionalization of DMA and BPO in the presence of coupling agent, while no attachment occurred in the absence of carbodiimide. The DRIFT spectrum of peroxide-functionalized particles showed two carbonyl stretches at 1790 and 1763 cm^{-1} which corresponded to the two carbonyl stretches of BPO **2** at 1793 and 1760 cm^{-1}. In the DRIFT spectrum of the aniline-functionalized resin, we observed the appearance of a relatively sharp carbonyl stretch at 1705 cm^{-1} corresponding to the ester and a methyl umbrella bend at 1261 cm^{-1}. Similar peaks are visible in the DRIFT spectrum of DMA **5** at 1697 and 1271 cm^{-1}. The spectral data thus confirmed successful conjugation of the two co-initiators to separate batches of resin.

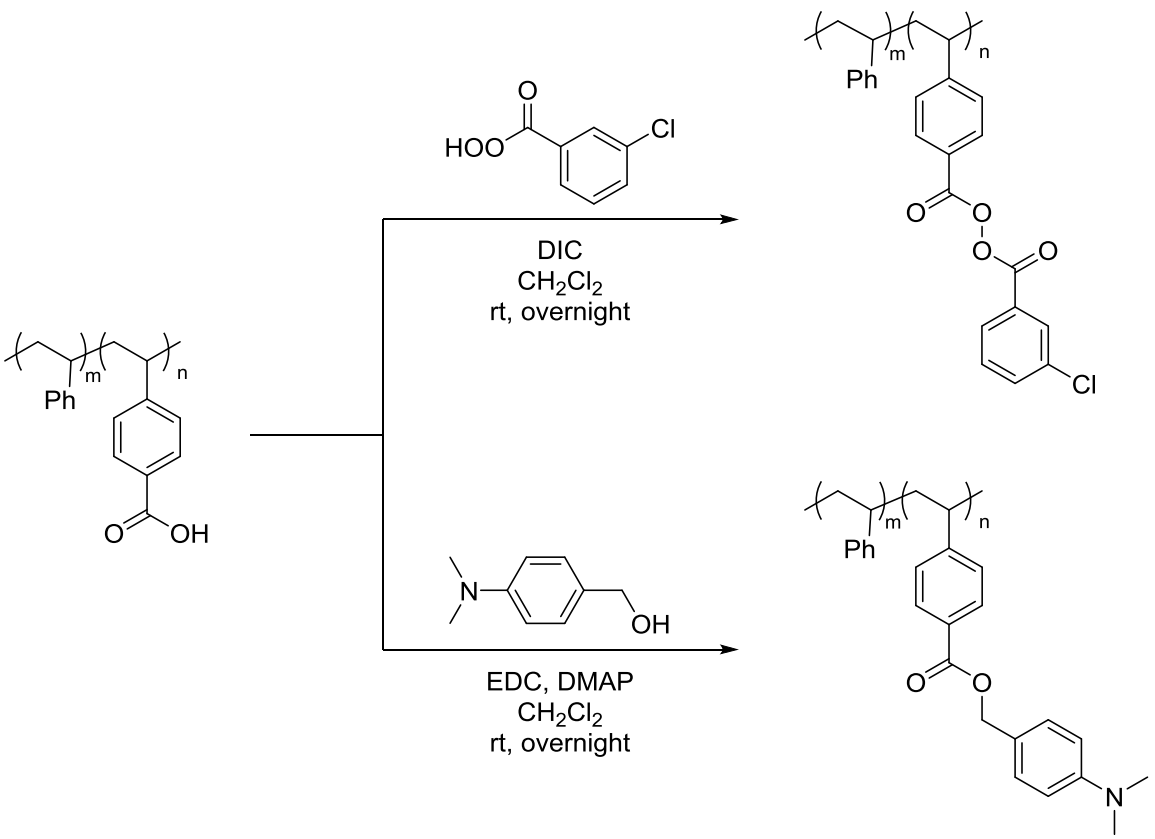

Scheme 3.5. Functionalization of commercial carboxyPS resins with peroxide and aniline derivatives.

To determine whether the resins show activity as co-initiators, polymerization tests were conducted in methyl acrylate (MA) with each initiator resin in the presence of its small molecule co-initiator. Methyl acrylate exhibits a rapid propagation rate with a low chain transfer rate, hence being an ideal choice for testing initiator activity. Additionally, the resins swell in MA, leading to increased contact surface area; thus, all of the initiator groups bound to the particle would be able to react with the small molecule co-initiator in solution. Various tests were conducted by swelling the functionalized resins in MA at 20 °C in the presence or absence of the small molecule complement. To determine whether polymerization had occurred for a given test at a certain time interval, the vial containing that test reaction was inverted; and gellation was noted as an indication of polymerization. As shown in Table 3.1 and Figure 3.4, polymerization was observed when the small molecule complements were present with the functionalized resins, which were chemically active as anticipated. The control experiments did not indicate polymerization within the same time frame, and a false positive result was not observed from

adsorbed molecules following particle functionalization. These tests confirmed that the functionalization route chosen would yield active co-initiators.

Vial	Functionalized resin	Small molecule	Time to Polym.
A	BPO	DMA **5**	10 min
B	BPO	-	-
C	BPO control	DMA **5**	-
D	Carboxy	DMA **5**	-
N	DMA	BPO **2**	40 min
O	DMA	-	-
P	DMA control	BPO **2**	-
Q	Carboxy	BPO **2**	-

Table 3.1. Polymerization tests of MA. Vials contained 25 mg of functionalized resin, 0.25 mL MA, and 0.2 M small molecule co-initiator. Polymerization was only observed when both the particle-bound initiator and its small molecule complement were present.

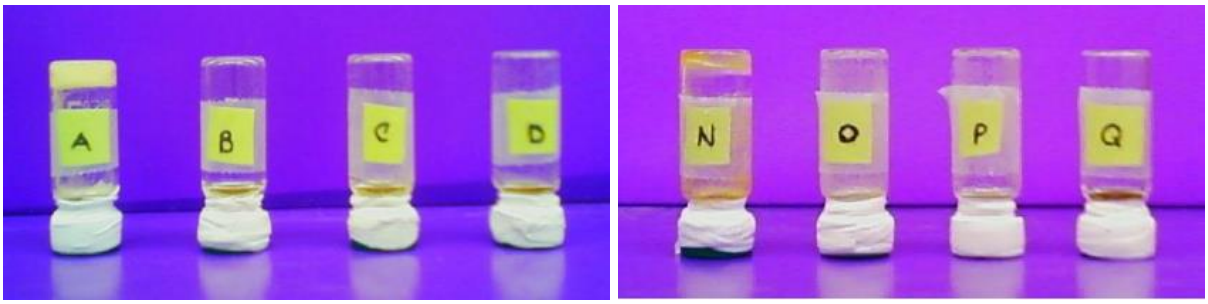

Figure 3.4. Tabletop rheology of polymerization tests with functionalized resins. Vials A-D are shown 10 min after addition of MA. Vials N-Q are shown 4 h after addition of MA.

3.4 Conclusion

In conclusion, we have synthesized particles bearing individual components of a co-initiator system and tested their activities for use in a TAG reaction. The BPO/DMA co-initiator system was selected as a suitable system for studying an interfacially controlled reaction. Reaction between small molecule derivatives of BPO and DMA in the presence of styrene or methyl acrylate indicated the successful initiation of a radical polymerization in the presence of both co-initiators. We further developed an appropriate functionalization route to attach both the peroxide and aniline derivatives to a

polymer surface. Grafted anilines and peroxides successfully initiated radical polymerization in the presence of their small molecule complements.

3.5 Synthetic and Experimental Procedures

Materials and Reagents:

Unless otherwise stated, all starting materials were obtained from commercial suppliers and used without purification. Carboxypolystyrene resin (200-400 mesh, 1.6-2.1 mmol/g) was purchased from Alfa Aesar. 4-(Dimethylamino)benzyl alcohol was synthesized according to the literature procedure.[27] Prior to use, *m*-chloroperbenzoic acid was washed with phosphate buffer, pH 7.5-8.5. All reactions were performed under ambient atmosphere unless otherwise specified.

Flash chromatography was conducted with silica gel 60 (230-400 mesh) from Silicycle. The ^{1}H and ^{13}C NMR spectra were obtained using either a Varian Unity 400 or 500 MHz spectrometer in the VOICE NMR laboratory at the University of Illinois; the residual solvent protons were used to reference the chemical shift. Coupling constants (*J*) are reported in Hertz (Hz), and splitting patterns are designated as s (singlet), d (doublet), t (triplet), q (quartet), m (multiplet), and br (broad). Mass spectra were obtained through the Mass Spectrometry Facility, SCS, University of Illinois and elemental analyses were performed by the University of Illinois MicroAnalytical services. Percent transmittance spectra were acquired on a Nicolet Nexus 670 FT-IR spectrometer with a diffuse reflectance attachment (DRIFTS) representing the sum of 128 individual scans for DRIFT spectra and 16 scans for transmission spectra at a resolution of 4 cm^{-1} from 800-4000 cm^{-1}. Iodometric titrations were performed to measure the amount of active oxygen in peroxides; the procedure outlined by Ma and Gerstein was followed.[28]

Synthesis of 2,4-Dinitrophenyl 4-Methylbenzoate, **S1**

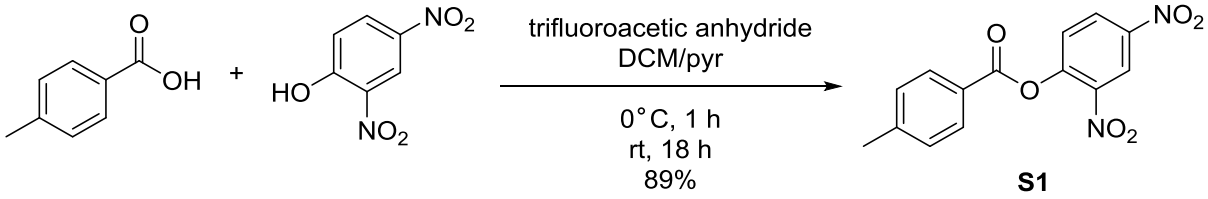

Scheme 3.6. Synthesis of an activated 2,4-dinitrophenyl ester.

A modified procedure by Leonard and Brunckova was followed.[29] In 37 mL DCM, pyridine (2.4 mL, 29 mmol), *p*-toluic acid (1.00 g, 7.34 mmol), and 2,4-dinitrophenol (2.73, 14.8 mmol) were dissolved. The mixture was cooled to 0 ºC and purged with N_2 before the addition of trifluoroacetic anhydride (2.05 g, 14.7 mmol). After 1 h, the reaction mixture was warmed to room temperature. The reaction mixture was stirred overnight at room temperature. After 18 h, the mixture was diluted to 200 mL and washed with 3 × 200 mL 1 M HCl and 4 × 100 mL $NaHCO_3$. The organic layer was dried over $MgSO_4$, and the solvent was removed *in vacuo* to yield 2.22 g (89% yield) of feathery yellow solid.

^{1}H-NMR (CD_2Cl_2) δ 8.97 (d, 1H, *J* = 2.7 Hz), 8.56 (dd, 1H, *J* = 8.9, 2.7 Hz), 8.08 (d, 2H, *J* = 8.5 Hz), 7.66 (d, 1H, *J* = 9.0 Hz), 7.38 (d, 2H, *J* = 8.4 Hz), 2.48 (s, 3H)

^{13}C-NMR ($CDCl_3$) δ 163.4, 149.0, 146.0, 144.9, 141.9, 130.7, 129.6, 128.8, 126.7, 124.6, 121.6, 21.9

HRMS-ESI (*m/z*): calcd for $C_{14}H_{10}N_2O_6Na$ $[M+Na]^+$, 325.0042; found, 325.0437

[1]H NMR Analysis of Reaction of *m*CPBA with Activated DNP Ester

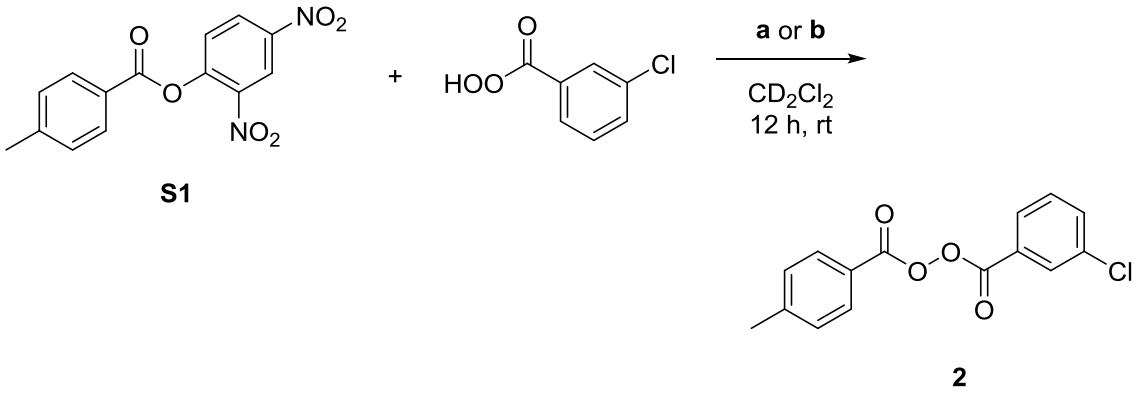

Scheme 3.7. Synthesis of unsymmetrical peroxide *via* activated DNP ester. Conditions: (**a)** 0.10 mL pyridine-d_5 (1.2 mmol) and (**b**) Cs_2CO_3 (24.2 mg, 74.3 µmol) and additional 0.10 mL CD_2Cl_2. Test reactions were monitored by ^{1}H NMR spectroscopy.

In a standard NMR tube, **S1** (10.1 mg, 33.4 µmol) and *m*CPBA (5.45 mg, 31.6 µmol) were dissolved in 0.50 mL CD_2Cl_2 with base as shown in the above scheme. ^{1}H NMR spectra were collected after 12 h. Integration of the methyl peak indicated formation of peroxide **2** in the presence of Cs_2CO_3 but not in the presence of pyridine.

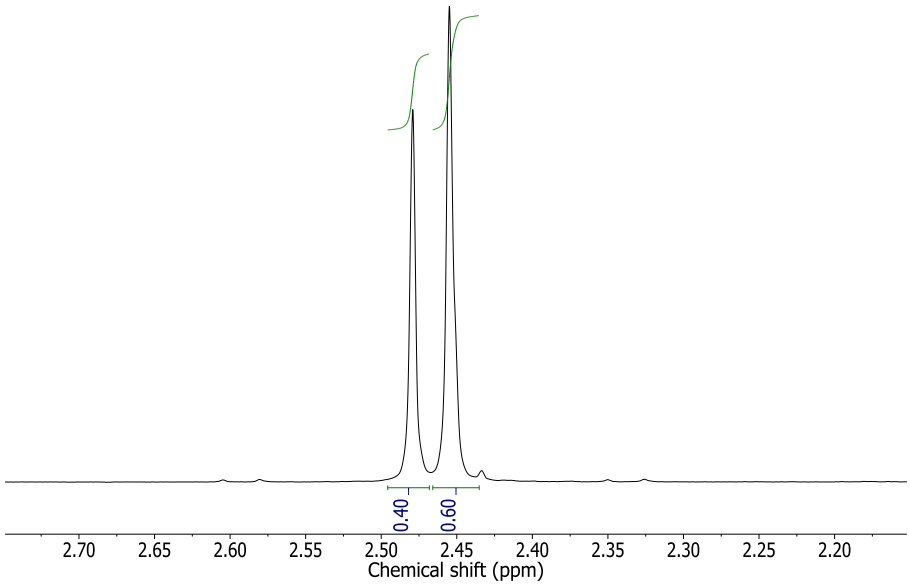

Figure 3.5. Detail of ^{1}H NMR spectrum of Cs_2CO_3 test showing integration of methyl peaks. The peak at δ 2.58 corresponds to **S1** while the peak at δ 2.45 corresponds to peroxide **2.**

Synthesis of 3-Chlorobenzoic 4-Formylbenzoic Peroxyanhydride, **S2**

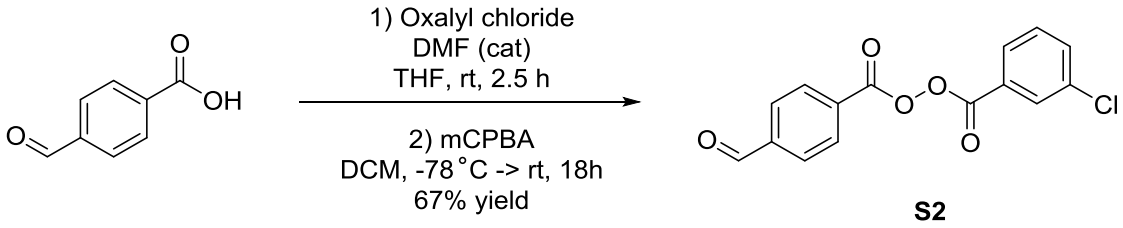

Scheme 3.8. Synthesis of a formyl-functionalized peroxide *via* an acid chloride.

A modified procedure by Linhardt was followed.[29] In a flame-dried flask, 4-formylbenzoic acid (1.00 g, 6.69 mmol) was dissolved in 50 mL of dry THF under N_2. To the solution, oxalyl chloride (0.63 mL, 7.22 mmol) was added dropwise followed by 5 drops of DMF. The mixture was stirred at room temperature for 2.5 h before solvent was removed under vacuum. The light yellow residue was dried under high vacuum overnight. The solid residue was dissolved in 30 mL DCM under N_2 and cooled in a dry ice/acetone bath. In 30 mL DCM, *m*-chloroperbenzoic acid (1.3140 g, 7.61 mmol) was dissolved. The *m*CPBA solution was then added to the acid chloride solution followed by pyridine (0.70 mL, 8.7 mmol). The mixture was stirred overnight and warmed to room temperature. The mixture was diluted to 100 mL and washed with 2 × 50 mL $NaHCO_3$, 1 × 50 mL DI water, and 1 × 50 mL brine. The organic layer was dried over $MgSO_4$. The white residue was purified by flash chromatography (SiO_2, 9:1 hexane/ethyl acetate). The first band was collected and concentrated to give 1.3602 g (4.46 mmol, 67% yield) of white solid.

EA: calcd: C 59.13, H 2.98, N 0, found: C 58.74, H 2.73, N 0.19

^{1}H-NMR ($CDCl_3$) δ 10.13 (s, 1H), 8.23 (d, 2H, *J* = 8.3 Hz), 8.07-8.00 (m, 3H), 7.96 (dt, 1H, *J* = 7.8, 1.4 Hz), 7.65 (ddd, 1H, *J* = 8.1, 2.2, 1.1 Hz), 7.48 (t, 1H, *J* = 7.9 Hz)

^{13}C-NMR ($CDCl_3$) δ 191.11, 161.94, 161.73, 140.01, 135.14, 134.53, 130.44, 130.29, 130.26, 129.78, 129.76, 127.87, 126.94

Iodometric titration: 5.2% active oxygen (5.3% theoretical)

Synthesis of 4-{[(Benzyloxy)imino]methyl}benzoic acid, **S3**

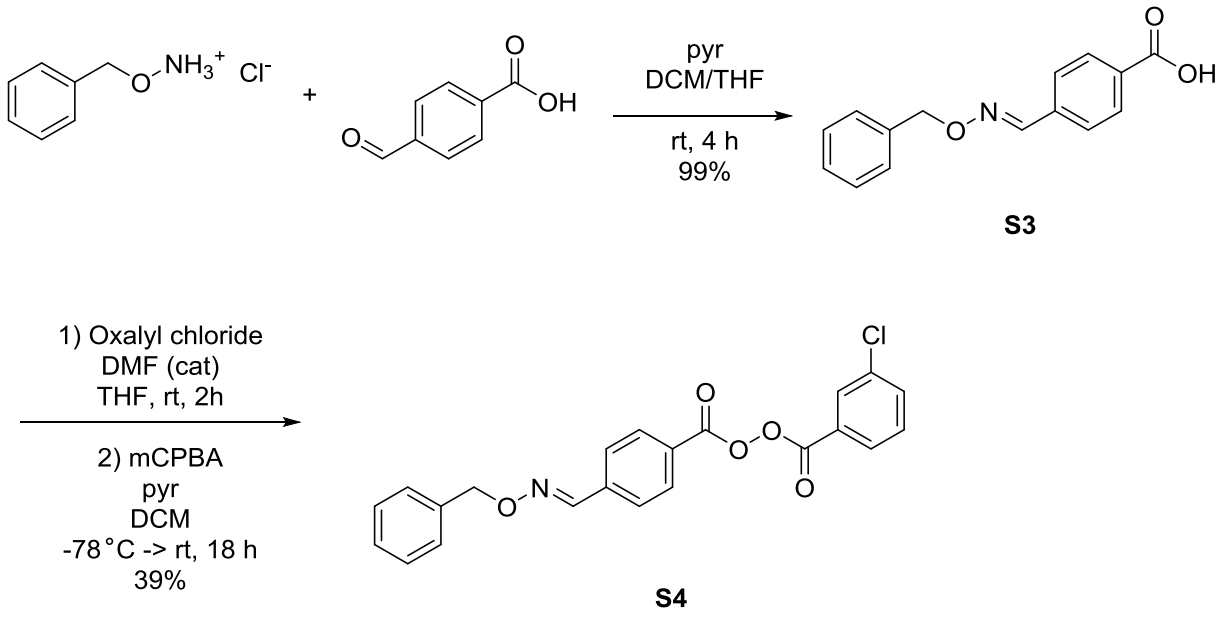

Scheme 3.9. Synthesis of an alkoxyamine-functionalized peroxide *via* an acid chloride.

A modified procedure of Dubost was followed.[30] In 5 mL DCM and 31 mL THF, 4-formylbenzoic acid (0.98 g, 6.6 mmol), *O*-benzylhydroxylamine HCl (2.0 g, 7.8 mmol), and pyridine (1.0 mL, 12 mmol) were dissolved. The mixture was stirred for 24 h. The solvent was removed under vacuum. The product was purified by silica plug (9:1 DCM/MeOH) to afford 1.65 g white solid (99% yield).

^{1}H-NMR ($CDCl_3$) δ 8.18 (s, 1H), 8.10 (d, 2H, *J* = 8.0 Hz), 7.69 (d, 2H, *J* = 8.0 Hz), 7.51-7.29 (m, 5H), 5.25 (s, 2H)

^{13}C-NMR ($CDCl_3$) δ 171.5, 147.9, 137.3, 137.1, 130.5, 130.1, 128.5, 128.1, 127.0, 122.7, 76.8

HRMS-ESI (*m/z*): calcd for $C_{15}H_{14}NO_3$ $[M+H]^+$, 256.0974; found, 256.0974

Synthesis of 4-{[(Benzyloxy)imino]methyl}benzoic 3-Chlorobenzoic Peroxyanhydride, **S4**

The modified procedure by Linhardt[23] was followed. This procedure presents an explosion hazard and was carried out behind a blast shield. In 50 mL dry THF under N_2, **S3** (0.99 g, 3.9 mmol) was dissolved. To the stirring mixture, oxalyl chloride (0.37 mL, 4.4 mmol) was added dropwise followed by 5 drops of

DMF. The mixture was stirred for 2 h. The solvent was removed by vacuum distillation. The residue was dissolved in 30 mL DCM and cooled in an acetone/dry ice bath. In another 30 mL DCM, *m*CPBA (0.67 g, 3.9 mmol) was dissolved; this solution and pyridine (0.37 mL, 4.6 mmol) were added to the first solution under N_2. The mixture was stirred overnight and warmed to room temperature. The reaction mixture was diluted to 200 mL and washed with 2 × 100 mL 2% K_2CO_3, 100 mL DI water, and 100 mL brine. The product was purified by flash chromatography (9:1 hexane/ethyl acetate) and collected as the first band to afford 0.62 g white crystalline solid (39% yield).

EA: calcd: C 64.48, H 3.94, N 3.42, found: C 64.22, H 3.93, N 3.26

^{1}H-NMR ($CDCl_3$) δ 8.17 (s, 1H), 8.09-8.03 (m, 3H), 7.99-7.93 (m, 1H), 7.72 (d, 2H, *J* = 8.4 Hz), 7.64 (ddd, 1H, *J* = 7.9, 2.1, 1.0 Hz), 7.53-7.30 (m, 6H), 5.26 (s, 2H)

^{13}C-NMR ($CDCl_3$) δ 162.4, 161.9, 147.6, 147.4, 137.9, 137.0, 135.1, 130.2, 130.1, 129.8, 129.7, 128.4, 127.9, 127.8, 127.3, 127.2, 126.0, 76.9

Iodometric titration: 3.9% active oxygen (3.9% theoretical)

<u>^{1}H NMR Analysis of Oxime Reaction of 3-Chlorobenzoic 4-Formylbenzoic Peroxyanhydride with Benzyloxyamine</u>

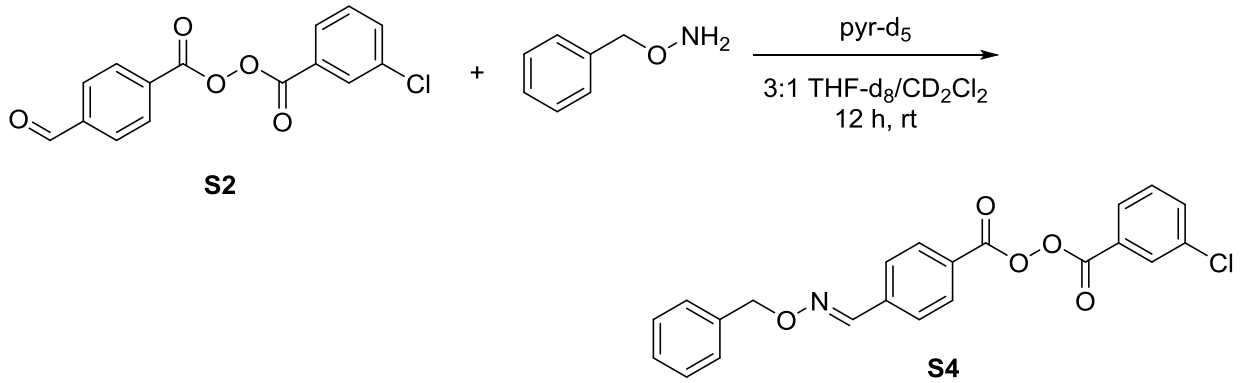

Scheme 3.10. Conjugation of a formyl-containing peroxide with an alkoxyamine *via* the oxime click reaction. The test reaction was monitored by ^{1}H NMR spectroscopy.

In a standard NMR tube, **S2** (14.6 mg, 47.8 µmol), benzyloxyamine (7.58 mg, 61.6 µmol), and pyridine-d_5 (0.02 mL, 0.2 mmol) were dissolved in 0.45 mL THF-d_8 and 0.16 mL CD_2Cl_2. ^{1}H NMR spectra were collected after 15 h. The aldehyde was mostly consumed. Several peaks were observed between δ 3.20-5.60 which did not correspond to a reagent or the desired product.

Synthesis of 4-Methylperbenzoic Acid, **S2**

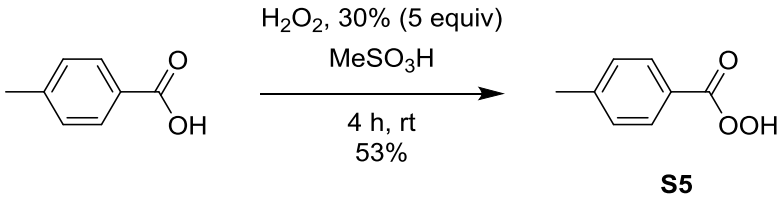

S5

Scheme 3.11. Acid-catalyzed synthesis of peracid.

A modified procedure by Swern was followed.[31] This procedure presents an explosion hazard and was carried out behind a blast shield. In 15 mL of methanesulfonic acid, *p*-toluic acid (1.01 g, 7.39 mmol) was dissolved. The mixture was immersed in a room-temperature water bath; and 30% hydrogen peroxide (4.1 mL, 37 mmol) was added dropwise. After 4 h of stirring, crushed ice was slowly added to the reaction mixture. The white precipitate was isolated by vacuum filtration, dissolved in 100 mL DCM and washed with 3 × 50 mL phosphate buffer, pH 7.5. The organic layer was dried over $MgSO_4$, and the solvent was removed *in vacuo* to yield 0.59 g of white solid (3.9 mmol, 53% yield).

EA: calcd: C 63.15, H 5.30, N 0, found: C 62.68, H 4.98, N 0.20

^{1}H-NMR ($CDCl_3$) δ 11.63 (s, 1H), 7.89 (d, 2H, *J* = 8.2 Hz), 7.30 (d, 2H, *J* = 7.9 Hz), 2.44 (s, 3H)

^{13}C-NMR ($CDCl_3$) δ 168.2, 145.5, 129.6, 129.3, 122.2, 21.8

Iodometric titration: 10.4% active oxygen (10.5% theoretical)

Synthesis of 4-Methylbenzoic Peroxyanhydride, **1**

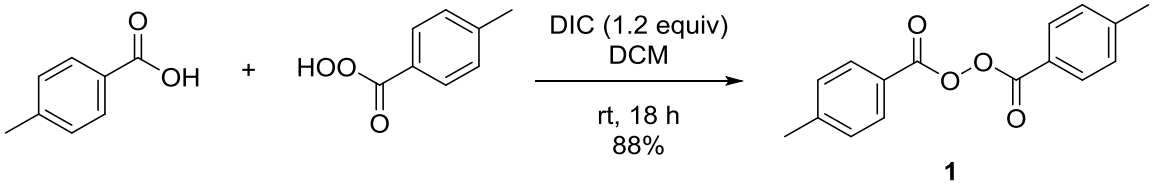

Scheme 3.12. Synthesis of an electron-rich symmetrical peroxide *via* carbodiimide coupling.

A modified procedure by Linhardt was followed.[23] This procedure presents an explosion hazard and was carried out behind a blast shield. In 30 mL DCM, *p*-toluic acid (0.48 g, 3.5 mmol) and **S5** (0.52 g, 3.4 mmol) were dissolved. The stirring solution was placed in a room temperature water bath, and diisopropylcarbodiimide (0.64 mL, 4.1 mmol) was added dropwise. The reaction mixture was stirred overnight. The reaction mixture was then diluted to 100 mL and washed with 3 × 50 mL phosphate buffer, pH 7.5. The organic layer was dried over $MgSO_4$. Solvent was removed *in vacuo*, and the solid was purified by flash chromatography (SiO_2, 9:1 hexane/ethyl acetate). The first band was collected. Removal of solvent *in vacuo* yielded 0.80 g white solid (3.0 mmol, 88% yield).

EA: calcd: C 71.10, H 5.22, N 0, found: C 70.92, H 5.27, N 0.28

^{1}H-NMR ($CDCl_3$) δ 7.97 (d, 2H, *J* = 8.3 Hz), 7.31 (d, 2H, *J* = 7.9 Hz), 2.44 (s, 3H)

^{13}C-NMR ($CDCl_3$) δ 163.1, 145.2, 129.7, 129.5, 122.7, 21.8

Iodometric titration: 5.52% active oxygen (5.92% theoretical)

Synthesis of 3-Chlorobenzoic 4-Methylbenzoic Peroxyanhydride, **2**

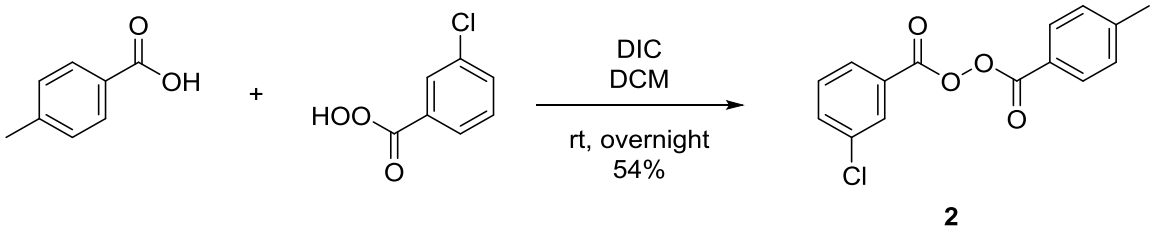

Scheme 3.13. Synthesis of an unsymmetrical peroxide with an electron-withdrawing group and an electron-donating group *via* carbodiimide coupling.

A modified procedure by Linhardt was followed.[32] This procedure presents an explosion hazard and was carried out behind a blast shield. In 30 mL DCM, *p*-toluic acid (0.47 g, 3.4 mmol) and washed *m*CPBA (0.71 g, 4.2 mmol) were dissolved. The stirring solution was placed in a room temperature water bath, and diisopropylcarbodiimide (0.65 mL, 4.1 mmol) was added dropwise. The reaction mixture was stirred overnight. The reaction mixture was then diluted to 100 mL and washed with 3 × 50 mL 2% K_2CO_3. The organic layer was dried over $MgSO_4$. Remaining diisopropylurea was removed by a celite plug (95:5 hexane/ethyl acetate). Recrystallization in hexane/$CHCl_3$ yielded white crystals (0.39 g, 3.2 mmol, 54% yield).

EA: calcd: C 61.98, H 3.81, N 0, found: C 61.26, H 3.61, N 0.31

^{1}H-NMR ($CDCl_3$) δ 8.06 (t, 1H, *J* = 1.9 Hz), 7.97-7.95 (m, 3H), 7.64 (m, 1H), 7.47 (t, 1H, *J* = 7.9 Hz), 7.32 (d, 2H, *J* = 7.9 Hz), 2.45 (s, 3H)

^{13}C-NMR ($CDCl_3$) δ 162.9, 162.0, 145.4, 135.0, 134.3, 130.2, 129.8, 129.7, 129.6, 127.8, 127.3, 122.4, 21.8

Iodometric titration: 5.63% active oxygen (5.50% theoretical)

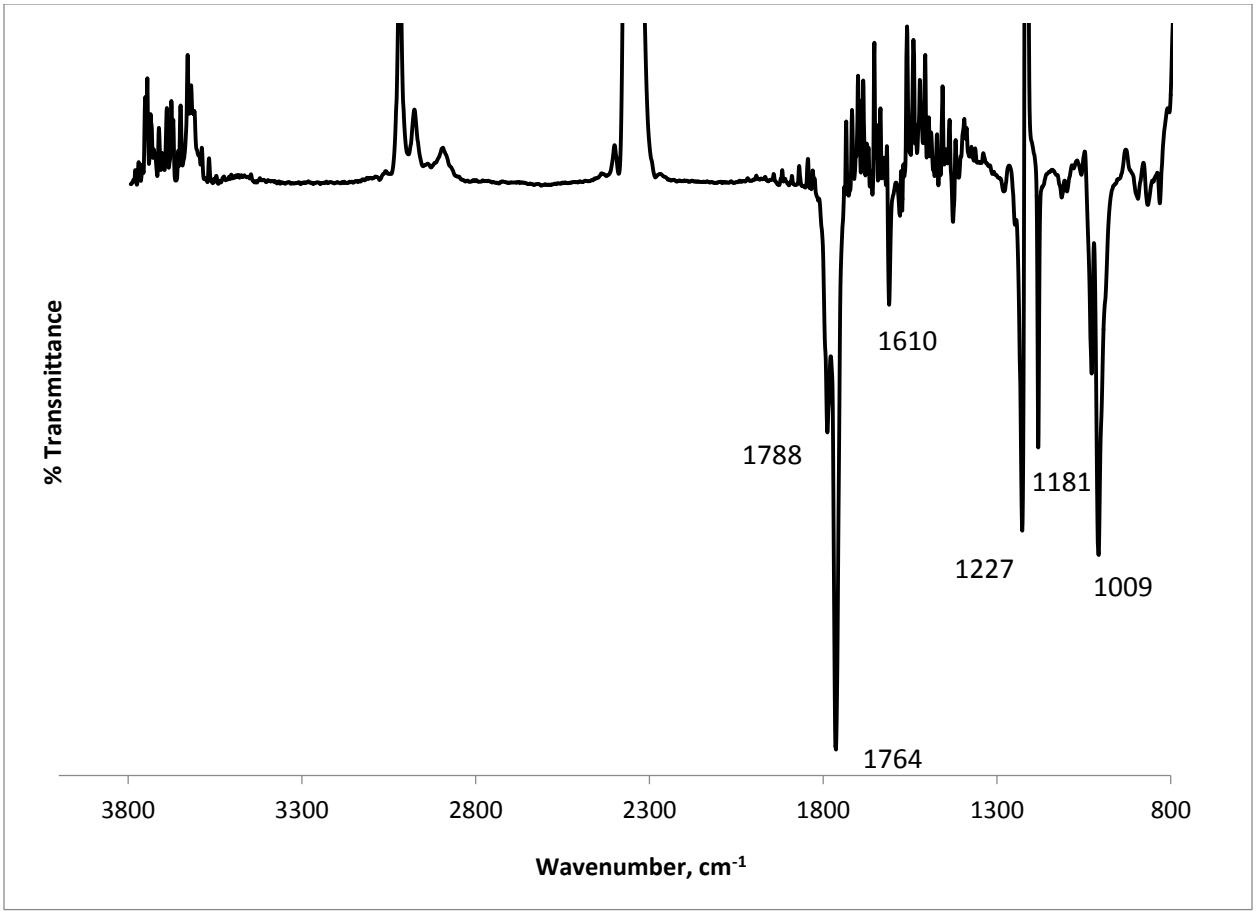

Figure 3.6. Transmission FTIR spectrum of peroxide **2** in $CHCl_3$.

Synthesis of 4-(Trifluormethyl)benzoic 4-Methylbenzoic Peroxyanhydride, **3**

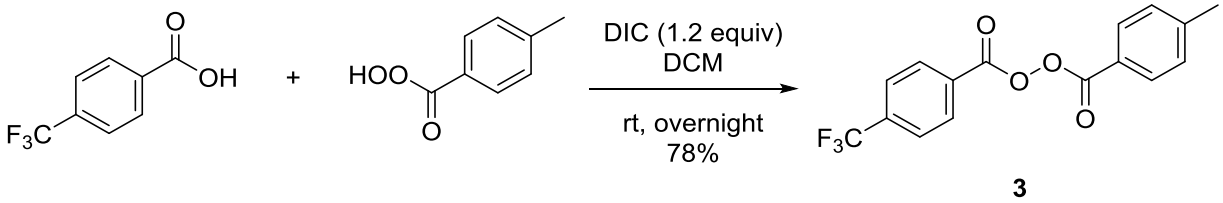

3

Scheme 3.14. Synthesis of an unsymmetrical peroxide with an electron-withdrawing group and an electron-donating group *via* carbodiimide coupling.

A modified procedure by Linhardt was followed.[32] This procedure presents an explosion hazard and was carried out behind a blast shield. In 30 mL DCM, 4-(trifluoromethyl)benzoic acid (0.40 g, 2.1 mmol) and **S5** (0.21 g, 1.4 mmol) were dissolved. Stirring solution was placed in a room temperature water bath, and diisopropylcarbodiimide (0.32 mL, 2.1 mmol) was added dropwise. The reaction mixture was stirred overnight. The reaction mixture was then diluted to 100 mL and washed with 3 × 50 mL phosphate

buffer, pH 7.5. The organic layer was dried over $MgSO_4$. Solvent was removed *in vacuo*, and the solid was purified by flash chromatography (SiO_2, 9:1 hexane/ethyl acetate). The first band was collect. Removal of solvent *in vacuo* yielded 0.35 g white solid (1.1 mmol, 78% yield).

EA: calcd: C 59.27, H 3.42, N 0, found: C 59.41, H 3.43, N 0.23

^{1}H-NMR ($CDCl_3$) δ 8.20 (d, 2H, J = 8.1 Hz), 7.96 (d, 2H, J = 8.2 Hz), 7.79 (d, 2H, J = 8.2 Hz), 7.32 (d, 2H, J = 8.0 Hz), 2.45 (s, 3H)

^{13}C-NMR ($CDCl_3$) δ 162.9, 162.0, 145.5, 130.2, 129.8, 129.8, 129.6, 129.1, 125.8 (q, $J_{C\text{-}F}$ = 3.7 Hz), 124.4, 122.3, 21.81

Iodometric titration: 4.75% active oxygen (4.93% theoretical)

Synthesis of N-[4-(Dimethylamino)phenyl]-4-methylbenzamide, **4**

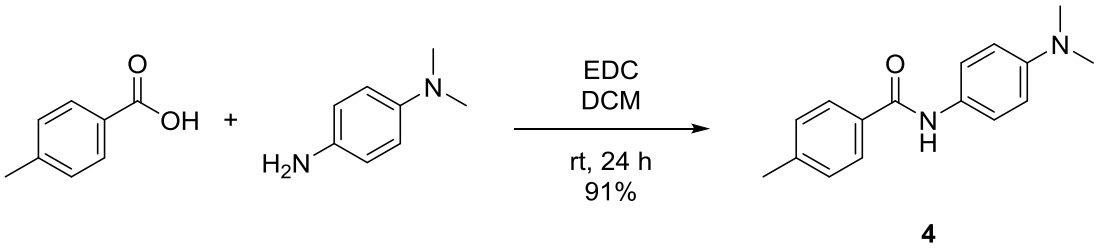

Scheme 3.15. Conjugation of electron-rich *N,N*-dimethylaniline derivative to a benzoic acid group *via* carbodiimide coupling.

A modified procedure by Zinzalla was followed.[33] In 20 mL DCM, *p*-toluic acid (0.53 g, 3.9 mmol), *p*-amino-*N*,*N*-dimethylaniline (0.65 g, 4.8 mmol), and *N*-(3-dimethylaminopropyl)-*N*′-ethylcarbodiimide hydrochloride (0.91 g, 4.8 mmol) were dissolved. The reaction mixture was stirred for 24 h. The reaction mixture was then diluted to 100 mL and washed with 3 × 50 mL phosphate buffer, pH 7.5. The organic layer was dried over $MgSO_4$. The solvent was removed *in vacuo* to yield 0.91 g of dark purple solid (3.6 mmol, 91% yield).

EA: calcd: C 75.56, H 7.13, N 11.01, found: C 75.48, H 7.21, N 11.06

^{1}H-NMR (CD_2Cl_2) δ 7.95 (br, 1H), 7.75 (d, 2H, *J* = 8.2 Hz), 7.46 (d, 2H, *J* = 9.0 Hz), 7.26 (d, 2H, *J* = 7.8 Hz), 6.72 (d, 2H, *J* = 9.0 Hz), 2.93 (s, 6H), 2.41 (s, 3H)

^{13}C-NMR (CD_2Cl_2) δ 165.6, 148.5, 142.3, 132.8, 129.5, 128.2, 127.3, 122.5, 113.0, 40.9, 21.5

HRMS-ESI (*m/z*): calcd for $C_{16}H_{19}N_2O$ $[M+H]^+$, 255.1497; found, 255.1498

Synthesis of 4-(Dimethylamino)benzyl 4-Methylbenzoate, **5**

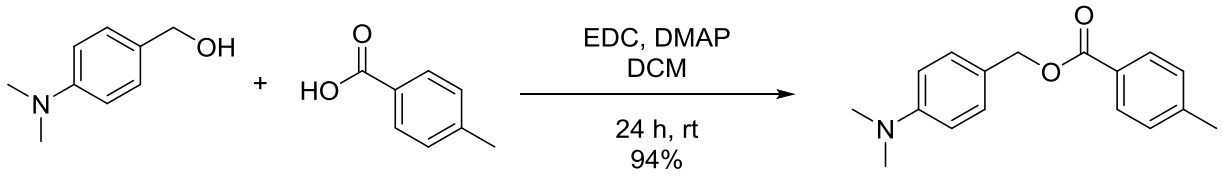

5

Scheme 3.16. Conjugation of an alcohol-functionalized *N*,*N*-dimethylaniline derivative to a benzoic acid group *via* carbodiimide coupling.

In 30 mL DCM, *p*-toluic acid (0.77 g, 5.6 mmol), 4-(dimethylamino)benzyl alcohol (0.51 g, 3.4 mmol), *N*-(3-dimethylaminopropyl)-*N*′-ethylcarbodiimide hydrochloride (1.08 g, 5.62 mmol), and 4-dimethylaminopyridine (0.53 g, 4.3 mmol) were dissolved. The reaction mixture was stirred for 24 h. The reaction mixture was then diluted to 100 mL and washed with 5 × 50 mL phosphate buffer, pH 7.5. The organic layer was dried over $MgSO_4$. Remaining *p*-toluic acid was removed by a celite plug (1:1 DCM/Et_3N). The product obtained was an off-white solid (0.85 g, 3.2 mmol, 94% yield). For analytical analysis, the product was further purified by flash chromatography (neutral Al_2O_3, 9:1 hexane/ethyl acetate) to give a white solid.

EA: calcd: C 75.81, H 7.11, N 5.20, found: C 75.33, H 7.19, N 5.32

^{1}H-NMR ($CDCl_3$) δ 7.96 (d, 2H, *J* = 8.2 Hz), 7.36 (d, 2H, *J* = 8.7 Hz), 7.22 (d, 2H, *J* = 8.2 Hz), 6.74 (d, 2H, *J* = 8.7 Hz), 5.27 (s, 2H), 2.97 (s, 6H), 2.40 (s, 3H)

^{13}C-NMR ($CDCl_3$) δ 166.7, 150.5, 143.3, 130.0, 129.6, 128.9, 127.7, 123.6, 112.2, 66.8, 40.5, 21.6

HRMS-ESI (*m/z*): calcd for $C_{17}H_{20}NO_2$ $[M+H]^+$, 270.1494; found, 270.1495

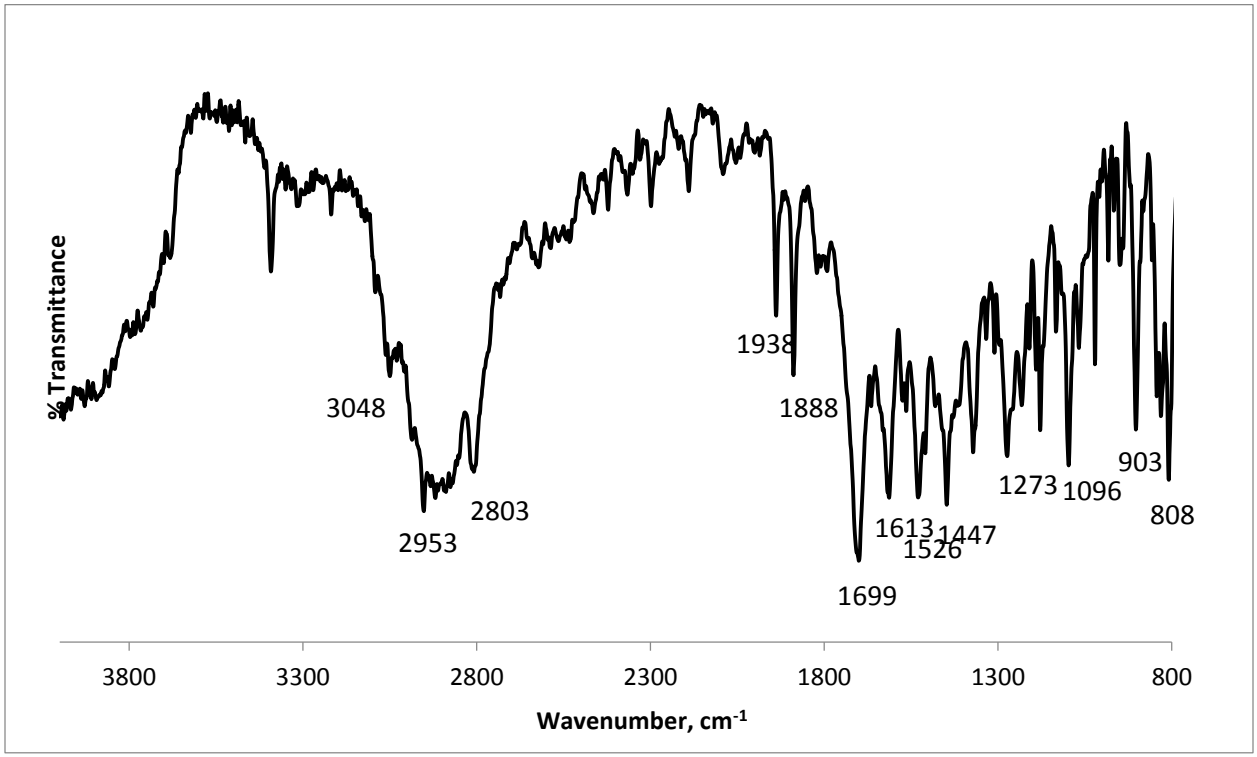

Figure 3.7. DRIFT spectrum of DMA **5**.

Coupling reaction of Carboxypolystyrene and Peracid

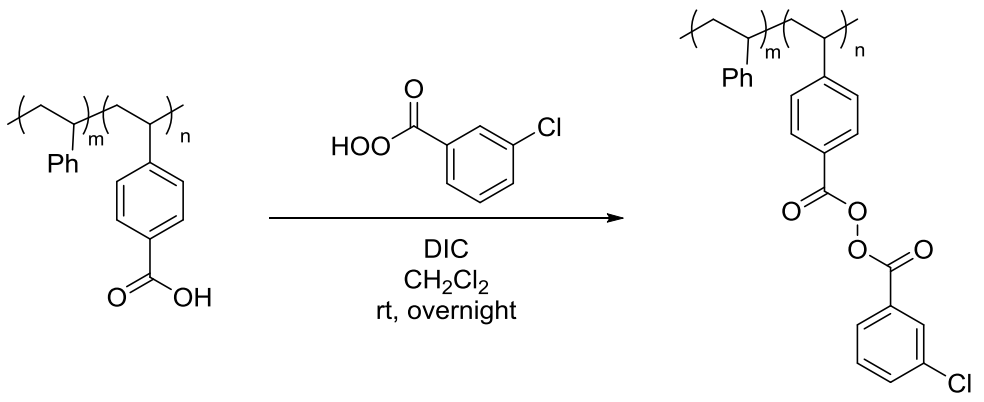

Scheme 3.17. Conjugation of a peroxide to a benzoic acid-functionalized resin *via* carbodiimide coupling.

In 15 mL DCM, *m*CPBA (0.75 g, 4.4 mmol) was dissolved in 15 mL DCM. The solution was added to carboxypolystyrene resin (0.50 g, 0.80-1.1 mmol benzoic acid). To the stirring mixture, diisopropylcarbodiimide (0.75 mL, 4.8 mmol) was added. The mixture was stirred at room temperature overnight. The next morning, 25 mL THF was added to the mixture. The mixture was centrifuged, and the supernatant was removed by decantation. The particles were subsequently washed with 5 × 30 mL THF/EtOH. The particles were dried under vacuum.

Iodometric titration: 0.755% active oxygen (2.1-2.6% theoretical)

Control Reaction for Coupling of Carboxypolystyrene and Peracid

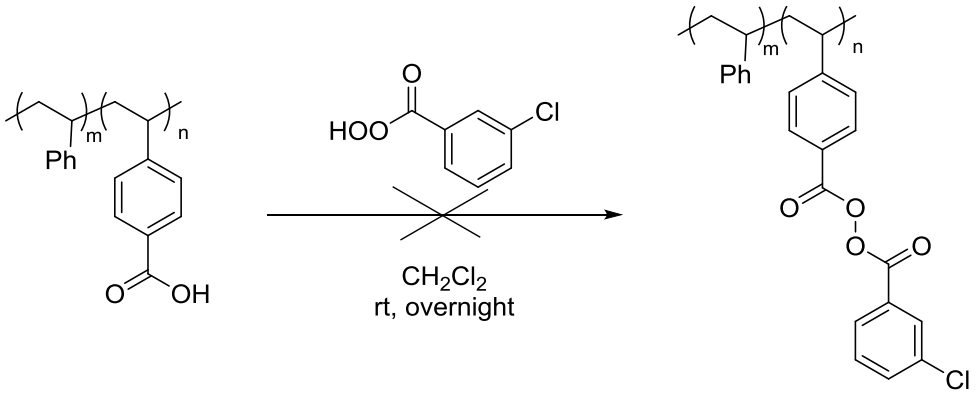

Scheme 3.18. Control for the conjugation of a peroxide to a benzoic acid-functionalized resin *via* carbodiimide coupling.

Procedure for the coupling reaction above was followed with the exception of the addition of carbodiimide. In 15 mL DCM, *m*CPBA (0.75 g, 4.4 mmol) was dissolved in 15 mL DCM. The solution was added to carboxypolystyrene resin (0.50 g, 0.80-1.1 mmol benzoic acid). The mixture was stirred at room temperature overnight. The next morning, 25 mL THF was added to the mixture. The mixture was centrifuged, and the supernatant was removed by decantation. The particles were subsequently washed with 5 × 30 mL THF/EtOH. The particles were dried under vacuum.

Iodometric titration: 0.195% active oxygen

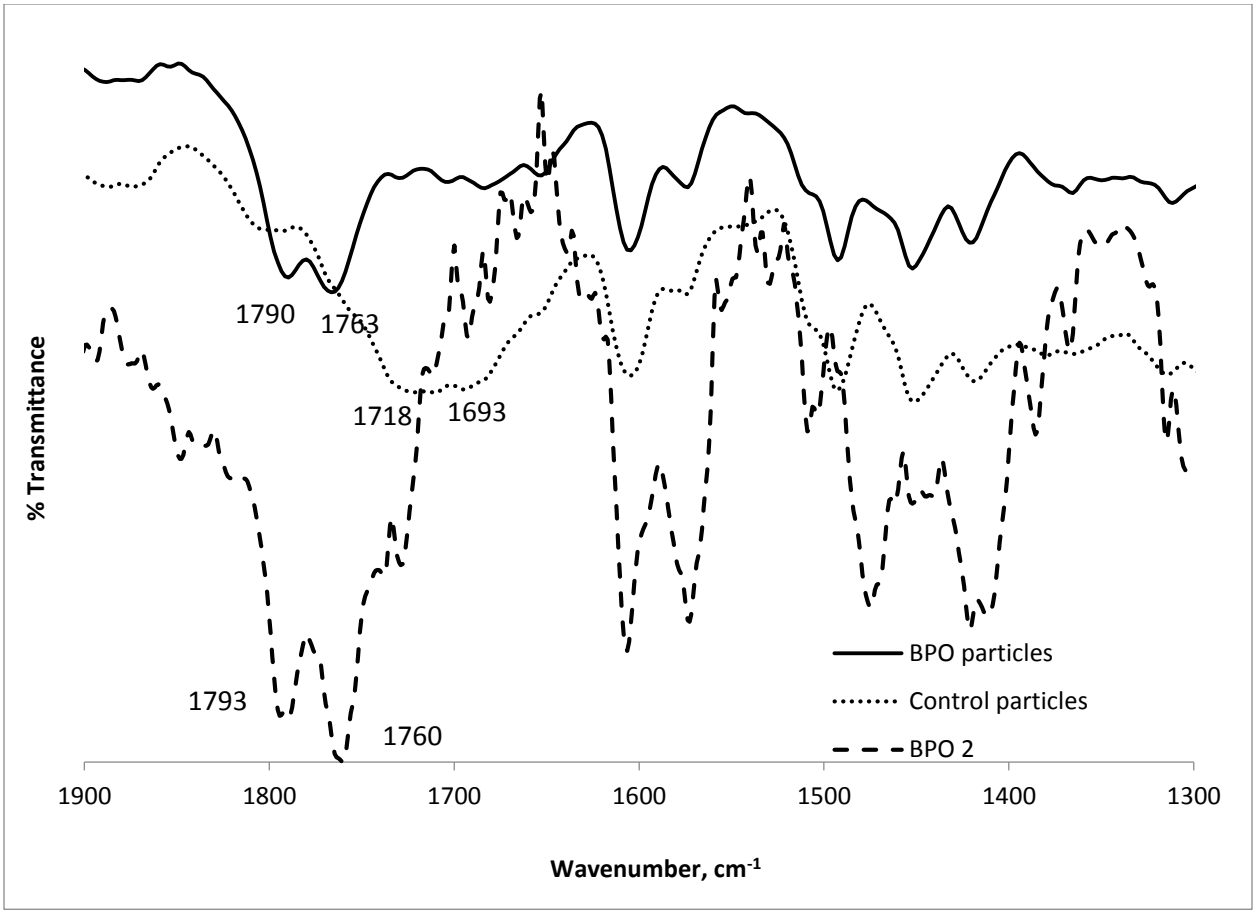

Figure 3.8. DRIFT spectrum of BPO **2**, peroxide-functionalized particles, and control particles.

Coupling Reaction of Carboxypolystyrene and 4-Dimethylaminobenzyl Alcohol

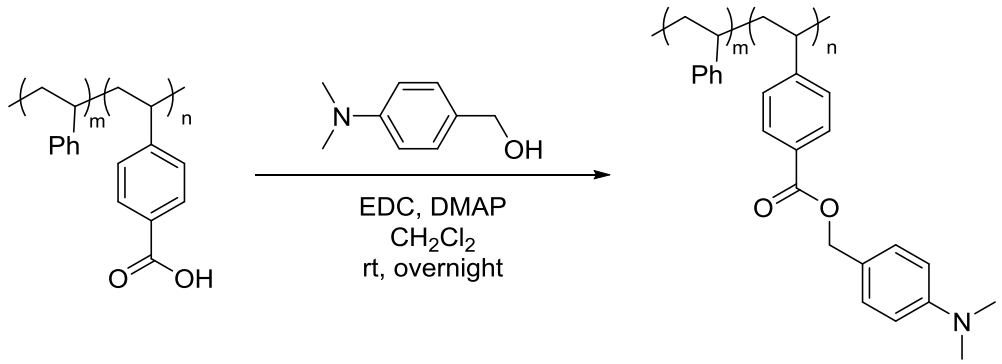

Scheme 3.19. Conjugation of a dimethylaniline derivative to a benzoic acid-functionalized resin *via* carbodiimide coupling.

In 15 mL DCM, 4-(dimethylamino)benzyl alcohol (0.62 g, 4.1 mmol) and 4-(dimethylamino)pyridine (0.50 g, 4.1 mmol) were dissolved in 15 mL DCM. The solution was added to carboxypolystyrene resin (0.50 g, 0.80-1.1 mmol benzoic acid). To the stirring mixture, *N*-(3-dimethylaminopropyl)-*N'*-ethylcarbodiimide hydrochloride (0.78 g, 4.1 mmol) was added. The mixture was stirred at room temperature overnight. The next morning, 25 mL THF was added to the mixture. The mixture was centrifuged, and the supernatant was removed by decantation. The particles were subsequently washed with 5 × 30 mL THF/EtOH. The particles were dried under vacuum.

Control Reaction for Coupling of Carboxypolystyrene and 4-Dimethylaminobenzyl Alcohol

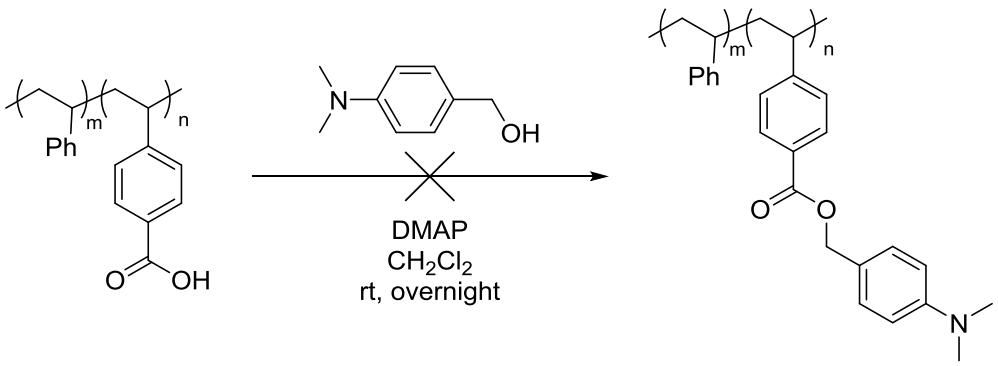

Scheme 3.20. Control for the conjugation of a dimethylaniline derivative to a benzoic acid-functionalized resin *via* carbodiimide coupling.

The procedure for the coupling reaction above was followed with the exception of the addition of carbodiimide. In 15 mL DCM, 4-(dimethylamino)benzyl alcohol (0.62 g, 4.1 mmol) and 4-(dimethylamino)pyridine (0.50 g, 4.1 mmol) were dissolved in 15 mL DCM. The solution was added to carboxypolystyrene resin (0.50 g, 0.80-1.1 mmol benzoic acid). The mixture was stirred at room temperature overnight. The next morning, 25 mL THF was added to the mixture. The mixture was centrifuged, and the supernatant was removed by decantation. The particles were subsequently washed with 5 × 30 mL THF/EtOH. The particles were dried under vacuum.

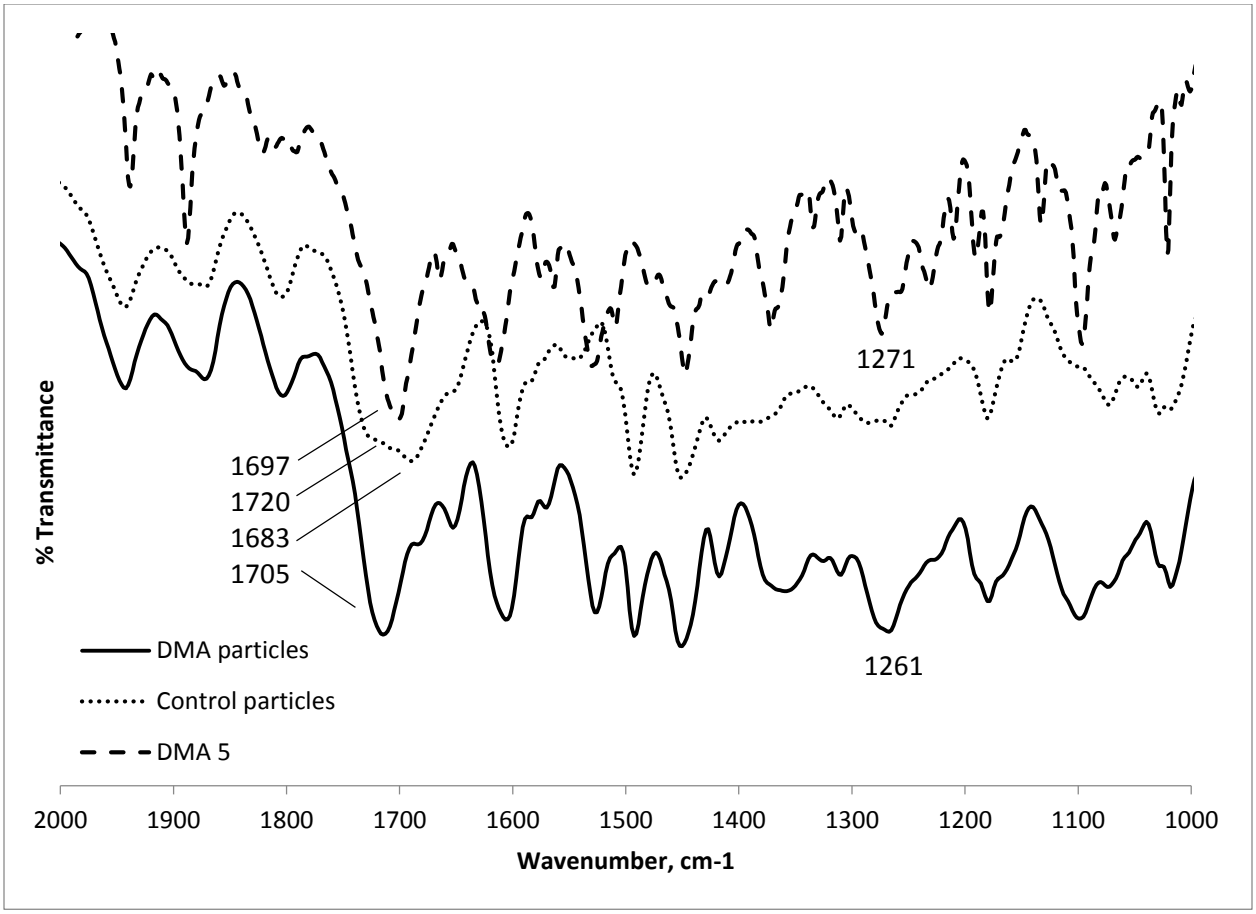

Figure 3.9. DRIFT spectrum of DMA **5**, aniline-functionalized particles, and control particles.

Tests of Functionalized Resins as Co-initiators with Small Molecule Complements

Tests were conducted in 2-mL vials under N_2. Resin (25 mg) was transferred to each vial followed by the addition of methyl acrylate, a 0.21 M solution of **2** in methyl acrylate, or 0.20 M solution of **5** in methyl acrylate. The results are recorded in Table 3.1.

3.6 References

(1) Ferscht, A., *Structure and Mechanism in Protein Science: A Guide to Enzyme Catalysis and Protein Folding*. W. H. Freeman and Company: New York, 1999.

(2) Van den Beuken, E. K.; Feringa, B. L., *Tetrahedron* **1998,** *54*, 12985-13022.

(3) Hegedus, L. S. *J. Am. Chem. Soc.* **2009,** *131*, 17995-17997.

(4) Sato, J.; Saito, N.; Nishiyama, H.; Inoue, Y. *J. Phys. Chem. B* **2001,** *105*, 6061-6063.

(5) Sato, J.; Saito, N.; Nishiyama, H.; Inoue, Y. *J. Phys. Chem. B* **2003,** *107*, 7965-7969.

(6) Nam, K. T.; Kim, D.-W.; Yoo, P. J.; Chiang, C.-Y.; Meethong, N.; Hammond, P. T.; Chiang, Y.-M.; Belcher, A. M. *Science* **2006,** *312*, 885-888.

(7) Lee, Y. J.; Yi, H.; Kim, W.-J.; Kang, K.; Yun, D. S.; Strano, M. S.; Ceder, G.; Belcher, A. M. *Science* **2009,** *324*, 1051-1055.

(8) Sakamoto, J. S.; Dunn, B. *J. Electrochem. Soc.* **2002,** *149*, A26-A30.

(9) Li, L.; Du, W.; Ismagilov, R. *J. Am. Chem. Soc.* **2010,** *132*, 106-111.

(10) Whitesides, G. M. *Nature* **2006,** *442*, 368-373.

(11) Jahnisch, K.; Hessel, V.; Lowe, H.; Baerns, M., *Ang. Chem. Int. Ed.* **2004,** *43*, 406-446.

(12) Kisailus, D.; Najarian, M.; Weaver, J. C.; Morse, D. E. *Adv. Mater*. **2005,** *17*, 1234-1239.

(13) Kisailus, D.; Truong, Q.; Amemiya, Y.; Weaver, J.C.; Morse, D. E. *Proc. Natl. Acad. Sci. USA* **2006**, *103*, 5652-5657.

(14) Elly, J.; Haward, R. N.; Simpson, W. *J. Appl. Chem.* **1951**, *1*, 347-353.

(15) Dove, A. P. Pratt, R. C.; Lohmeijer, B. G. G.; Waymouth, R. M.; Hedrick, J. L. *J. Am. Chem. Soc.* **2005**, *127*, 13798-13799.

(16) Pryor, W. A.; Hendrickson Jr, W. H. *J. Am. Chem. Soc.* **1983**, *105*, 7114-7122.

(17) Pryor, W. A.; Hendrickson Jr, W. H. *Tetrahedron* **1983**, *24*, 1459-1462.

(18) Walling, C.; Indictor, N. *J. Am. Chem. Soc.* **1958**, *80*, 5814-5818.

(19) Leffler, J. E.; Barbas, J. T. *J. Am. Chem. Soc.* **1981**, *103*, 7768-7773.

(20) Theato, P. *J. Polym. Sci. Part A: Polym. Chem.* **2008**, *46*, 6677-6687.

(21) Iha, R. K.; Wooley, K. L.; Nyström, A. M.; Burke, D. J.; Kade, M. J., Hawker, C. J. *Chem. Rev.* **2009**, *109*, 5620-5686.

(22) Callau, L.; Mantecón, A.; Reina, J. A. *J. Polym. Sci., Part A.* **2002**, *40*, 2237-2244.

(23) Linhardt, R. J.; Murr, B. L.; Montgomery, E.; Osby, J.; Sherbine, J. *J. Org. Chem.* **1982**, *47*, 2242-2251.

(24) Vazquez, B.; Elvira, C.; Levenfeld, B.; *et al*. *J. Biomed. Mater. Res.* **1997**, *34*, 129-136.

(25) O'Driscoll, K. F.; Ricchezza, E. N. *Die Makromol. Chem.* **1961**, *47*, 15-18.

(26) Meltzer, T. H.; Tobolsky, A. V. *J. Am. Chem. Soc.* **1954**, *76*, 5178-5180.

(27) Wiles, C.; Watts, P.; Haswell, S. *Tetrahedron Lett.* **2006**, *47*, 5261-5264.

(28) Ma, T. S.; Gerstein, T. *Microchem. J.* **1961**, *5*, 163-174.

(29) Leonard, N. M.; Brunckova, J. *J. Org. Chem.* **2011**, *76*, 9169-9174.

(30) Dubost, E.; Fossey, C.; Cailly, T.; Rault, S.; Fabis, F. *J. Org. Chem.* **2011**, *76*, 6414-6420.

(31) Silbert, L. S.; Siegel, E.; Swern, D. *J. Org. Chem.* **1962**, *27*, 1336-1342.

(32) Linhardt, R. J.; Murr, B. L.; Montgomery, E.; Osby, J.; Sherbine, J. *J. Org. Chem.* **1982**, *47*, 2242-2251.

(33) Antonow, D.; Marrafa, T.; Dawood, T.; Haque, M. R.; Thurston, D. E.; Zinzalla, G. *Chem. Commun.* **2010**, *46*, 2289-2291.

Chapter 4: Demonstration of a Touch-and-Go Reaction: Radical Polymerization Initiated by Contact between Peroxide- and Aniline-Functionalized Microparticles

4.1 Abstract

The concept that two chemical groups must come into proximity in order to react is one of the fundamental concepts of chemistry. Herein, we demonstrated this theory on a macroscopic scale. Particle resins were functionalized with dimethylaniline and benzoyl peroxide groups. Swelling the particles in vinyl monomer enabled contact between particles with complementary functionalities which initiated a radical polymerization. This reaction and the accompanying controls demonstrated a touch-and-go reaction, one in which contact is necessary for the ensuing reaction to occur. This project illustrates the fundamental concept of the necessity of proximity of reacting groups in an intermolecular reaction.

4.2 Introduction

Touch-and-go (TAG) chemistry hypothesizes that a reaction can be controlled when two complementary, reactive surfaces come into contact. The previous chapter discusses the choice of the dimethylaniline (DMA)/benzoyl peroxide (BPO) system to test for a TAG reaction. BPO and DMA co-initiate free radical polymerizations under oxygen-depleted conditions.[1] The initiation mechanism proceeds through a benzoyloxyanilinium cation which homolytically cleaves to form active radicals, subsequently initiating polymerization.[2] Thus, the ensuing polymerization requires initial contact between

the BPO and DMA groups. We explored conjugation routes for attaching these complementary groups to a polymer bead or nanoparticle (Scheme 4.1). In particular, the carbodiimide coupling between a benzoic acid and peracid provided an efficient route to synthesizing an unsymmetrical dibenzoyl peroxide-functionalized particle that maintains the integrity of the peroxide bond. Attachment of these functional groups to commercially available carboxypolystyrene (carboxyPS) resins resulted in co-initiators that were active in the presence of small molecule complements but did not react with each other upon preliminary testing. The carboxyPS starting material would require alteration in order to demonstrate the desired TAG reaction. As discussed in the second chapter of this work, methods were developed to synthesize carboxyPS particles of sizes ranging from 50 nm to 360 μm. The carboxyPS microparticles showed varying swelling ratios based on the identity and amount of cross-linker used in the suspension polymerization. These materials and methods provide a toolkit for testing our hypothesis and optimizing TAG reactions.

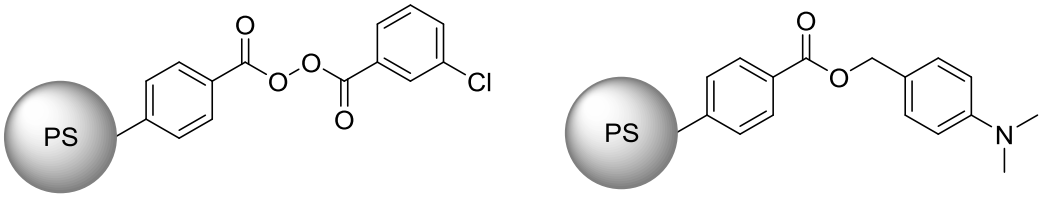

Scheme 4.1. BPO- and DMA-functionalized particles for TAG experiments.

4.3 Results and Discussion

4.3.1 TAG Test between a Functionalized Bead and a Planar Substrate

To demonstrate a TAG reaction, we investigated two interfacial systems, one involving a microparticle and planar surface and the other testing complementary microparticles. Previously, the activity of BPO- or DMA-functionalized particles had been demonstrated in the presence of their small molecule complements. The initial experimental design called for a mixed dispersion of BPO and DMA nanoparticles in monomer. Polymerization would generate free polymer that would induce aggregation of the particles via the depletion effect. However, this experiment involves a variety of unknown variables

such as the threshold particle concentration, optimal particle size, and rate of sedimentation. Initial trials of dispersed nanoparticles and swollen microparticles did not indicate polymerization of the dispersing medium. Thus, we simplified the experimental design to verify the viability of the TAG hypothesis by compressing a BPO-functionalized microparticle on a complementary DMA-functionalized surface (Figure 4.1). BPO-functionalized particles were swollen in a methyl acrylate (MA) on top of the DMA-functionalized microscope slide and then compressed under a Teflon stir blade for 2 min. Upon removal of the applied pressure and washing of the slide, pieces of particle remained on the functionalized slide (Figure 4.2). This result indicated that a reaction had occurred. When swollen, unfunctionalized carboxyPS particles were compressed on a DMA-functionalized slide, we did not observe any bonding between the particles and the slide. Likewise, when swollen BPO particles were compressed on a slide that had not been functionalized, bonding or polymerization was not observed. However, these tests were ambiguous. Attempted ATR-FTIR characterization of the slides before and after testing did not yield conclusive data.

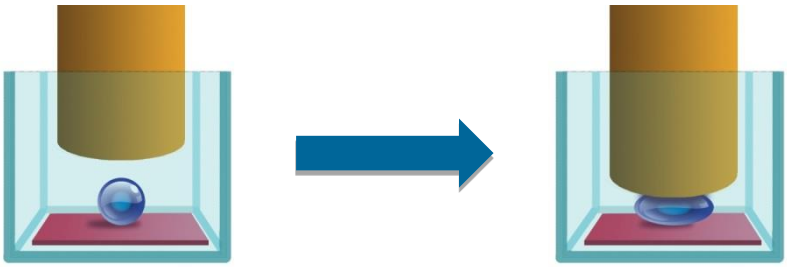

Figure 4.1. Proposed compression test of a TAG reaction. BPO particle swollen in monomer and compressed on complementary DMA surface. Surface contact between the particle and planar substrate increases upon compression.

4.3.2 TAG Test between Complementary Functionalized Beads

Another simple experimental protocol that probes a TAG reaction involves using both types of microparticles. In preparation for the experiments with a particle and complementary planar substrate, large carboxyPS particles with low degrees of cross-linking were synthesized. Initial tests to swell more highly cross-linked resins in methyl acrylate (MA) had not resulted in a reaction, and we attributed this

result to the low surface contact between the particles. In contrast, the particles synthesized with a low degree of cross-linker had displayed a higher volume swelling ratio than the highly cross-linked microparticles. We anticipated that by placing these synthesized resins in high loading within a monomer that is a good solvent for polystyrene, the particles would come into contact as they swelled and their volume increased. Thus, DMA- and BPO-functionalized particles were swollen in methyl acrylate inside a beaker. To further ensure contact between the particles, a glass stopper or inverted, weighted centrifuge tube was placed on top of the particles during swelling. This weight could be expected to compress the resins and prevent the particles from floating or drifting in the monomer medium. Figure 4.3 illustrates the experimental design involving both sets of functionalized beads. After 1 h of swelling in MA in an oxygen-depleted atmosphere, the particles were removed and washed. FTIR-ATR spectra indicated the polymerization of PMA from the particles. Some of the particles were visibly larger while others remained roughly the same size as previous to the experiment. This result stems from one of two causes. First, polymer chains initiated by the TAG reaction may propagate from the surface of one type of particle, either the DMA or the BPO beads. Second, certain particles may not come into physical contact with their complementary partners, resulting in no TAG initiation reaction and no grafted PMA chains. These two questions remained as well as the basic question of whether contact was necessary for the reaction to proceed.

To verify that the reaction was in fact initiated upon contact of or proximity between the particles, a separator was incorporated in the experiment. BPO particles were isolated within a doubled cotton cloth separator and placed inside a beaker. DMA particles were placed outside the cloth in the beaker. After 1 h of swelling in MA under a weight, the particles were washed in separate vessels. FTIR-ATR of the particles matched that of the starting materials. The particles appeared to be the same size both before and after the experiment (Figure 4.4). When the particle diameters were measured, no significant difference was observed. The particles that came into contact averaged 500 ± 200 μm in diameter while the control DMA particles averaged 400 ± 100 μm and the control BPO particles averaged 390 ± 90 μm in

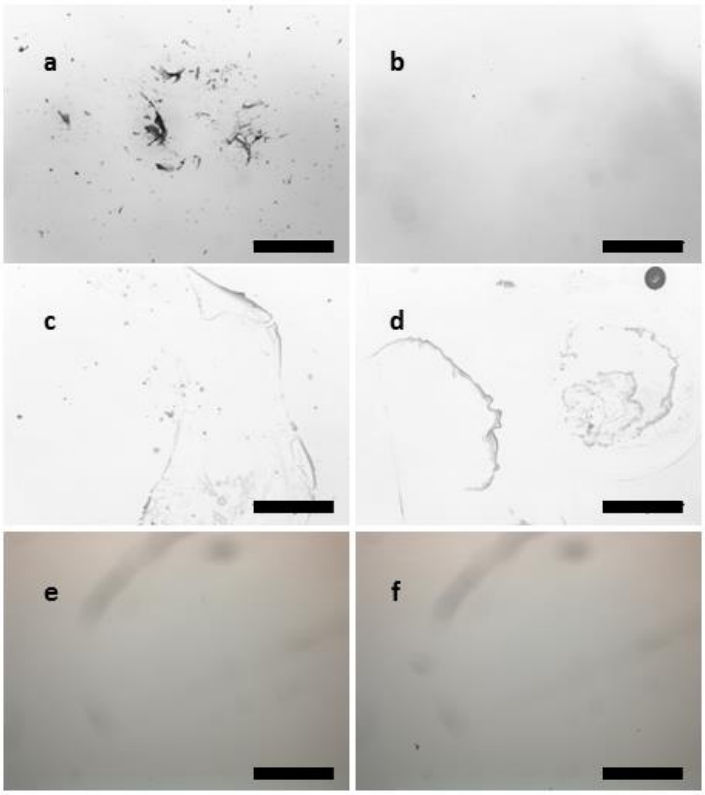

Figure 4.2. Optical images of microscope slides following compression tests. Images of DMA-functionalized slide tested with BPO resin (a) in stamped region and (b) outside stamped region. Images of a second DMA-functionalized slide tested with carboxyPS resin (c) in stamped region and (d) outside stamped region. Images of azide-functionalized slide tested with BPO resin (e) in stamped region and (f) outside stamped region. Polymer only appeared bonded to slide when (a) BPO particles were compressed on a DMA-functionalized surface. All scale bars represent 500 µm.

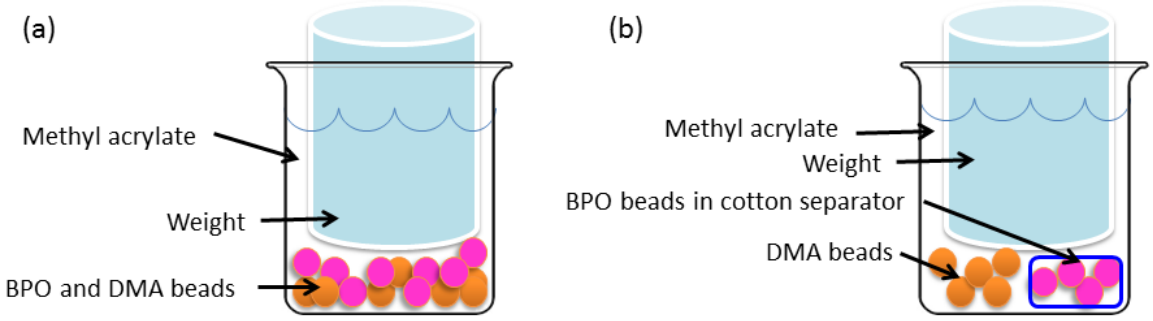

Figure 4.3. Schematic of experimental design for TAG reaction testing complementary microparticles. (a) Experimental set involving contact between BPO- and DMA-functionalized particles. (b) Control set in which BPO- and DMA-functionalized particles are physically separated by a cotton separator.

diameter. However, both the imaging and the histogram (Figure 4.5) display the particle growth for the beads that come into contact in comparison to those that are physically separated.

While the control above indicated that contact was in fact necessary for the TAG reaction to occur, a further control was needed to verify that the cotton square and string were not inhibiting the polymerization. Inside a beaker, a doubled cotton square with cotton string was placed in addition to both DMA- and BPO-functionalized particles. After 1 h of swelling in MA under a weighted centrifuge tube, the particles were washed. For this experiment, the FTIR-ATR spectrum indicated the presence of PMA following washing. Additionally, the particles were visibly larger in size for this control experiment. This control set showed that the use of cotton did not inhibit MA polymerization and succeeded to verify the result from the previous control. When the particles were in contact, a reaction proceeded as predicted. When the particles were physically separated, the TAG reaction did not occur although solvent, small molecules, and linear polymer could flow between the particles. This simple experimental design allowed us to demonstrate a preliminary system in which physical contact between two macroscale objects controls a chemical reaction.

4.3.3 Characterization of Beads and Solution Following the TAG Test

Although the two controls above verified the occurrence of a TAG reaction, they did not indicate whether PMA polymer had been incorporated into both types of particles or was free in solution. These results could elucidate the debated role of the radical cation formed from DMA; thus, additional experiments were performed. Table 4.1 lists the resins and small molecules used for each experiment. The first experiment involved the polymerization of methyl acrylate, which has a low chain transfer constant, as initiated by particle-bound BPO and the small molecule DMA. The second involved the polymerization of methyl acrylate as initiated by particle-bound DMA and small molecule BPO. The third was a control which followed the polymerization of methyl acrylate as initiated by small molecule BPO and DMA in the presence of carboxyPS. In the fourth, complementary BPO and DMA particles initiated the polymerization of MA. All four experiments displayed a significant amount of PMA incorporated in

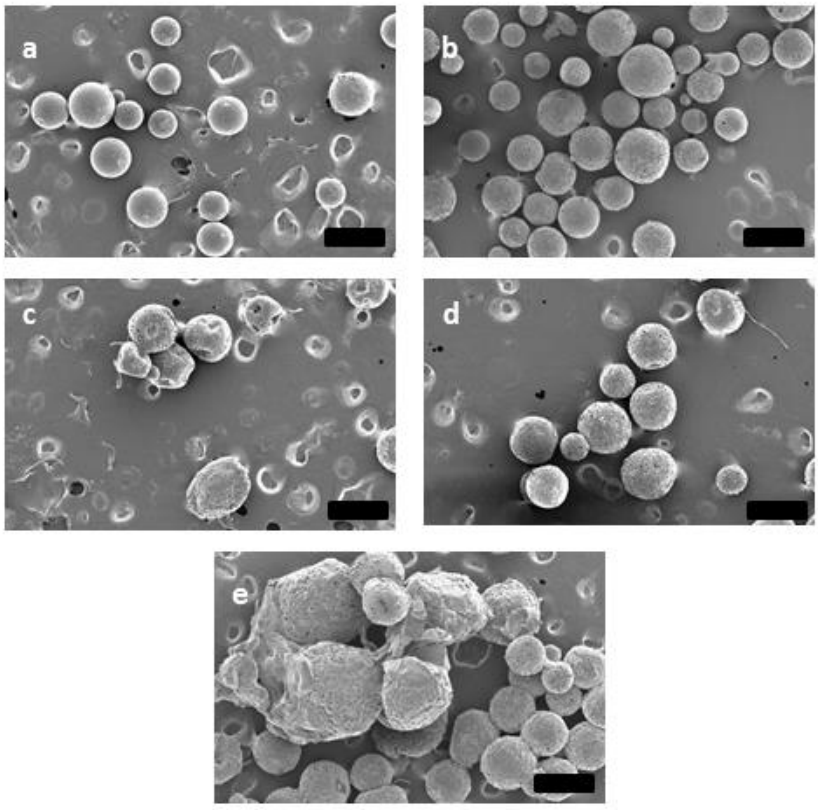

Figure 4.4. SEM images of control TAG experiments: (a) DMA particles before test, (b) BPO particles before test, (c) DMA particles after cotton membrane test, (d) BPO particles after cotton membrane test, and (e) mixture of BPO and DMA particles after contact test. Scale bar represents 500 µm.

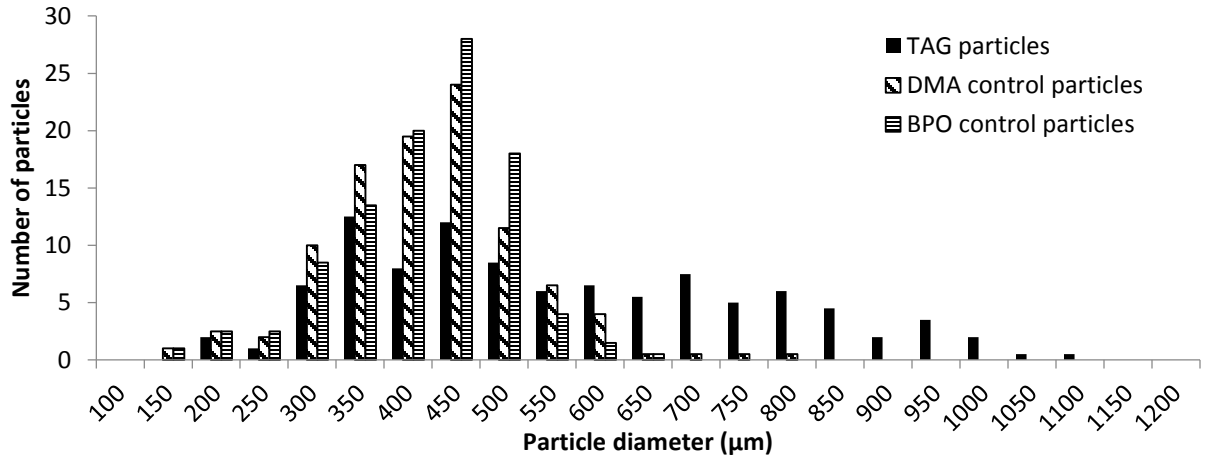

Figure 4.5. Histogram of diameters of complementary microparticles used in TAG experiments. Black bars represent complementary beads that were brought into contact. Diagonally striped bars represent control DMA beads that were physically separated from BPO beads, and horizontally striped bars represent BPO particles of the same control experiment. For each set, 100 particles were measured. Particles from the TAG experiment averaged 500 ± 200 µm in diameter while the control DMA particles and control BPO particles averaged 400 ± 100 µm and 390 ± 90 µm in diameter, respectively.

the beads. Since PMA should not have been chemically attached to the carboxyPS particles, it can be assumed that the PMA chains were entangled in or adsorbed to the beads. Thus, no conclusions can be drawn from the polymer observed on the beads. However, one significant hypothesis can be formed based on the polymerization in solution. In the first experiment, the particle-bound BPO is unsymmetric, meaning that one benzoate should be a better leaving group than the other. If the more stable anion is displaced, the 3-chlorobenzoate anion, then the benzoyloxy and phenyl radicals will be attached to the beads (Scheme 4.2). Thus, polymerization should only be significant in the solution if the anilinium radical cation is involved with initiating polymer chains. However, it is possible that the S_N2 attack is not specific for one of the peroxide oxygens. If the aniline nitrogen attacks the other oxygen (Scheme 4.3), benzoyloxy and phenyl radicals will be formed in solution. Polymer chains in solution might either be initiated by these radicals or by the anilinium radical cation. From the second experiment which involved particle-bound DMA and the small molecule BPO, one could expect radical initiation in solution based on the mechanism (Scheme 4.4). Benzoyloxy and phenyl radicals, both of which are known to initiate polymer chains, will be formed in solution. The results from the first experiment were more informative than those from the second. Likewise, one would expect polymerization to occur in solution for the third experiment. The last experiment provided the most helpful information of the four. Barring significant chain transfer, a radical should only be generated in solution if the benzoate attached to the particle is the leaving group (Scheme 4.5). Since polymerization is observed in solution and MA has a low chain transfer constant, it can be assumed that such is the case. Hence, it is likely that the S_N2 attack is not specific for one of the peroxide oxygens.

Experiment	Functionalized resin	Small molecule	PMA in solution	PMA on bead
1	BPO	DMA	yes	yes
2	DMA	BPO	yes	yes
3	Carboxy	DMA and BPO	yes	yes
4	BPO and DMA	-	yes	yes

Table 4.1. Polymerization tests of MA as initiated by beads and small molecule complements. An aliquot of the solution was removed after 1 h and characterized by ^{1}H NMR spectroscopy. Beads were washed and dried under vacuum before characterization by ATR-FTIR spectroscopy. All tests showed that PMA had been incorporated in the beads and that polymerization had occurred in solution.

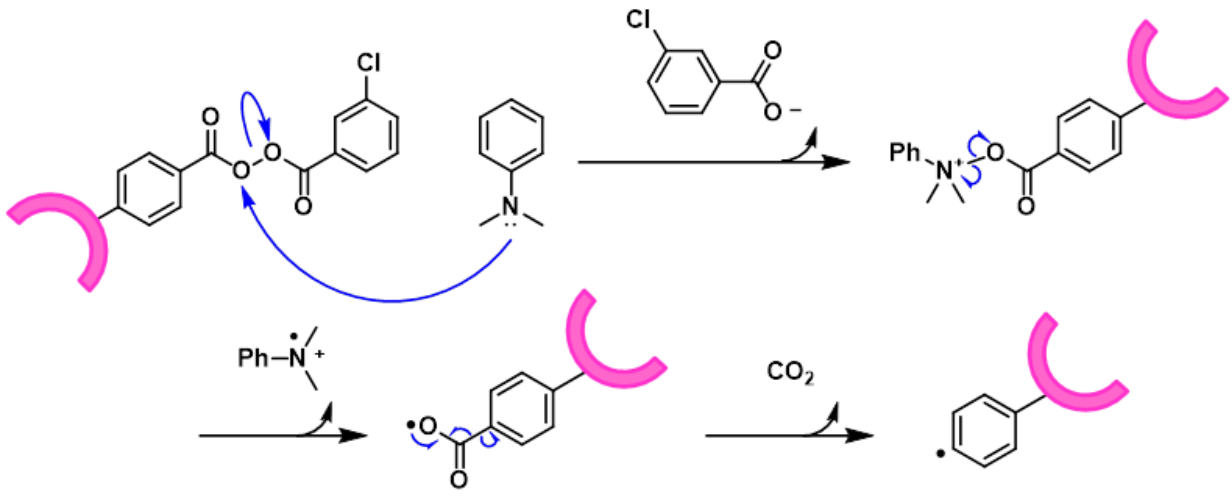

Scheme 4.2. First proposed radical initiation mechanism involving BPO particles and small molecule DMA. A radical is bound to the particle which can initiate polymer chain growth. The anilinium radical cation is free in solution and may be involved with intitiation of polymer chain growth.

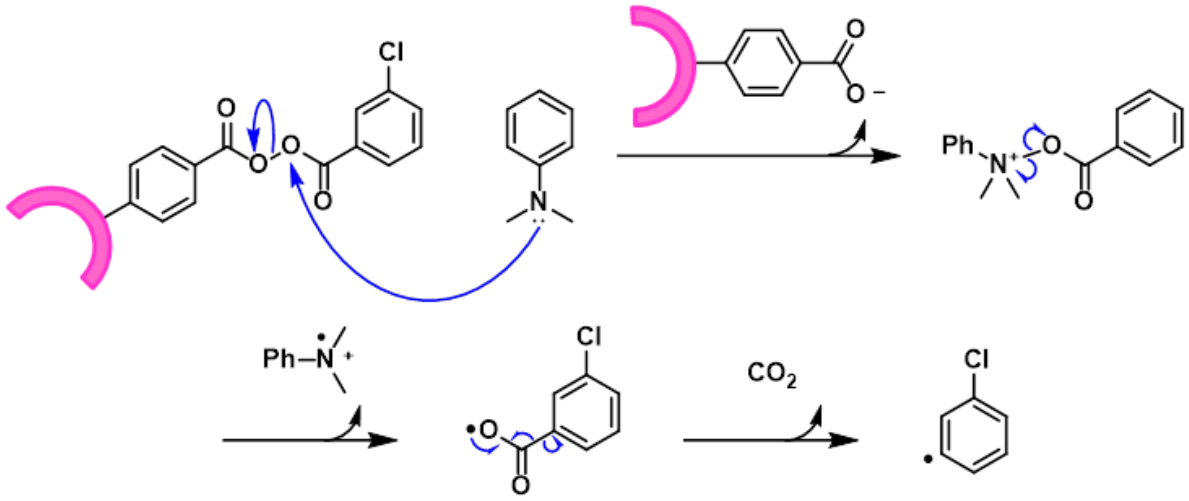

Scheme 4.3. Second proposed radical initiation mechanism involving BPO particles and small molecule DMA. This mechanism would follow in addition to the first if the attack on the peroxide is not specific for one of the oxygens. The *m*-chorophenyl radical which can initiate polymer chain growth is free in solution in addition to to the radical cation which may be involved with initiating polymer chain growth.

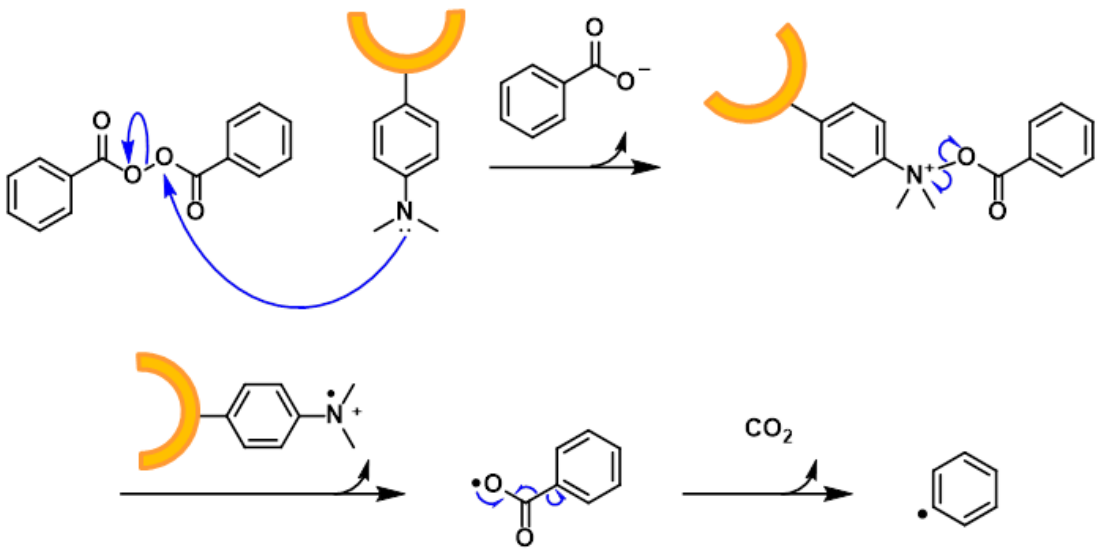

Scheme 4.4. Proposed radical initiation mechanism involving DMA particles and small molecule BPO. The phenyl radical is free in solution which is known to initiate polymer chain.

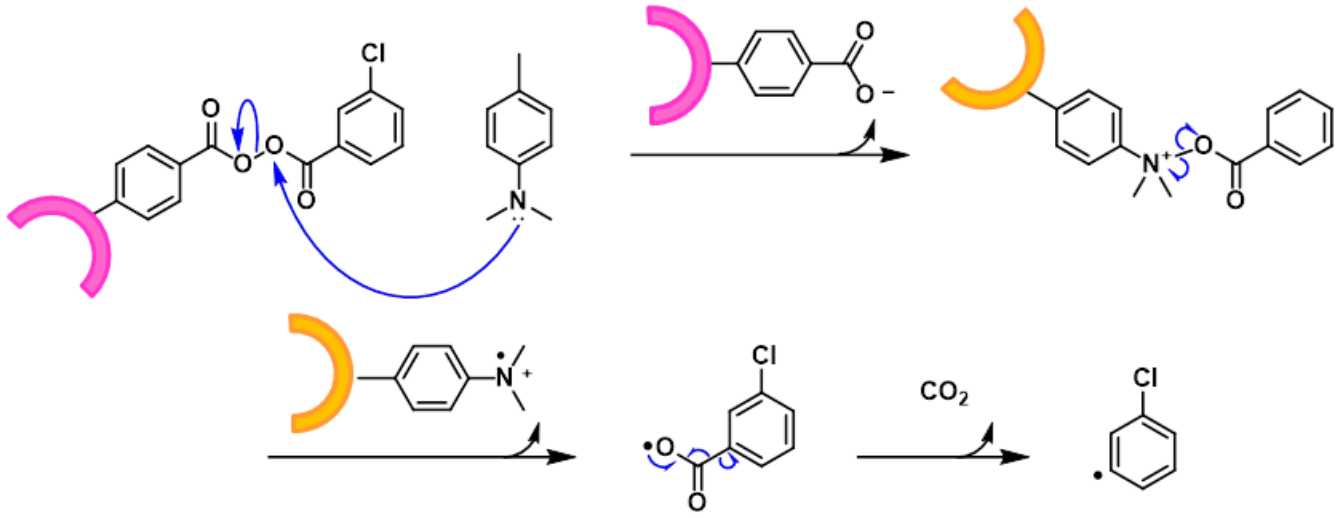

Scheme 4.5. Proposed radical initiation mechanism involving BPO particles and DMA particles. This mechanism would follow if the attack on the peroxide is not specific for one of the oxygens, thereby generating the *m*-chorophenyl radical in solution which can initiate polymer chain growth.

4.4 Conclusion

BPO- and DMA-functionalized microparticles displayed activity as co-initiators upon contact. This reaction confirmed the hypothesis of touch-and-go chemistry, that a reaction can be controlled by the proximity of two complementary macroscopic objects. Experiments are currently being conducted to

probe the mechanism of BPO/DMA initiation of radical polymerization and indicate that the nucleophilic attack of an amine on an unsymmetrical peroxide is not specific for one of the oxygens. Future experiments will seek to quantify the polymer produced as a function of interfacial contact.

4.5 Synthetic and Experimental Procedures

Materials and Reagents:

Unless otherwise stated, all starting materials were obtained from commercial suppliers and used without purification. Ethanol, 200 proof, (EtOH) and tetrahydrofuran (THF) were purchased from Fisher Scientific. 4-(Dimethylamino)benzyl alcohol was synthesized according to the literature procedure.[3] The monomer *tert*-butyl 4-vinylbenzoate was synthesized as reported previously. Inhibitor was removed from styrene, methyl acrylate, and *tert*-butyl 4-vinylbenzoate by passage through a basic alumina column. All other reagents were purchased from Sigma Aldrich. Prior to use, *m*-chloroperbenzoic acid (*m*CPBA) was washed with phosphate buffer, pH 7.5-8.5. Water was obtained from a Millipore (Billerica, MA) MilliQ water purification system. An IKA 20 digital mechanical stirrer and a Glas-Col GT Series mechanical stirrer were used for emulsion and suspension polymerizations. ^{1}H NMR spectra were recorded on a Varian Unity 500 MHz or 400 MHz spectrometer. Chemical shifts (δ) are reported in ppm from tetramethylsilane with the solvent resonance as the internal standard (deuterochloroform: 7.26 ppm, deuterated THF: 1.73 ppm). Data are reported as follows: chemical shifts, multiplicity (s = singlet, d = doublet, t = triplet, m = multiplet), and coupling constant (Hz). FTIR spectra were recorded on a Nicolet Nexus 670 spectrometer with DRIFTS and iTR attachments, and ESI-HRMS spectra were recorded on a Waters Q-TOF Ultima mass spectrometer. Scanning electron microscopy (SEM) images were acquired on a JEOL 6060LV at 10 kV. The SEM samples were prepared by drying suspensions on aluminum stubs followed by sputter coating with a Au/Pd alloy. Optical images were obtained on a Leica microscope. Contact angles were measured with a contact angle goniometer.

Synthesis of *N*,*N*-Dimethyl-4-((prop-2-yn-1-yloxy)methyl)aniline, **S1**

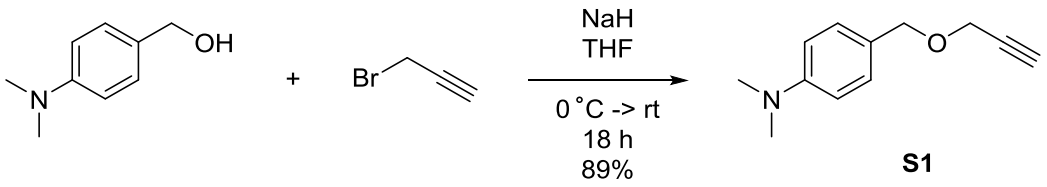

Scheme 4.6. Synthesis of an alkynyl-functionalized DMA.

At 0 ºC, 4-(dimethylamino)benzyl alcohol (0.86 g, 5.7 mmol) was dissolved in 20 mL THF. Sodium hydride (60% dispersion in mineral oil, 1.2 g, 30 mmol) was added to the solution. Propargyl bromide (80 wt% in toluene, 1.3 mL, 12 mmol) was then added dropwise to the reaction mixture. The reaction mixture was allowed to warm to room temperature after the addition. After 18 h, the reaction was quenched by slow addition of 20 mL deionized water. THF was removed under reduced pressure. The product was extracted with 3 × 50 mL DCM, and the combined organic layers were dried over $MgSO_4$. The product was separated from excess propargyl bromide *via* a short SiO_2 column (100:0 to 0:100 Hex/DCM) to yield 0.95 g of dark red oil (89% yield).

^{1}H-NMR ($CDCl_3$) δ 7.24 (d, 2H, J = 8.6 Hz), 6.71 (d, 2H, J = 8.7 Hz), 4.52 (s, 2H), 4.11 (d, 2H, J = 2.4 Hz), 2.95 (s, 6H), 2.44 (t, 1H, J = 2.4 Hz)

MS-ESI (*m/z*): calcd for $C_{12}H_{15}NO$ $[M+H]^+$, 190.1; found, 190.0

Functionalization of Microscope Slides

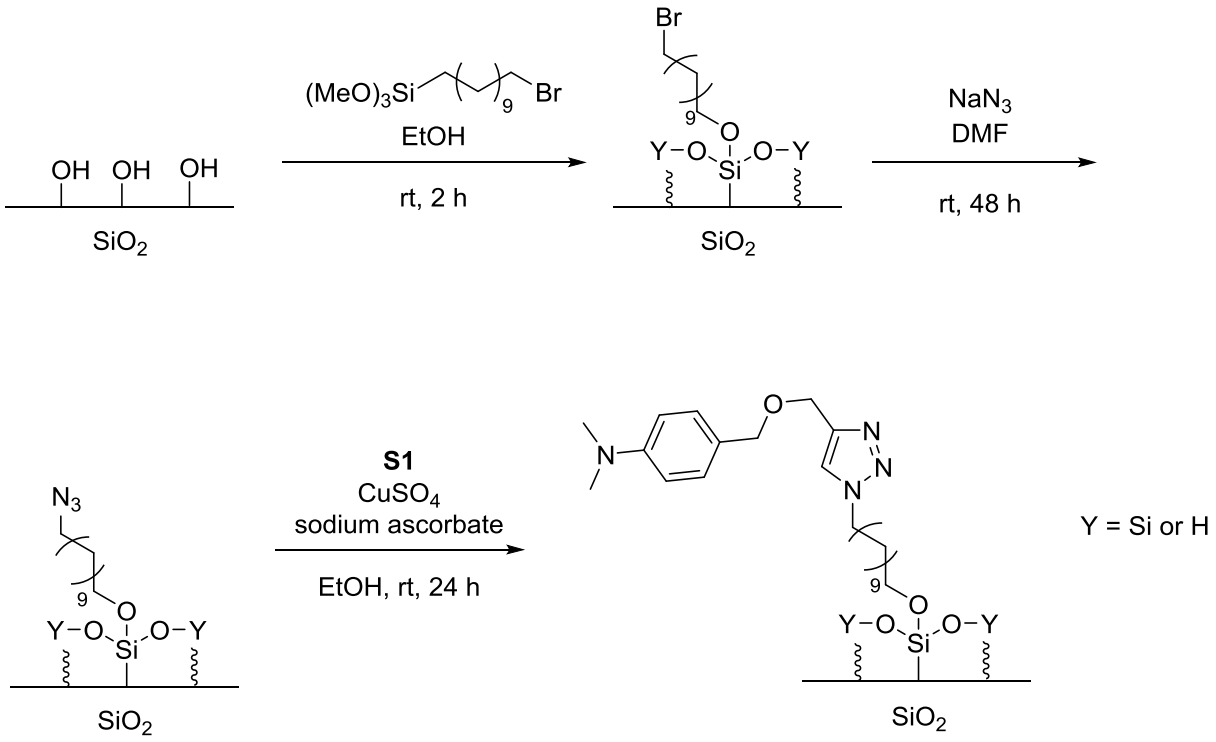

Scheme 4.7. Functionalization of microscope slides with a DMA derivative.

Procedures by Bailey, Hoffmann, Brittain, and Rudolf were modified.[4-7] Microscope slides were washed with piranha solution prior to functionalization. The average contact angle of 6 droplets of milli-Q water on the surface was 5.4 ± 1.4º. Nine slides were immersed in a solution of (11-bromoundecyl)trimethoxysilane (1.0 mL) in 200-proof EtOH (50 mL). After 2 h, slides were washed by sonicating in EtOH 5 times. The average contact angle of 6 droplets of milli-Q water on the surface was 15.7 ± 1.4º. Slides were immersed in a saturated solution of sodium azide in DMF (50 mL). After 48 h, slides were washed by sonicating in DMF five times and twice in EtOH. The contact angle was 26.1º. Slides were immersed in a solution of **S1** (0.11 g), copper sulfate pentahydrate (5.2 mg), and sodium L-ascorbate (51 mg). After 24 h, slides were washed by sonicating in EtOH 5 times. The contact angle was 33.1º. Contact angles indicated functionalization of the slides, although ATR-FTIR did not indicate any functionality.

Synthesis of Protected CarboxyPS Microspheres with EGDMA Cross-Linker

In a 250-mL Morton flask, water (110 g), Mowiol 40-88 (M_W ~205,000 g/mol, 88% hydrolyzation, 0.25 g), styrene (16.1 g, 155 mmol), ethylene glycol dimethacrylate (EGDMA) (0.11 g, 0.58 mmol), *tert*-butyl 4-vinylbenzoate (2.0 g, 9.8 mmol), and benzoyl peroxide (BPO, Luperox, 0.50 g, 1.5 mmol) were stirred at 235 rpm by an IKA 20 digital mechanical stirrer, purged with nitrogen for 15 min, and heated to 70 °C. The reaction mixture was cooled to room temperature 12 h after heating. The particles were isolated by centrifugation for 3 min at 3000 rpm, washed 5 times in 3:7 THF/EtOH by redispersion and centrifugation for 3 min at 3000 rpm, and dried *in vacuo* to yield 11.9 g particles (65% yield).

Removal of *tert*-Butyl Protecting Group on CarboxyPS Particles

At room temperature, protected carboxyPS particles (5.55 g) were suspended in 1:1 DCM/trifluoroacetic acid (100 mL). The mixture was stirred for 12 h. DCM and trifluoroacetic acid were removed *in vacuo*. The carboxyPS particles were washed 5 times in THF/EtOH by redispersion and centrifugation, and dried *in vacuo* to yield 4.32 g particles (80% yield).

Functionalization of CarboxyPS Particles with 3-Chloroperbenzoic Acid

CarboxyPS particles (1.1 g) were swollen in a solution of *m*CPBA (0.98 g, 5.7 mmol) in DCM (25 mL). To this mixture, diisopropylcarbodiimide (DIC, 0.55 mL, 3.6 mmol) was added. After 12 h, 25 mL EtOH were added to the reaction mixture. The particles were isolated by centrifugation, washed 5 times in THF/EtOH by redispersion and centrifugation, and dried *in vacuo* to yield 1.1 g (96% yield).

Functionalization of CarboxyPS Particles with 4-(Dimethylamino)benzyl Alcohol

CarboxyPS particles (1.1 g) were swollen in a solution of 4-dimethylaminopyridine (0.34 g, 2.8 mmol) and 4-(dimethylamino)benzyl alcohol (0.42 g, 2.8 mmol) in DCM (35 mL). To this mixture, DIC (0.44 mL, 2.8 mmol) was added. After 12 h, 15 mL EtOH was added to the reaction mixture. The

particles were isolated by centrifugation, washed five times in THF/EtOH by redispersion and centrifugation, and dried *in vacuo* to yield 0.63 g (66% yield).

Test of Functionalized Particles on a Planar Substrate

A DMA-functionalized slide was immersed in MA at room temperature under ambient atmosphere. About 3 mg of BPO-functionalized particles were placed on the DMA-functionalized surface. A Teflon stirring blade was placed on top of the particles on the surface, and pressure was applied for two minutes. The slide was then gently rinsed with milli-Q water and wiped with a Kimwipe. This procedure was repeated for an azide-functionalized slide with BPO-functionalized particles and for a DMA-functionalized slide with carboxyPS particles.

Compression Tests of Complementary Particles

Compression tests were conducted inside a nitrogen-filled glovebag. In a 10-mL beaker, BPO particles (34 mg) and DMA particles (32 mg) were mixed with a spatula. A stopper was placed on top of the dry particles before addition of 1.5 mL methyl acrylate (MA). The particles were allowed to swell and react for 1 h before removal from the glovebag and washing with THF and EtOH. The particles were dried *in vacuo*. The ATR-FTIR spectrum of the particles is included below (Figure 4.6). The PMA polymer was observed in the spectrum.

For the first control set, BPO particles (29 mg) were tied inside two 3”x3” pieces of 100% cotton. The bundle of particles was placed inside a 40-mL beaker with DMA particles (29 mg). A weighted centrifuge tube was placed on top of the particles inside the beaker before the addition of 7 mL MA. The particles were allowed to swell and react for 1 h before removal from the glovebag and washing with THF and EtOH. The particles were dried *in vacuo*. PMA was not observed in the ATR-FTIR spectra of these particles.

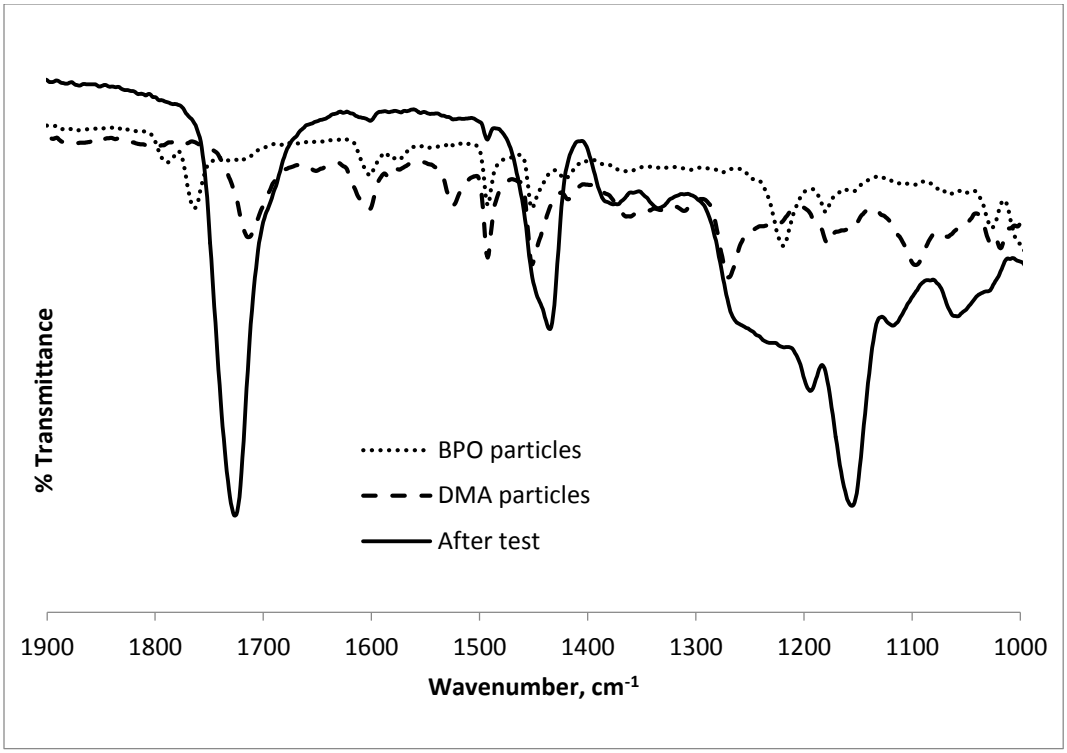

Figure 4.6. ATR-FTIR spectra of functionalized particles before and after the compression tests indicating the formation of PMA following contact.

For the second control set, two 3"x3" pieces of 100% cotton and two pieces of cotton string were placed in the bottom of a 40-mL beaker. Inside this beaker, BPO particles (29 mg) and DMA particles (29 mg) were mixed with a spatula. A weighted centrifuge tube was placed on top of the particles inside the beaker before the addition of 7 mL MA. The particles were allowed to swell and react for 1 h before removal from the glovebag and washing with THF and EtOH. The particles were dried *in vacuo*. PMA was observed in the ATR-FTIR spectrum of these particles.

Tests of Functionalized Particles with Small Molecule Complements

Isophthalic acid (1.0 g) was dissolved in MA (80 mL) and THF (160 mL). Solutions (0.20 M) of benzoyl peroxide (BPO) and *N*,*N*-dimethylaniline (DMA) were made from the isophthalic acid solution. In a nitrogen-purged vial, BPO particles (11 mg) were swollen in 1.0 mL 0.20 M DMA. After 1 h, 0.10 mL of the supernatant was added to 0.75 mL 0.08 mM butylated hyrdoxytoluene solution in $CDCl_3$. The

particles were washed with THF and EtOH and dried *in vacuo*. In a second nitrogen-purged vial, DMA particles (12 mg) were swollen in 1.0 mL 0.20 M BPO. After 1 h, 0.10 mL of the supernatant was added to 0.75 mL 0.08 mM butylated hyrdoxytoluene solution in $CDCl_3$. The particles were washed with THF and EtOH and dried *in vacuo*. In a third nitrogen-purged vial, carboxyPS particles (12 mg) were swollen in 0.5 mL 0.20 M DMA + 0.5 mL 0.20 M BPO. After 1 h, 0.10 mL of the supernatant was added to 0.75 mL 0.08 mM butylated hyrdoxytoluene solution in $CDCl_3$. The particles were washed with THF and EtOH and dried *in vacuo*. ATR-FTIR spectra of all three sets of particles indicated the presence of PMA. Polymer was also present in the supernatant as characterized by ^{1}H NMR spectroscopy.

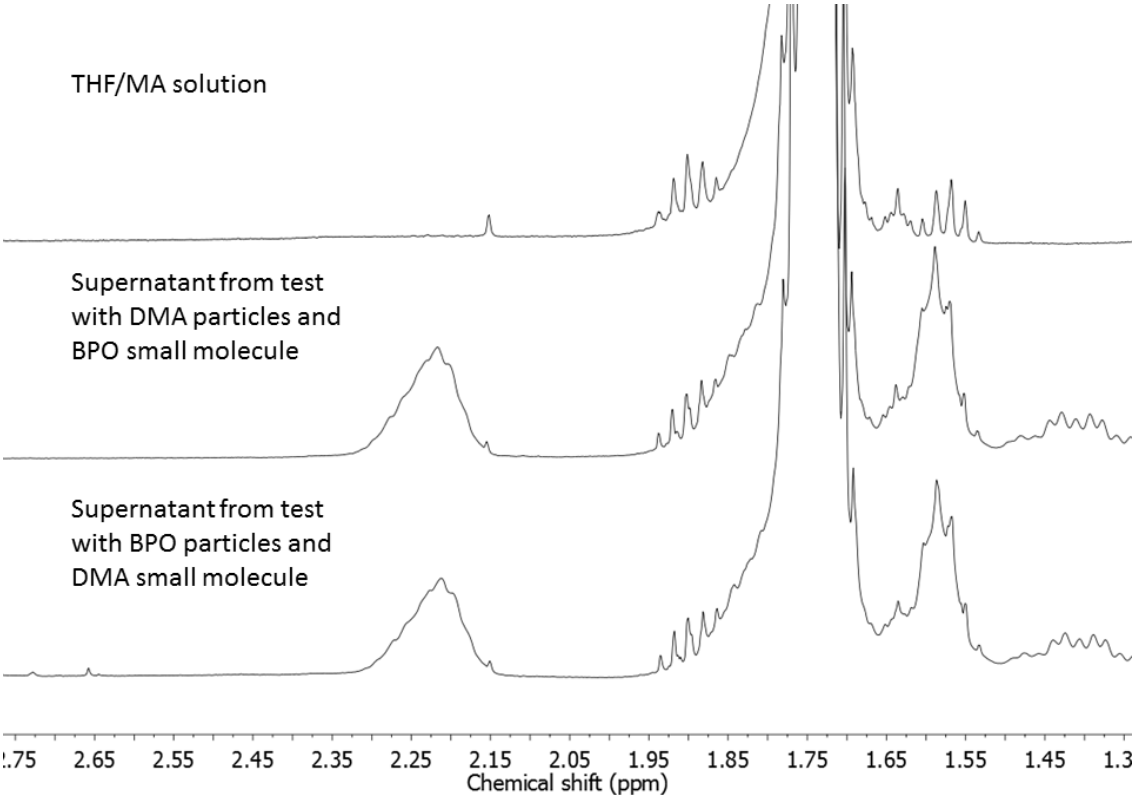

Figure 4.7. ^{1}H NMR spectra of supernatant in tests of particles with small molecule co-intiator. Methine and methylene protons of PMA chains are observed at δ 2.22 and 1.59 ppm.

A final compression test was conducted inside a nitrogen-filled glovebag. In a 10-mL beaker, BPO particles (~30 mg) and DMA particles (~30 mg) were mixed with a spatula. A stopper was placed on top of the dry particles before addition of 1.5 mL methyl acrylate (MA). The particles were allowed to swell

and react for 1 h before removal from the glovebag and washing with THF and EtOH. The washes were collected and concentrated in vacuo to yield a white, sticky residue. This residue was dissolved in THF-d_8 and characterized by ^{1}H NMR spectroscopy, which indicated the presence of the methine protons of PMA by a broad peak at δ 2.33 ppm. The particles were dried *in vacuo*. The ATR-FTIR spectrum of the particles indicated the presence of PMA.

4.6 References

(1) *Angew. Chem.* **1949**, *61*, 433-460.

(2) Pryor, W. A.; Hendrickson, W. H. *Tetrahedron Lett.* **1983**, *24*, 1459-1462.

(3) Wiles, C.; Watts, P.; Haswell, S. *Tetrahedron Lett.*, **2006**, *47*, 5261-5264.

(4) Washburn, A. L.; Luchansky, M. S.; Bowman, A. L.; Bailey, R. C. *Anal. Chem.* **2010**, *82*, 69-72.

(5) Lummerstorfer, T.; Hoffmann, H. *J. Phys. Chem. B* **2004**, *108*, 3963-3966.

(6) Ranjan, R.; Brittain, W. J. *Macromolecules* **2007**, *40*, 6217-6223.

(7) Cecchet, F.; Pilling, M.; Hevesi, L.; Schergna, S.; Wong, J. K. Y.; Clarkson, G. J.; Leigh, D. A.; Rudolf, P. *J. Phys. Chem. B* **2003**, *107*, 10863-10872.

Appendix: Moore Group Raps and Carols

At Prof. Jeffrey Moore's request, the raps performed during group meetings are included in this dissertation, with the exception of one rap that cannot be located. The two Moore group carols are also recorded in this appendix for future reference and inspiration.

Moore Group Rap

(Fall 2012)

Yo! Here at the Moore group, it's all about the delta!
Yeah, bring on the change, 'cause it's enough to melt ya.
Mike's online, startin' a revolution
In educatin'; yeah, statistics he's computin'.
Preston's system is a purple shining star—
A mechanophore with arms that stretch so far.
For shock wave power, you should look to Nag.
Charles and Tomo are workin' on some PAG's,
While Nina's in lab at night playin' games like TAG.
Polymers degrade in the labs of Josh and Bora
'Cause signaled release really has an aura.
For macrocycles, Sisco's really at the top.
James has a filter that toxic ions stops.
Alzheimer's on a peg'll be hung
By the work of Pin-Nan, Li-juan, and our Yang.

Hefei's all about them disappearin' fibers;
And Grolman makes capsules that make the field wider.
Cat's makin' vesicles of polymers with blocks.
Windy's gels will heal at the ticking of a clock.
Daniel's research will make our autos safer.
Xinghong may make some nano-polywafers.
Ke's small molecules are actin' pretty sweet.
Ashley's orderin' and keepin' up on tweets.
But Jeff's the one in charge; yeah, he's our man.
And he's the reason why I'll always be a Moore group fan.

CarboxyPS Particle Rap

(Summer 2014)
We got some particles, both big and small;
See those mushroom caps and those ones so spherical.
Yeah, they'll blow your mind with their orders of mag;
And soon they'll be used for mechanochem and TAG.
You see we's got particles that are covered in carboxies;
Or maybe you want some spheres with aminoalkoxies.
'Cause it's conjugation that these spheres are all about;
So let's functionalize before you get the gout.
And when we've made our spheres, let's go for a spin
In our new centrifuge, which is gonna make you grin.

Tips for Seminars Rap

(Spring 2015)
So's you'se getting' all ready for some big research talk
Or some seminar you don't want folks to mock.
Well, I've got a few suggestions for my peeps in da hood-
Just some don't's and some do's, the should not and the should.

Background should be short; just cut to the chase;
And don't forget to bluntly state the question that you face.
Just say what that question is;
Express your hypothesis
'Cause too many times we miss
The science speaker's gist.

And when it comes to those slides, remember that they're free.
Keep it just to one point – not two, or five, or three.
And when it comes to that point, make sure you write it clear
On the bottom of that slide in case your hearers didn't hear.

On the wiki you will find clear directions for those ChemDraws,
The alumni's advice, and Silverman's slide laws.
It's true in the Moore group that it's all about the delta;
But let's keep those slides clean so Jeffy don't melt ya.

O Mechanochem

To the tune of "O Christmas Tree"

(Winter 2013)

O mechanochem, O mechanochem,
How stretched out are your polymers.
O mechanochem, O mechanochem,
How stretched out are your polymers.
The sonication bubbles break;
Mechanophore acts in their wake.
O mechanochem, O mechanochem,
How stretched out are your polymers.

Mickey the Microcapsule

To the tune of "Rudolph the Red-Nosed Reindeer"

(Winter 2013)

Mickey the microcapsule
Had a very thick shell wall
To hold his self-healing contents;
To heal he was made special.

All of the other capsules
Used to leak and lose their load.
They couldn't last like Mickey
Whose great qualities now showed.

Then one fateful research day,
The pressure was applied.
The crack was formed, and Mickey broke.
The crack with his contents was soaked.

But his load set and cured soon,
Healing what was the crack.
Thank you to Mickey's failure;
Matrix performance is back!